

UNIVERSIDADE FEDERAL DO PARANÁ
SETOR DE CIÊNCIAS BIOLÓGICAS
DEPARTAMENTO DE FARMACOLOGIA

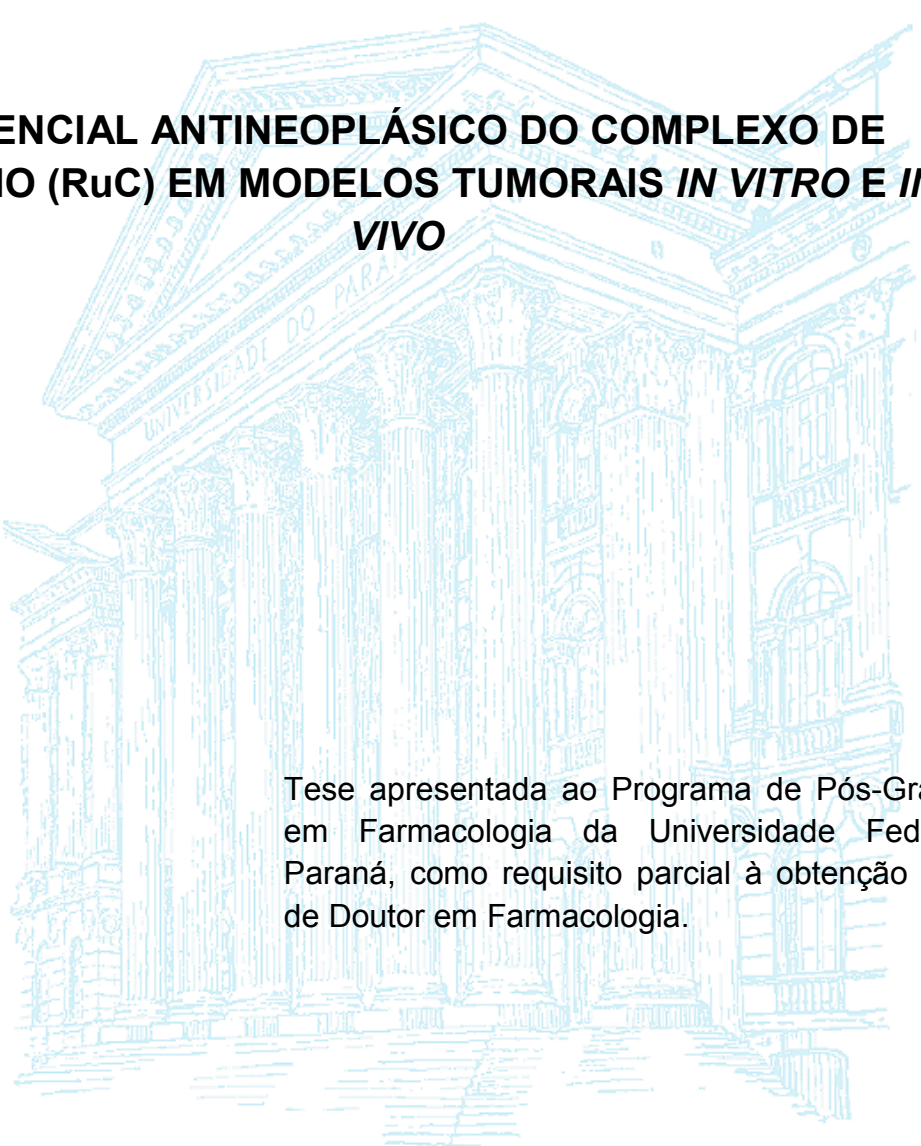
**POTENCIAL ANTINEOPLÁSICO DO COMPLEXO DE
RUTÊNIO (RuC) EM MODELOS TUMORAIS *IN VITRO* E *IN*
*VIVO***

Carlos Eduardo Alves de Souza

CURITIBA
2017

Carlos Eduardo Alves de Souza

**POTENCIAL ANTINEOPLÁSICO DO COMPLEXO DE
RUTÊNIO (RuC) EM MODELOS TUMORAIS *IN VITRO* E *IN*
*VIVO***



Tese apresentada ao Programa de Pós-Graduação
em Farmacologia da Universidade Federal do
Paraná, como requisito parcial à obtenção do título
de Doutor em Farmacologia.

Orientadora: Prof^a Dr^a Alexandra Acco

Co-orientadora: Prof^a Dr^a Sílvia Maria Suter Correia Cadena

CURITIBA
2017



MINISTÉRIO DA EDUCAÇÃO
UNIVERSIDADE FEDERAL DO PARANÁ
PRÓ-REITORIA DE PESQUISA E PÓS-GRADUAÇÃO
Setor CIÊNCIAS BIOLÓGICAS
Programa de Pós Graduação em FARMACOLOGIA
Código CAPES: 40001016038P0

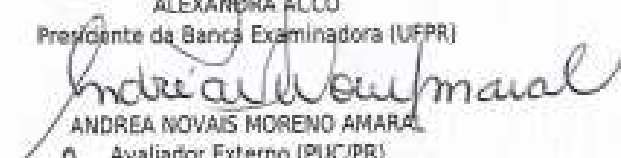
ATA DE SESSÃO PÚBLICA DE DEFESA DE TESE PARA A OBTENÇÃO DO GRAU DE DOUTOR EM FARMACOLOGIA

No dia trinta de junho de dois mil e dezessete às 08:30 horas, na sala 107 - Anfiteatro, Anexo I do Setor de Ciências Biológicas - Farmacologia, do Setor de CIÊNCIAS BIOLÓGICAS da Universidade Federal do Paraná, foram instalados os trabalhos de arguição do doutorando **CARLOS EDUARDO ALVES DE SOUZA** para a Defesa Pública de sua Tese intitulada: **"Potencial Antineoplásico do Complexo de Rutênio (Ruphenimh) em Modelos Tumorais *in vitro* e *in vivo*"**. A Banca Examinadora, designada pelo Colegiado do Programa de Pós-Graduação em FARMACOLOGIA da Universidade Federal do Paraná, foi constituída pelos seguintes Membros: ALEXANDRA ACCO (UFPR), ANDREA NOVAIS MORENO AMARAL (PUC/PR), JULIANA GEREMIAS CHICHORRO (UFPR), RÔNISE MARTINS SANTIAGO (UNIANDRADE), SHEILA MARIA BROCHADO WINNISCHÖFER (UFPR). Dando início à sessão, a presidência passou a palavra ao discente, para que o mesmo expusesse seu trabalho aos presentes. Em seguida, a presidência passou a palavra a cada um dos Examinadores, para suas respectivas arguições. O aluno respondeu a cada um dos arguidores. A presidência retomou a palavra para suas considerações finais. A Banca Examinadora, então, e, após a discussão de suas avaliações, decidiu-se pela APROVAÇÃO do aluno. O doutorando foi convidado a ingressar novamente na sala, bem como os demais assistentes, após o que a presidência fez a leitura do Parecer da Banca Examinadora. A aprovação no rito de defesa deverá ser homologada pelo Colegiado do programa, mediante o atendimento de todas as indicações e correções solicitadas pela banca dentro dos prazos regimentais do programa. A outorga do título de doutor está condicionada ao atendimento de todos os requisitos e prazos determinados no regimento do Programa de Pós-Graduação. Nada mais havendo a tratar a presidência deu por encerrada a sessão, da qual eu, ALEXANDRA ACCO, lavrei a presente ata, que vai assinada por mim e pelos membros da Comissão Examinadora.


Observações: _____

Curitiba, 30 de junho de 2017.


ALEXANDRA ACCO
Presidente da Banca Examinadora (UFPR)


ANDREA NOVAIS MORENO AMARAL
Avaliador Externo (PUC/PR)


JULIANA GEREMIAS CHICHORRO
Avaliador Interno (UFPR)


RÔNISE MARTINS SANTIAGO
Avaliador Externo (UNIANDRADE)


SHEILA MARIA BROCHADO WINNISCHÖFER
Avaliador Externo (UFPR)



MINISTÉRIO DA EDUCAÇÃO
UNIVERSIDADE FEDERAL DO PARANÁ
PRÓ-REITORIA DE PESQUISA E PÓS-GRADUAÇÃO
Setor CIÊNCIAS BIOLÓGICAS
Programa de Pós Graduação em FARMACOLOGIA
Código CAPES: 40001016038P0

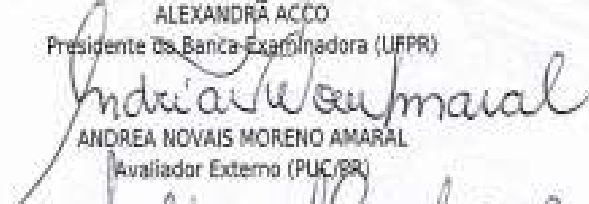
TERMO DE APROVAÇÃO

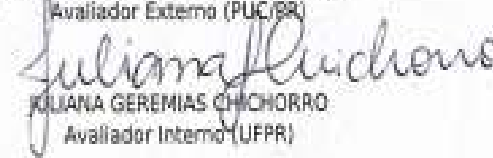
Os membros da Banca Examinadora designada pelo Colegiado do Programa de Pós-Graduação em FARMACOLOGIA da Universidade Federal do Paraná foram convocados para realizar a arguição da Tese de Doutorado de **CARLOS EDUARDO ALVES DE SOUZA**, intitulada: "**Potencial Antineoplásico do Complexo de Rutênio (Ruphenimh) em Modelos Tumerais *in vitro* e *in vivo***", após terem inquirido o aluno e realizado a avaliação do trabalho, são de parecer pela sua Aprovação no rito de defesa.


A outorga do título de doutor está sujeita à homologação pelo colegiado, ao atendimento de todas as indicações e correções solicitadas pela banca e ao pleno atendimento das demandas regimentais do Programa de Pós-Graduação.

Curitiba, 30 de junho de 2017.


ALEXANDRA ACCO
Presidente da Banca Examinadora (UFPR)


ANDREA NOVAIS MORENO AMARAL
Avaliador Externo (PUC/RR)


JULIANA GEREMIAS CHICHORRO
Avaliador Interno (UFPR)


RONISE MARTINS SANTIAGO
Avaliador Externo (UNIANDRADE)


SHEILA MARIA BROCHADO WINNISCHOFER
Avaliador Externo (UFPR)

Dedico este trabalho a todos que participaram direta ou indiretamente durante esta etapa da minha vida, principalmente minha esposa Helen, meu filho Otávio e minha família. Tenham certeza que sem o apoio incondicional de vocês eu não teria conseguido.

AGRADECIMENTOS

Agradeço primeiramente a Deus, por me conceder o presente de ter chegado até o presente momento com saúde mental e física, permitindo-me imensa disposição, força, paciência, sabedoria e coragem para enfrentar os obstáculos durante toda minha formação acadêmica. Tais agradecimentos não poderiam deixar de ser estendidos aos amigos espirituais que com amor, carinho e paciência auxiliaram a mim e minha família a caminhar sobre as luzes de Deus. Um grande amigo me disse algumas palavras que marcaram meu coração: “Somos como uma semente que Deus planta e cuida para que esta pequena semente cresça, e tornando-se uma bela árvore dê lindas flores e magníficos frutos para que na próxima estação, suas sementes sejam propagadas a novos frutos, que serão propagadas novamente por Deus”.

Antes de mais nada, meus principais agradecimentos a minha amada, carinhosa, atenciosa, compreensiva, dedicada, equilibrada, paciente e humana esposa que me acompanha nesta linda trajetória com dedicação e abnegação. Em 2010, quando decidimos fazer o mestrado, sei que foi a decisão mais difícil que tomamos, mas com coragem, muito amor e companheirismo, chegamos ao final de mais um ciclo neste imenso espiral da vida, mais fortalecidos, maduros, conscientes das responsabilidades da vida e com o maior presente de todos que foi nosso filho Otávio. Agradeço pelo imenso amor que você me deu desde o dia em que nos conhecemos, porque este amor me agiganta e me motiva a crescer cada vez mais ao seu lado. OBRIGADO MEU AMOR.

Nunca poderia deixar de mencionar as pessoas que participaram ativamente na formação do meu caráter, princípios e ética, que refletem diretamente na tese aqui apresentada e estiveram presentes fortemente em meu coração e pensamentos nesta caminhada, tornando-a cada dia mais prazerosa e feliz. A estes os meus agradecimentos. À minha mãe Rejane sempre muito presente em todos os momentos. A meu irmão Cesar Vinícius, minha cunhada Cristina e a meu sobrinho César, que mesmo distantes fisicamente, estão presente nos pequenos detalhes de minha vida e principalmente desta tese. Agradeço a meus avós (Glória, Rita, Benedita e falecidos Crispim e Crispiniano) pelo enorme carinho e amor que recebo e recebi ao longo da minha vida. Agradeço a todos os membros da minha família (tias, tios, primos e primas) que abdicaram de confraternizações e visitas para que esta tese fosse concluída.

Não somente de familiares herdados tive o imenso privilégio de conviver e aprender, mas de familiares a que fui apresentado, que conquistaram e conquistam com enorme força cada milímetro do meu coração, com um mar de carinho, afeto, ternura, atenção, diálogo, alegria, humor, amor e essenciais “puxões de orelha”, fundamentais para a construção do caráter e equilíbrio refletido hoje. A estas contribuições, agradeço ao meu sogro e sogra Jair e

Helena, a minha cunhada Hely que me ensina a arte da paciência e da reflexão da vida, e às tias, tios, primos, primas e a tantas pessoas maravilhosas que participaram desta trajetória. Sem o apoio de vocês nada disso seria possível.

Minha história acadêmica é marcada por pessoas e instituições que tiveram cada qual seu papel, mas que no conjunto foram indispensáveis nesta caminhada. É para estas pessoas e instituições que dirijo meus agradecimentos.

É costume começar pelo orientador. É o que faço. Não só porque ele foi o primeiro a acreditar que eu merecia a oportunidade de viver esta experiência acadêmica, mas principalmente porque seu apoio e supervisão não subtraiu a liberdade necessária para que eu ganhasse autonomia no pensar e no agir: condição indispensável na formação do pesquisador. Professora Dr^a Alexandra Acco, muito obrigado! Hoje, tenho certeza que aprender é, antes de tudo, aprender a caminhar, a perguntar e buscar as respostas possíveis. É parar e duvidar dos caminhos escolhidos é percorrê-los novamente, se necessário. Ao fazer-me caminhar sozinho, algumas vezes aos tropeços, pelo caminho das pedras, permitiu que eu construísse minha estrada. Estrada, que tenho certeza, continuará interpondo pedras para remover. Mas hoje, sei que posso removê-las.

Agradeço imensamente à minha Co-orientadora, Prof^a Dr^a Sílvia Maria Suter Correia Cadena (que é minha co-orientadora somente no papel, mas minha orientadora na minha formação), uma pessoa, mãe, e uma cientista maravilhosa. São quatro anos de convivência que não poderiam ser melhores, tanto no aspecto científico, quanto no aspecto pessoal. Agradeço por todo apoio, as conversas, a paciência, os momentos de consolo após desequilíbrio e desesperança do futuro, mas que com seu carinho imediatamente tudo passava, acompanhado de um bom café ou uma xícara de chá. Principalmente agradeço por tudo que eu aprendi e aprendo com você. MUITO OBRIGADO.

Sou particularmente grato às professoras Dr^a Glaucia R. Martinez, Dr^a Guilhermina Rodrigues Noletto, Dr^a Maria Eliane Merlin Rocha e Dr^a Sheila M. B. Winnischofer que me receberam no laboratório do grupo de Oxidações Biológicas e Cultivo Celular no Departamento de Bioquímica, acolhendo-me sempre, como um de seus alunos. As professoras tiveram um papel importantíssimo na minha formação, pois com paciência e atenção tive a oportunidade de aprender com cada professora as melhores características que cada uma tem no âmbito científico. Minha convivência no laboratório me deu a certeza de que bons resultados não acontecem facilmente e nem por acaso. A generosa acolhida e participação nos momentos de “escuridão” ensinaram-me que aprendemos muito mais do que aquilo que ansiosamente buscamos. Sempre digo que tive o prazer de ter 4 co-orientadoras e 2 orientadoras que me auxiliaram na minha formação profissional e científica. Sem isso, nada seria possível.

Agradecer aos amigos é a tarefa mais delicada. Alguns estavam ali sempre, dentro ou fora do laboratório. Alguns passaram rapidamente, mas

tiveram um impacto que muitas vezes nem conseguimos compreender como e porque foi. Seja como for, todos foram importantes para que eu pudesse manter o foco, o ritmo e principalmente a saúde mental. São os amigos as principais vítimas de nosso estresse e de nossas inseguranças, mas que tudo se esvaiu com muita facilidade por ter pessoas tão companheiras e pacientes. Por isso, mas também pela amizade e pelos bons momentos de descontração e pelo estímulo intelectual, agradeço aos companheiros dos laboratórios de Farmacologia e Metabolismo Aline, Arturo, Amanda, Flávia, Claudia, Carol, Larissa e Thaisa; e do grupo de Oxidações Biológicas e Cultivo Celular: Diego, Ana Paula, Aninha, Monique, Elaine, Gustavo, Amanda, Juan, Stephane, Otávio, Carol, Rafaela, Juliana e Wilian. Muito embora apareçam elencados de forma impessoal, “num pacote”, saibam que cada um de vocês teve um papel singular nesta minha trajetória.

Palavras não são capazes de expressar meu sentimento de dívida. MUITO OBRIGADO por todos os sacrifícios, se não fosse por vocês com certeza eu não estaria aqui hoje. Este trabalho nada mais é do que o fruto de um trabalho que todos nesta trajetória participaram!

O agradecimento final é dedicado à CAPES e ao CNPQ pelo apoio financeiro e pela bolsa de doutorado que me foi concedida. A impessoalidade desta referência não significa que agradeço para cumprir formalidade. Sem estas instituições não chegaria ao bom termo deste trabalho, na verdade, seria impensável iniciá-lo.



Caminhante sobre o mar de névoa (1818)

Óleo sobre tela: 98.4 x 74.8 cm

(Caspar David Friedrich)

“A vida é como andar de bicicleta.
Para manter o equilíbrio, é preciso
se manter em movimento”.

(Albert Einstein, em carta a seu filho Eduard, 1930)

“Noventa por cento do sucesso se
baseia simplesmente em insistir”.

(Woody Allen)

NOTA EXPLICATIVA

Esta tese é apresentada em formato alternativo, como artigos científicos para publicação, de acordo com as normas do Programa de Pós-Graduação em Farmacologia da Universidade Federal do Paraná. A tese consta de uma revisão bibliográfica, objetivos gerais e específicos do trabalho e dois artigos científicos com os experimentos realizados, resultados e discussão, além das considerações finais sintetizando os achados dos mesmos.

RESUMO

O índice de pessoas diagnosticadas com câncer vem aumentando consideravelmente no mundo todo. Em 2020 estima-se que o número de novos casos mundiais alcance a ordem de 15 milhões de pessoas, sendo que 60% destes deverão ocorrer nos países em desenvolvimento. O tratamento de escolha para esta enfermidade são os quimioterápicos, mas sabe-se que eles são agentes altamente citotóxicos, possuem baixo índice terapêutico, vários efeitos colaterais e baixa seletividade em relação às células tumorais, características que restringem o seu uso. A cisplatina, por exemplo, utilizada com sucesso no tratamento de alguns tipos de tumor, apresenta efeitos adversos tempo e dose-dependentes. Assim, novos compostos formulados com metais de transição da mesma família da platina têm surgido como uma opção mais satisfatória, uma vez que promovem menos efeitos colaterais. Neste contexto, complexos de Rutênio têm apresentado seletividade para algumas células tumorais, associada ao favorecimento de sua redução no microambiente ácido tumoral. O objetivo deste trabalho foi avaliar a atividade antineoplásica do composto de rutênio denominado *cis*-[Ru(phen)₂(ImH)₂]²⁺ ou RuC, em cultura (*in vitro*) de células HepG2 (carcinoma hepatocelular), HeLa (adenocarcinoma de cervix humana), U87MG (glioblastoma humano), NDAmb234 (adenocarcinoma mamário humano), B16F10 (melanoma murino) e HEK293 (não-tumoral renal embrionária humana), e no carcinoma Walker-256 de ratos (*in vivo*), bem como analisar parâmetros metabólicos, de estresse oxidativo, morfológicos e a expressão de genes associados à apoptose. Em todos os experimentos, a cisplatina foi usada como controle positivo. O RuC reduziu a viabilidade de células HepG2 e HeLa em várias concentrações testadas (10, 50 e 100 nmol/L), após 48 horas de exposição, nos ensaios de MTT, Cristal Violeta e Vermelho Neutro. O RuC inibiu todos os estados da respiração celular e aumentou os níveis dos metabólitos piruvato e lactato em ambas as linhagens celulares. Em consonância, diante do tumor sólido Walker-256 em ratos, a dose de 10 mg/kg RuC, administrada por via intraperitoneal durante 13 dias, mostrou-se mais efetiva, pois reduziu o volume e o peso tumoral, induziu estresse oxidativo e necrose no tecido tumoral, e reduziu a respiração em células tumorais, mas não induziu apoptose. Em adicional, o RuC melhorou parâmetros antioxidantes sistemicamente, avaliados em fígado e rins de animais portadores do tumor Walker-256. Estes resultados foram corroborados pela ausência de toxicidade observada em ratos sem tumor e tratados com a mesma dose de RuC (10 mg/kg), diferindo dos achados com a cisplatina, que provocou nefrotoxicidade. Os resultados sugerem que o RuC tem atividade antineoplásica através da modulação do estresse oxidativo e fosforilação oxidativa das células tumorais, sem causar toxicidade sistêmica. Estes efeitos tornam o RuC uma promissora droga anticancerígena. Outras investigações com este composto, incluindo estudos clínicos, devem ser encorajadas.

ABSTRACT

The number of people diagnosed with cancer has increased considerably worldwide. By 2020, it is estimated that the number of new global cases will reach 15 million people, with 60% occurring in developing countries. The treatment of choice for this disease is chemotherapy, but it is known that chemotherapeutic agents are highly cytotoxic, have low therapeutic index, several side effects and low selectivity in relation to tumor cells, characteristics that restrict its use. Cisplatin, for example, used successfully in the treatment of some types of tumor, has both time-dependent and dose-dependent adverse effects. Thus new compounds formulated with transition metals of the same platinum family have emerged as a more satisfactory option as they promote fewer side effects. In this context, Ruthenium complexes have shown selectivity for some tumor cells, associated with its favorable reduction in the tumor acidic microenvironment. The objective of this work was to evaluate the antineoplastic activity of the ruthenium compound named cis- $[\text{Ru}(\text{phen})_2(\text{ImH})_2]^{2+}$ or RuC, in culture (*in vitro*) of HepG2 (hepatocellular carcinoma), HeLa (adenocarcinoma of human cervix), U87MG (human glioblastoma), NDAmb234 (human breast adenocarcinoma), B16F10 (murine melanoma cells) and HEK293 (non-tumor human embryonic kidney), and Walker-256 rat carcinoma (*in vivo*), as well as to analyze metabolic, oxidative stress and morphological parameters, and gene expression associated with apoptosis. In both experiments cisplatin was used as a positive control. RuC reduced the viability of HepG2 and HeLa cells at various concentrations tested (10, 50 and 100 nmol/L) after 48 hours of exposure in the MTT, Violet Crystal and Neutral Red assays. RuC inhibited all cellular respiration states and increased levels of pyruvate and lactate metabolites in both cell lines. Accordingly, in the presence of the Walker-256 solid tumor in rats, the dose of 10 mg/kg RuC, administered intraperitoneally for 13 days, was more effective, because it reduced the volume and tumor weight, induced oxidative stress and necrosis in tumor tissue, and reduced respiration in tumor cells, but did not induce apoptosis. In addition, RuC improved systemic antioxidant parameters assessed in the liver and kidneys of Walker-256 tumor-bearing animals. These results were corroborated by the absence of toxicity observed in rats without tumor and treated with the same dose of RuC (10 mg/kg), differing from the findings with cisplatin, which caused nephrotoxicity. The results suggest that RuC has antineoplastic activity through the modulation of oxidative stress and oxidative phosphorylation of tumor cells, without cause systemic toxicity. These effects make the RuC a promising anticancer drug. Further investigations with this compound, including clinical studies, should be encouraged.

LISTA DE FIGURAS

REVISÃO LITERÁRIA

FIGURA 1. (A) Imagem de microscopia de luz da forma sólida do tumor de Walker 256 transplantada em ratos. (B) Imagem de microscopia de luz do fluído peritoneal de um rato portador de tumor ascítico de Walker 256.....33

FIGURA 2. Principais vias de formação de espécies reativas de oxigênio/nitrogênio. SOD - superóxido dismutase; MPO mieloperoxidase; CAT catalase; GPX glutathiona peroxidase; LH lipídios, LO - radical alcóxila, LOO - radical peróxila. ONOOCO₂-radical peroximonocarbonato.....37

FIGURA 3. Estrutura da (A) cisplatina e (B) transplatina representada em forma estrutural espacial.....42

FIGURA 4. Estrutura química do (cis-[Ru(1,10-fenantrolina)₂(imidazol)₂]²⁺), onde 1,10-fenantrolina (phen) e imidazol (ImH), sendo denominado RuphenImH ou RuC neste trabalho.....44

PRIMEIRO ARTIGO CIENTÍFICO

FIGURE 1. Chemical structure of RuC, according to IUPAC nomenclature, cis-[Ru(1,10-phen)₂(ImH)₂]²⁺, which *phen* refers to 1,10-phenanthroline and *ImH* refers to imidazole.....51

FIGURE 2. Toxicity of RuC complex on cell lines. Different cell lines were treated with RuC at concentration of 100 nmol/L for (A) 24, (B) 48 and (C) 72 hours. The experimental conditions are described in the Materials and Methods. Briefly, the cells (10⁴ cell/ well) were seeded in 96-well plates with RuC at 100 nmol/L and treatment with RuC for 24, 48 and 72 hours and cell viability was evaluated by MTT. The values represent the mean ± SEM of four experiments.....56

FIGURE 3. Toxicity of cisplatin and RuC on HepG2 and HeLa cells. (A and B) MTT assay, (C and D) crystal violet, and (E and F) neutral red assay. The experimental conditions are described in the Materials and Methods. Briefly, the cells (10⁴ cell/ well) were seeded in 96-well plates with cisplatin (5 and 10 µmol/L) or RuC (10, 50 and 100 nmol/L) for 48 h. The values represent the mean ± SEM of six experiments. The results are expressed as % of control

(DMSO 0.1%). Symbols: * significantly different from the control; # significantly different from cisplatin 10 $\mu\text{mol/L}$; one, two, and three symbols refer to $p < 0.05$, $p < 0.01$, and $p < 0.001$, respectively.....58

FIGURE 4. Effect of RuC and cisplatin on proliferation of HepG2 (A) and HeLa cells (B). The experimental conditions are described in the Materials and Methods. The cells were cultured by 48 hours prior the addition of cisplatin (5 and 10 $\mu\text{mol/L}$) or RuC (10, 50 and 100 nmol/L). The values represent the mean \pm SEM of six experiments. The results are expressed as % of control (DMSO 0.1%). Symbols: * significantly different from the control in the same time of treatment; one, two, and three symbols refer to $p < 0.05$, $p < 0.01$, and $p < 0.001$, respectively.....59

FIGURE 5. Effect of cisplatin and RuC in the respiration of HepG2 cells (A, C and E) and HeLa cells (B, D and F). The experimental conditions are described in the Materials and Methods. Briefly, cells (10^6 cell/ well) were seeded in 60 mm plates, treated and transferred to the Oroboros 2-K oxygraph chambers, where the oxygen consumption was determined in the absence of inhibitors or uncouplers (basal state), in the presence of oligomycin (leak state) and in the presence of FCCP (uncoupled state). The results were expressed as respiration ($\text{pmolO}_2/1 \times 10^6 \text{cells}$) relatively to the control. Values represent the mean \pm SEM of four independent experiments. Symbols: * significantly different from the control (DMSO 0.1% - vehicle); # significantly different from cisplatin 10 $\mu\text{mol/L}$; one, two, and three symbols refer to $p < 0.05$, $p < 0.01$, and $p < 0.001$, respectively.....60

FIGURE 6. Levels of pyruvate (A and B) and lactate (C and D) released by HepG2 and HeLa cells treated with Cisplatin or RuC. The experimental conditions are described in the Materials and Methods. The cells (10^6 cell/ well) were seeded in 60 mm plates and treated with cisplatin (5 and 10 $\mu\text{mol/L}$) and RuC (10, 50 and 100 nmol/L) for 48 h. The pyruvate and lactate concentrations were measured in the culture medium. The results are expressed as the mean \pm SEM of four independent experiments. Symbols: * significantly different from the control (DMSO 0.1% - Vehicle); # significantly different from cisplatin 10 $\mu\text{mol/L}$; one, two, and three symbols refer to $p < 0.05$, $p < 0.01$, and $p < 0.001$, respectively.....61

FIGURE 7. Recovery proliferation curve of HepG2 (A) and HeLa (B) cells. The experimental conditions are described in the Materials and Methods. The cells (10^6 cell/well) were plated in 6-well plate with a cell density of 1.5×10^4 cell and treated with cisplatin or RuC during the first 48h of the experiment protocol. After the treatment the proliferation of the cells were monitored during 9 days. The results are expressed as the numbers of cells (no cells $\times 10^4/\text{mL}$) of four independent experiments.....62

SEGUNDO ARTIGO CIENTÍFICO

FIGURE 1. Synthetic route and chemical structure of ruthenium complex (RuphenImH [RuC]) (A), tumor growth curve (cm³) (B), tumor weight (g) (C), and weight gain (D) in healthy (baseline) and tumor-bearing rats that were treated with RuC, cisplatin, and vehicle (control) for 13 days. The data are expressed as mean ± SEM. The statistical analyses were performed using two-way (B) or one-way (C, D) ANOVA followed by the Bonferroni test. ^{b, *} #Significant difference from baseline, control, and cisplatin groups, respectively (one, two, and three symbols refer to $p < 0.05$, $p < 0.01$, and $p < 0.001$, respectively).....88

FIGURE 2. Relative weight (%) of the kidney (A), liver (B), spleen (C), and lung (D) in the healthy (baseline) group and tumor-bearing control, cisplatin, and RuC groups. The data are expressed as mean ± SEM. The statistical analyses were performed using one-way ANOVA followed by the Bonferroni test. ^{b, *} #Significant difference from baseline, control, and cisplatin groups, respectively (one, two, and three symbols refer to $p < 0.05$, $p < 0.01$, and $p < 0.001$, respectively).....89

FIGURE 3. Gene expression of *p53* (A), *Bax* (B), *Bcl-2* (C), *caspase 3* (D), *catalase* (E), and *Nrf2* (F) in tumor tissue from animals that were treated i.p. with vehicle, cisplatin (2 mg·kg⁻¹), or RuC (10 mg·kg⁻¹) for 13 days at 3 days intervals. The data are expressed as mean ± SEM and were analyzed by one-way ANOVA followed by the Bonferroni test. * $p < 0.05$, ** $p < 0.01$, significant difference from control group; # $p < 0.05$, ## $p < 0.01$, significant difference from cisplatin group.....91

FIGURE 4. DPPH free radical-scavenging activity of RuC (A) and cisplatin (B) at various concentrations (1-300 µg·ml⁻¹). The negative control was distilled water. The positive control was ascorbic acid (AA, 50 µg·ml⁻¹). The data are expressed as mean ± SEM and were analyzed by one-way ANOVA followed by the Bonferroni test. * $p < 0.05$, and *** $p < 0.001$, compared with negative control.....92

FIGURE 5. Oxidative stress parameters in Walker-256 tumor-bearing rats that were treated with vehicle, cisplatin (2 mg·kg⁻¹), and RuC (5 and 10 mg·kg⁻¹) for 13 days. The following parameters were analyzed in tumor tissue (1st column), liver tissue (2nd column), and kidney tissue (3rd column): SOD activity (A-C), Cat activity (D-F), GST activity (G-I), GSH rate (J-L), and LPO rate (M-O). The data are expressed as mean ± SEM and were analyzed by one-way ANOVA followed by the Bonferroni test. ^{b, *} #Significant difference from baseline, control, and cisplatin groups, respectively (one, two, and three symbols refer to $p < 0.05$, $p < 0.01$, and $p < 0.001$, respectively).....93

FIGURE 6. Walker-256 tumor histology in rats that were treated with vehicle (A), 5 mg·kg⁻¹ RuC (B), 10 mg·kg⁻¹ RuC (C), or cisplatin (D) for 13 days. Moderate (A-B) to severe (C) necrosis (*) was observed, accompanied by

diffuse mononuclear infiltration (arrowhead). Cell contraction and cytoplasmic eosinophilia with pycnosis and cariorexis (arrows) were intensely observed in D.....94

FIGURE 7. Effects of RuC and cisplatin on Walker-256 cell respiration. Oxygen consumption was determined immediately (1st column) or 10 min after (2nd column) the addition of compounds. Oxygen flow was determined by an Oroboros 2-K device in the absence of inhibitors or uncouplers (basal state) (A, B), in the presence of oligomycin (leak state) (C, D), and in the presence of FCCP (uncoupled state) (E, F). The data are expressed as the mean \pm SEM of six independent experiments. The data were analyzed by one-way ANOVA followed by the Tukey test. *, #Significant difference from control and cisplatin groups, respectively (one, two, and three symbols refer to $p < 0.05$, $p < 0.01$, and $p < 0.001$, respectively).....96

FIGURE 8. Relative weights of the liver (A), spleen (B), lung (C), and kidney (D) and body weight gain (E) in non-tumor-bearing rats that were treated with vehicle, cisplatin (2 mg·kg⁻¹), and RuC (10 mg·kg⁻¹), i.p., for 13 days at 3 day intervals. (F) Representative section of the kidney after cisplatin treatment (hematoxylin and eosin staining). Black circles indicate discrete to moderate tumefaction of the tubular epithelium. The data are expressed as mean \pm SEM and were analyzed by one-way ANOVA followed by the Bonferroni test. ** $p < 0.01$, *** $p < 0.001$, significant difference from control group; ## $p < 0.01$, ### $p < 0.001$, significant difference from cisplatin group.....97

SUPPLEMENTARY FIGURE S1. Histological observations of liver (A) and kidney of healthy rats treated with vehicle (B), 10 mg·kg⁻¹ RuC (C) or 2 mg·kg⁻¹ cisplatin (D) for 13 days. Typical tubular cells are represented in B and C. White circles indicate discrete to moderate tumefaction of the tubular epithelium, stained with hematoxylin and eosin.....111

LISTA DE TABELAS

SEGUNDO ARTIGO

TABLE 1. Plasma biochemistry and hematological parameters in Walker-256 tumor-bearing rats that were treated for 13 days with vehicle (control), cisplatin (2 mg·kg⁻¹), and RuC (5 and 10 mg·kg⁻¹) p.o. or i.p.....90

LISTA DE ABREVIATURAS: REVISÃO LITERÁRIA

2-DA - 2-desoxiglicose

AMBRA1 - Molécula ativadora regulada por Beclin 1

ARE - Elemento em Resposta a Antioxidante

ATG12 - proteína que regula a Autofagia 12

ATG5 - proteína que regula a Autofagia 5

ATP - Adenosina Trifosfato

CDKs - Ciclina dependente de Quinases

CHC - Carcinoma Hepatocelular

DCFDA - Sonda para detecção de EROS

DMEM - Meio Dulbecco's Modified Eagle

DNA - Ácido desoxirribonucleico

EGFR - Receptores dos genes de fatores de crescimento PDGF

EROS - Espécies Reativa de Oxigenio

Fas-L - Proteína Transmembrana do tipo II

FDA - Administração Federal para Drogas e Alimentos (tradução do inglês)

GSH/GSSG - Razão da glutatona reduzida e glutatona dissulfeto

INCA - Instituto Nacional de Câncer

IUPAC - União Internacional de Química Pura e Aplicada

Keap1 - Proteína Keap do tipo I

MAPK - Proteína quinase ativadas por Mitógenos

MDR - Resistência a Múltiplas Drogas

NAD⁺ - Dinucleotido de nicotinamida e adenina oxidado

NADH - Dinucleotido de nicotinamida e adenina reduzido

NADPH - Dinucleotido de nicotinamida e adenina 2'-fosfato

Nrf2 - fator transcricional sensível ao equilíbrio redox celular

Nrf2-Keap1 - Proteína associada a *Kelch-like ECH*

OXPHOS - Fosforilação oxidativa

PBS - Solução salina com fosfato

PDGF - Genes de fatores de crescimento

pRB - Proteína envolvida no ciclo celular

PTEN - Homólogo de fosfatase e tensão eliminada no cromossomo 10

QET - Químio-embolização Transarterial

RAS - Moléculas transdutoras de sinal

RIP-1 - Proteína quinase de interação ao receptor RIP do tipo I

RIP-2 - Proteína quinase de interação ao receptor RIP do tipo II

Ru (II) - Átomo de Rutênio com valência 2⁺

Ru (III) - Átomo de Rutênio com valência 3⁺

RuC - Complexo de Rutênio (cis-[Ru(1,10-fenantrolina)₂(imidazol)₂]²⁺)

SUS - Sistema Único de Saúde

TCA - Ciclo dos Ácidos Tricarboxílicos

TNF-α - Fator de Necrose Tumoral do tipo α

TRAIL - Ligante indutor de apoptose relacionado ao TNF

VEGF - Fator de crescimento vascular endotelial

VHB - Vírus da hepatite B

VHC - Vírus da Hepatite C

WR - Walker-256 resistentes à cisplatina e clorambucil

WS - Walker-256 sensível à cisplatina e clorambucil

LISTA DE ABREVIATURAS: PRIMEIRO ARTIGO CIENTÍFICO

^{13}C NMR - Ressonância Magnética Nuclear de Carbono

^1H NMR - Ressonância Magnética Nuclear de Hidrogênio

ANOVA - Análise de Variância

ATCC – American Type Culture Collection

ATP - Adenosina Trifosfato

B16F10 - Célula de Melanoma de Murino

BSA - Albumina do Soro Bovino

DMEM HG - Meio Dulbecco's Modified Eagle alta glicose

DMSO - Dimetilsulfóxido

ERAD - Degradação de proteínas associadas à membrana do Retículo Endoplasmático

FBS - Soro Fetal Bovino

FCCP - Carbonil cianeto p-trifluormetoxifenilhidrazona

HEK293 - Célula Embriônica de Rim Humano

HeLa - Adenocarcinoma de Cérvix Humana

HEPES - Ácido 4- (2-hidroxietil) -1-piperazinoetanosulfônico

HepG2 – Linhagem celular de Carcinoma Hepatocellular

HK-II - Hexokinase II

HT116 – Célula de Carcinoma Coloretal

LDH - Lactato Desidrogenase

MEM – Meio Mínimo Essencial

MTT - 3-(4,5-dimetilazol-2il)-2,5-difeniltetrazólio

NDAmb234 - Célula de Adenocarcinoma de Mama Humano

p53^{-/-} - Proteína 53 com Gene Supressor de Tumor Inibido

p53^{+/+} - Proteína 53 com Gene Supressor de Tumor Presente

PBS - Solução de tampão fosfato

PFK-1 - 6-fosfofruto-1-quinase

Ru (II) - Átomo de Rutênio com valência 2⁺

Ru (III) - Átomo de Rutênio com valência 3⁺

RuC - Complexo de Rutênio (cis-[Ru(1,10-fenantrolina)₂(imidazol)₂]²⁺)

RuphenImH - Complexo de Rutênio (cis-[Ru(1,10-fenantrolina)₂(imidazol)₂]²⁺)
ou RuC

U87MG - Célula de Glioblastoma Humano

LISTA DE ABREVIATURAS: SEGUNDO ARTIGO CIENTÍFICO

ALT - Alanina aminotransferase

ANOVA - Análise de Variância

AST - Aspartato aminotransferase

Cat - Catalase

cDNA - Ácido desoxirribonucleico complementar

DMEM - Meio Dulbecco's Modified Eagle

DNA - Ácido desoxirribonucleico

DPPH - 2,2-difenil-1-picrilhidrazil

FCCP - Carbonil cianeto p-trifluormetoxifenilhidrazona

GSH - Glutathiona reduzida

GST - Glutathiona-S-transferase

H₂O₂ - Peróxido de Hidrogênio

HEPES - N-(2-hidroxietil) piperina N' (ácido 2-etano sulfônico)

HO[•] - Hidroxil

HO₂[•] - Superóxido protonado

i.p. - Administração por via intra peritoneal

IUPAC - União Internacional de Química Pura e Aplicada

KP1019 - ([Hind]-[trans-(RuCl₄[ind]₂), ind = indazole),

LPO - Peroxidação lipídica

NAMI-A - ([Him][trans-RuCl₄(DMSO)(im)], im = imidazole),

NO[•] - Óxido Nítrico

O₂^{•-} - Ânion superóxido

ONOO⁻ - Peróxido nítrico

p.o. - Administração por via oral

PBS – Solução de tampão fosfato

ROS - Espécies Reativa de Oxigênio

RPMI - Roswell Park Memorial Institute

Ru (II) - Átomo de Rutênio com valência 2⁺

Ru (III) - Átomo de Rutênio com valência 3⁺

RuC - Complexo de Rutênio (cis-[Ru(1,10-fenantrolina)₂(imidazol)₂]²⁺)

SOD - Superóxido dismutase

SUMÁRIO

1. REVISÃO LITERARIA

1.1. CÂNCER, UM BREVE PANORAMA.....	25
1.1.1. Carcinogênese.....	27
1.2. CARCINOMA HEPATOCELULAR (CHC).....	29
1.2.1. Diagnóstico e Tratamento do CHC.....	29
1.3. CÂNCER DE COLO DE ÚTERO.....	32
1.4. TUMOR DE WALKER-256.....	34
1.5. ALVOS E PROCESSOS DE MORTE CELULAR.....	36
1.5.1. Mecanismos de Morte Celular.....	37
1.5.2. Radicais Livres e Espécies Reativas.....	38
1.6. METABOLISMO DE CÉLULAS TUMORAIS.....	41
1.6.1. O Efeito Warburg.....	41
1.7. QUIMIOTERAPIA.....	43
1.7.1. Química Inorgânica Medicinal.....	43
1.7.2. Cisplatina.....	43
1.7.3. Complexo de Rutênio.....	45

2. OBJETIVOS

2.1. Objetivo Geral.....	48
2.2. Objetivos Específicos.....	48

3. PRIMEIRO ARTIGO CIENTÍFICO: **Antineoplastic activity of a ruthenium complex against human hepatocellular carcinoma (HepG2) and human cervix adenocarcinoma (HeLa) cells.**

3.1. ABSTRACT.....	49
3.2. INTRODUCTION.....	51
3.3. MATERIALS AND METHODS.....	52
3.3.1. Chemicals.....	52
3.3.2. Cell culture.....	53
3.3.3. Toxicity screening of the RuC.....	53
3.3.4. Cellular viability assays.....	54

3.3.4.1. MTT.....	54
3.3.4.2. Crystal violet.....	54
3.3.4.3. Neutral red.....	54
3.3.5. Cellular proliferation.....	55
3.3.6. Cellular respiration.....	55
3.3.7. Determination of lactate and pyruvate released by cultured cells.....	56
3.3.8. Proliferation recovery curve of HepG2 and HeLa cells.....	56
3.3.9. Protein determination.....	56
3.3.10. Statistical analysis.....	57
3.4. RESULTS.....	57
3.4.1. RuC toxicity screening in cell lines.....	57
3.4.2. RuC is toxic for HepG2 and HeLa cells.....	59
3.4.3. RuC affects HepG2 and HeLa proliferation.....	60
3.4.4. RuC affects the respiration of HepG2 and HeLa cells.....	61
3.4.5. RuC increases the levels of pyruvate and lactate.....	62
3.4.6. Recovery curve of HepG2 and HeLa cells.....	64
3.5. DISCUSSION.....	64
3.6. CONFLICT OF INTEREST.....	67
3.7. ACKNOWLEDGEMENTS.....	67
3.8. REFERENCES.....	68
 4. SEGUNDO ARTIGO CIENTÍFICO: Ruthenium complex exerts antineoplastic effects that are mediated by oxidative stress without inducing toxicity in Walker-256 tumor-bearing rats.	
4.1. ABSTRACT.....	76
4.2. INTRODUCTION.....	77
4.3. MATERIALS AND METHODS.....	79
4.3.1. Chemicals.....	79
4.3.2. Methods.....	80
4.3.2.1. Animal Handling and Ethical Issues.....	80
4.3.2.2. Handling and Inoculation of Walker-256 Tumor Cells...80	
4.3.2.3. Experimental Design and Sample Collection.....	81
4.3.2.4. Biophysical Measurements.....	81

4.3.2.5. Plasma Biochemistry and Hematological Assays.....	82
4.3.2.6. Tumor Gene Expression.....	83
4.3.2.7. In vitro Free Radical-Scavenging Activity of RuC.....	84
4.3.2.8. <i>In vivo</i> Oxidative Stress Parameter Assays.....	84
4.3.2.8.1. Lipid peroxidation rate.....	84
4.3.2.8.2. Catalase, superoxide dismutase, and glutathione-S-transferase activity.....	85
4.3.2.8.3. Reduced glutathione levels.....	85
4.3.2.9. Quantification of Tissue Proteins.....	86
4.3.2.10. Tumor and Organ Histology.....	86
4.3.2.11. Oxygen Uptake of Walker-256 Ascitic Cells.....	87
4.3.2.12. Statistical Analysis.....	88
4.4. RESULTS.....	88
4.4.1. Biophysical Parameters.....	88
4.4.2. Plasma Biochemistry and Hematology.....	90
4.4.3. Tumor Gene Expression.....	92
4.4.4. In vitro Free Radical-Scavenging Activity.....	93
4.4.5. <i>In vivo</i> Oxidative Stress Parameters.....	95
4.4.6. Walker-256 Tumor Histology.....	95
4.4.7. Walker-256 Cell Respiration.....	96
4.4.8. Toxicity Parameters in Healthy Rats.....	98
4.5. DISCUSSION.....	99
4.6. CONFLICT OF INTEREST.....	104
4.7. ACKNOWLEDGEMENTS.....	104
4.8. AUTHOR CONTRIBUTIONS.....	104
4.9. REFERENCES.....	105
4.10. SUPPLEMENTARY FIGURE.....	111
5. CONSIDERAÇÕES FINAIS.....	112
6. REFERÊNCIAS BIBLIOGRÁFICAS.....	114

1. INTRODUÇÃO

1.1. CÂNCER, UM BREVE PANORAMA

A terminologia “câncer” é originária do latim e tem como significado a palavra caranguejo, fazendo menção à característica infiltrativa das patas deste crustáceo e relacionando-a ao potencial caráter evolutivo da doença (CROCE *et al.*, 2008). Outras terminologias também são comumente utilizadas para a designação da doença, como “processo polimitótico” fazendo referência ao crescimento expressivo das lesões; e ainda “neoplasia” (neo = novo e plasia = tecido), sendo diferenciada entre benigna e maligna, determinando desta forma, a característica biológica das lesões (KUMAR *et al.*, 2010; CHABNER, 2012).

Os cânceres abrangem mais de 100 tipos de doenças diferentes que são determinadas pela invasão de células a órgãos e tecidos através de seu crescimento desordenado (INCA, 2016). Com maior rigor é possível afirmar que as neoplasias malignas se caracterizam por uma proliferação anormal e desordenada de um determinado tecido, que passa a agir de forma autônoma e anárquica; portanto, sem controle pelo organismo hospedeiro. Tal autonomia celular se deve, basicamente, às alterações genéticas encontradas em tais células. O poder de invadir os tecidos vizinhos, assim como migrar pelo organismo provocando metástases, são os grandes responsáveis por levar o paciente ao óbito (CHABNER, 2012).

Em relação à evolução da doença, o câncer pode ser classificado em não invasivo ou carcinoma *in situ* e câncer invasivo. O câncer não invasivo caracteriza-se por ser o 1º estágio de classificação da doença, com exceção apenas dos cânceres do sistema sanguíneo. Nesta fase o câncer ainda se encontra somente no tecido de origem, não tendo se espalhado para outras camadas. A importância do diagnóstico precoce é fundamental, pois a maioria dos cânceres neste estágio é passível de cura. Já o câncer invasivo tem a potencialidade de se disseminar para outras partes do organismo humano, levando ao aparecimento da doença a outras áreas distintas do local de origem (INCA, 2016).

Durante muitos séculos o câncer foi uma doença própria dos países desenvolvidos. Entretanto, nas últimas décadas ele vem atingindo de forma

avassaladora tanto as grandes potências quanto os países em desenvolvimento. Por este motivo, o câncer tem se apresentado como um relevante problema de saúde pública em nível mundial (INCA, 2016). Dados da Organização Mundial da Saúde (OMS) estimam para 2030, 27 milhões de casos novos de câncer, sendo que destes, 17 milhões chegarão a óbito e 75 milhões de pessoas viverão com a doença. Chama-se atenção ao fato de que o grande impacto causado por esta doença incidirá fortemente nos países em desenvolvimento (INCA, 2016). Esta realidade indica que os países com menos recursos deverão arcar em grande parte com o elevado ônus decorrente da doença. Torna-se, portanto, fundamental que os serviços de saúde estejam preparados e organizados para intervir nesta realidade através de ações de educação e promoção da saúde, prevenção de agravos e garantia de diagnóstico precoce, tratamento e reabilitação.

Vale ressaltar que o nível de desenvolvimento socioeconômico de um país mantém estreita relação com os tipos de câncer mais incidentes na população. Neste sentido, os cânceres que derivam de um alto status socioeconômico são os de mama, próstata, cólon e reto, e os que estão associados à pobreza são os de estômago, pênis, cavidade oral e colo de útero (GUERRA; GALLO; MENDONÇA, 2005). Dados recentes divulgados em relação aos tipos mais incidentes de câncer incluem no rol dos cânceres derivados de alto status socioeconômico o de pulmão, e no caso dos cânceres associados à pobreza, insere-se o câncer de fígado (INCA, 2016).

Em relação ao sexo, com exceção do câncer de pele não melanoma, os cânceres mais frequentes no sexo masculino são os cânceres de próstata, pulmão, cólon e reto, estômago, fígado e cavidade oral, enquanto que na população feminina são os cânceres de mama, cólon e reto, colo do útero, pulmão e glândula tireoide (INCA, 2016).

Considerando que o câncer do colo do útero é o quarto tipo de câncer mais incidente na população feminina (INCA, 2016), o presente trabalho se propôs a estudar, dentre outros modelos, células neoplásicas HeLa, que são derivadas de câncer de colo uterino. Ainda, células HepG2, derivadas de hepatocarcinoma, também serviram de ferramentas de investigação neste trabalho.

1.1.1 Carcinogênese

As células tumorais originam-se de células normais que sofreram alterações no DNA (fatores genéticos) ou em mecanismos que controlam a expressão gênica (fenômenos epigenéticos) em um ou mais locos envolvidos no controle da divisão e na diferenciação celular (HANAHAHAN *et al.*, 2011). A transformação dessas células, decorrente de uma lesão genética não-letal (mutação) pode ser herdada na linhagem germinativa, ou surgir de modo espontâneo, assim como pode ser causada por agentes ambientais, como substâncias químicas, radiação ou vírus (HEIDI *et al.*, 2009; KUMAR *et al.*, 2010). As etapas da carcinogênese são: (1) Iniciação (ou transformação celular) – lesão permanente (mutação) no DNA da célula por exposição aos agentes carcinogênicos físicos, químicos ou biológicos. Esta etapa refere-se a uma mudança no fenótipo de uma célula com controle normal de seu desenvolvimento em outra com crescimento descontrolado, que se torna menos responsiva a fatores que inibem a proliferação celular, a indutores de diferenciação celular ou à apoptose; (2) Promoção – a célula iniciada é estimulada a proliferar, amplificando o clone transformado; e (3) Progressão – o clone transformado prolifera e múltiplas mutações se acumulam, gerando subclones com habilidades variadas de crescimento, invasão, metástase e resistência, tornando o tumor mais agressivo e com maior potencial maligno (HEIDI *et al.*, 2009; KUMAR *et al.*, 2010).

A proliferação autônoma, a senescência replicativa e a insensibilidade a sinais que inibem mitose e a evasão da apoptose, conferem às células neoplásicas a propriedade de imortalidade, possibilitando sua multiplicação excessiva e descontrolada. A autonomia nos sinais de proliferação que essas células neoplásicas adquirem, é resultante de mutações ativadoras de oncogenes, que são os genes que promovem o crescimento celular na ausência de sinais promotores de crescimento. Essas mutações são frequentes em genes de fatores de crescimento (p. ex., PDGF), de seus receptores (p. ex., EGFR no carcinoma de mama), de moléculas transdutoras de sinal (p. ex., RAS) e de amplificação em genes que acionam o ciclo celular (p. ex., ciclina D1). A insensibilidade aos sinais inibidores de mitose decorre de: mutação inativadora em genes que codificam moléculas reguladoras da via MAPK (p. ex., PTEN, que desfosforila moléculas nessa via), de fatores de transcrição

ativadores de genes que controlam o ciclo celular (p. ex., pRB, inativador natural de E2F, que ativa a entrada em G1), além de mutação inativadora no gene p53, que inativa o complexo ciclina/CDK. A evasão da apoptose resulta da inibição de genes pró-apoptóticos, de hiperexpressão de genes antiapoptóticos ou de inativação do gene p53, que promove interrupção do ciclo celular por lesão no DNA e induz a apoptose. As células tumorais apresentam ainda a capacidade de evasão de senescência replicativa, que ocorre por meio da ativação de telomerase, permitindo a duplicação do DNA. No decorrer dessas alterações o genoma torna-se instável, como resultado do estresse oxidativo durante a duplicação do DNA. Essa instabilidade persistente facilita alterações na regulação genética e epigenética associada à progressão maligna (BOGLIOLO; BRASILEIRO, 2011). No decorrer desse intenso processo de proliferação e formação de um tumor, as células malignas, assim como as células normais, necessitam de um suprimento sanguíneo para receber nutrientes e oxigênio e para remover produtos de excreção. Portanto, há uma expressiva indução da formação de novos vasos sanguíneos, por processo angiogênico. As células tumorais promovem um aumento na atividade angiogênica por meio da liberação de fatores como o VEGF (fator de crescimento vascular endotelial). A angiogênese apresenta uma correlação com a malignidade tumoral, já que é requerida não somente para o crescimento celular, mas também para o acesso à vasculatura e posterior formação de metástases. Assim, quanto maior essa atividade, maior é a potência de metastatização do câncer e mais rápida é a sua progressão. Adicionalmente, sabe-se que a modificação na expressão de moléculas de adesão (perda de caderina E) e ativação de genes que favorecem a produção de metaloproteinases, em conjunto com a angiogênese, aumentam a capacidade das células tumorais malignas de invadir tecidos e originar metástases, uma das principais causas de morbidade e mortalidade relacionadas ao câncer (KUMAR *et al.*, 2010; BOGLIOLO; BRASILEIRO, 2011; HANAHAN; WEINBERG, 2011). Frente a este panorama, modelos de estudo que simulam estas condições são aplicados para entender as neoplasias e seus tratamentos.

1.2. CARCINOMA HEPATOCELULAR (CHC)

O carcinoma hepatocelular humano (CHC) é o tipo de câncer mais frequente no fígado e corresponde a 60-70% dos tumores primários originários deste órgão (HATZARAS *et al.*, 2016). São observadas mais de 600 mil mortes por ano decorrentes desta doença (CHENG *et al.*, 2014; LEE *et al.*, 2014; WOO; HEO, 2015) e são estimados cerca de 700 mil novos casos de CHC anualmente (CHENG *et al.*, 2014), tornando-o o sexto tipo de câncer mais prevalente no mundo (LEE *et al.*, 2014; WOO *et al.*, 2016). Quanto ao sexo, o CHC é o quinto tipo de tumor prevalente em homens e o sétimo em mulheres (EL-SERAG, 2011).

Dentre os principais fatores de risco para o desenvolvimento de CHC estão: as infecções por (i) vírus da hepatite B (VHB) e (ii) vírus da hepatite C (VHC), (iii) doenças alcoólicas do fígado, e (iv) esteatose hepática alcoólica e esteatose hepática não alcoólica. A distribuição mundial destes fatores de risco é variável e depende principalmente da região geográfica e etnia (EL-SERAG, 2007). Aproximadamente 50% dos casos de CHC são provenientes de infecção com VHB, chegando a 90% em regiões endêmicas, como Ásia e África. O risco de desenvolver CHC em pessoas infectadas por VHB pode ainda aumentar quando expostas a aflatoxina, tabaco, álcool ou ainda co-infectadas com VHC (EL-SERAG, 2011).

Portadores do VHC apresentam risco 15 a 20 vezes maior de desenvolver CHC, quando comparados a pessoas não infectadas (DONATO *et al.*, 2002). Entretanto, alguns estudos em países do ocidente mostraram que entre 30 a 40% dos pacientes com CHC não apresentavam infecção com VHB e VHC, sugerindo outros fatores envolvidos, como obesidade e diabetes tipo 2 (EL-SERAG, 2011). Alguns avanços têm sido feitos para prevenção da doença, pois desde que os programas de vacinação contra a hepatite B começaram há mais de 20 anos, a incidência de CHC em crianças de 6 a 12 anos diminuiu em aproximadamente 70% (ZANETTI *et al.*, 2008).

1.2.1. Diagnóstico e Tratamento do CHC

Os tratamentos considerados eficazes são recomendados para os estágios iniciais do CHC (CHENG *et al.*, 2014; KIM, 2016), no entanto apenas 20-30% dos diagnósticos são realizados nesta fase (BUPATHI *et al.*, 2015), o

que leva a um prognóstico desfavorável (CHENG *et al.*, 2014; KIM, 2016). Existem muito fatores que devem ser considerados para a escolha da terapêutica, como o tamanho e localização tumoral, relação tumor/estruturas próximas, número de lesões, presença de invasão vascular e doenças hepáticas e extra-hepáticas existentes (HATZARAS *et al.*, 2014). Em alguns casos, o diagnóstico de CHC pode ser feito através de métodos não invasivos (uso de imagens), mas o recomendado é o uso de imagens somado à biópsia de fígado (EL-SERAG, 2011).

Geralmente a ressecção cirúrgica é o tratamento padrão para pacientes com CHC em estágios iniciais da doença com a função hepática preservada (CHENG *et al.*, 2014; TABRIZIAN *et al.*, 2014), proporcionando uma taxa de sobrevivência em cinco anos de 42-62% (HATZARAS *et al.*, 2014), ou até 70% quando não há fatores de risco associados, como pressão portal e/ou bilirrubina aumentada (TABRIZIAN *et al.*, 2014). Altos casos de reincidências de aparecimento do tumor são observados após a ressecção cirúrgica, acometendo em média 70% dos pacientes cinco anos após o procedimento (CHENG *et al.*, 2014; FITZMORRIS; SINGAL, 2015).

O transplante de fígado é o tratamento de primeira escolha para pacientes com pequenos tumores multinodulares (≤ 3 nódulos com área ≤ 3 cm²) ou tumores únicos (≤ 5 cm²) e disfunção hepática avançada (EASL-EORTC, 2012). Além destas, outras condições devem estar presentes para que possa ocorrer o transplante, como níveis reduzidos de invasão vascular e ausência de doenças extra-hepáticas (HATZARAS *et al.*, 2014). A principal desvantagem relacionada ao transplante, além da indução da imunossupressão enquanto o paciente estiver com o órgão doado, é o grande tempo de espera para um doador (ATTWA; EL-ETREBY, 2015; FITZMORRIS; SINGAL, 2015).

A ablação local é considerada a primeira linha de escolha para pacientes em estágios iniciais do CHC quando os mesmos não são elegíveis para terapias cirúrgicas (EASL-EORTC, 2012; HATZARAS *et al.*, 2014). Nesta terapia, são realizadas injeções locais de substâncias químicas ou modificações na temperatura do microambiente tumoral, induzindo a necrose tumoral com efeitos reduzidos sobre o parênquima hepático (MÉNDEZ-SÁNCHEZ *et al.*, 2014). Entretanto, as altas taxas de remissão representam

um fator limitante na utilização destes tratamentos (KHAN *et al.*, 2000), podendo alcançar até 34% de retorno da proliferação tumoral em dois anos após o procedimento em pacientes que apresentaram tumores menores 3 cm² (KHAN *et al.*, 2000).

A quimioembolização transarterial (QET) é um tratamento bem estabelecido para pacientes em estágios intermediários do CHC (TABRIZIAN *et al.*, 2014), sendo utilizado em casos de tumores múltiplos e grandes (≥ 5 cm²), incluindo pacientes com função hepática moderada (MURATA *et al.*, 2014; ATTWA, 2015). A ação antitumoral da QET baseia-se na aplicação local de um agente citotóxico seguido por indução de isquemia através de embolização dos vasos sanguíneos responsáveis pelo suprimento tumoral (MÉNDEZ-SÁNCHEZ *et al.*, 2014). Para pacientes com estágios avançados de CHC ou tumores reincidentes após terapias loco-regionais e com função hepática bem preservada, a quimioterapia sistêmica é o tratamento mais indicado (EASL-EORTC, 2012). Em geral, esta abordagem é bastante limitada devido à capacidade de retorno do tumor (ATTWA; EI-ETREBY, 2015), decorrente principalmente da expressão aumentada ou mutações de proteínas promotoras de resistência, como p53, glutathione-S-transferase e glicoproteína P (AKIMOTO *et al.*, 2006). Além disso, outro fator que dificulta o tratamento é a baixa seletividade de determinados compostos para as células tumorais, e a consequente toxicidade em hepatócitos saudáveis. Estes são fatores que frequentemente determinam a interrupção do tratamento devido à perda da função hepática (ATTWA; EI-ETREBY, 2015).

O primeiro quimioterápico que foi capaz de aumentar as taxas de sobrevivência em pacientes com CHC em estágio avançado foi o sorafenibe (ALVES *et al.*, 2011), o único medicamento aprovado pela *Food and Drug Administration* (FDA) desde 2007 para este tipo de câncer (EASL-EORTC, 2012; BUPATHI *et al.*, 2015). Seu efeito antitumoral deve-se à ação inibitória sobre algumas quinases responsáveis pela sinalização da proliferação celular e angiogênese (ALVES *et al.*, 2011). Estima-se que o uso de sorafenibe diminua em 31% a chance de morte associada ao CHC em estágio avançado, aumentando a sobrevida dos pacientes em 2 a 3 meses (LLOVET *et al.*, 2008; CHENG *et al.*, 2009).

Devido ao modesto benefício clínico e baixa eficácia obtidos com as terapias sistêmicas atuais para CHC (BUPATHI *et al.*, 2015), é essencial encontrar novas drogas com maior eficácia terapêutica e/ou novos alvos que atuem de maneira seletiva sobre as células tumorais (WRZESINSKI *et al.*, 2011; ALVES *et al.*, 2011).

1.3. CANCER DE COLO DE ÚTERO

Dentre os cânceres mais incidentes na população feminina, com aproximadamente 530 mil casos novos por ano no mundo, o câncer do colo do útero é o quarto tipo de câncer mais comum entre as mulheres, excetuando-se os casos de câncer de pele não-melanoma. Este tipo é responsável por 265 mil óbitos por ano, sendo a quarta causa mais frequente de morte por câncer em mulheres, representando de 10 a 15% dos casos mundiais (INCA, 2016).

O câncer do colo do útero é uma enfermidade de fácil diagnóstico, de evolução lenta e com fases pré-clínicas que podem ser detectadas, tratadas e curadas. Com a detecção precoce é possível que quase 100% dos casos sejam prevenidos e curados (WHO, 2017). Este tipo de câncer mantém extrema relação com a pobreza, sendo 80% de seus casos e mortes provenientes dos países em desenvolvimento (ALBUQUERQUE *et al.*, 2009). Nestes países, identifica-se baixo índice de desenvolvimento humano, ausência ou fragilidade de ações de promoção da saúde e prevenção de agravos e dificuldades no acesso aos serviços de diagnóstico precoce e tratamento dos casos diagnosticados. A incidência no Brasil em 2016 foi de 16.340 casos de câncer do colo do útero, apresentando um risco estimado de 15,85 casos a cada 100 mil mulheres (INCA, 2016).

Em relação à sobrevida por este tipo de câncer, estima-se que a sobrevida média em 5 (cinco) anos para os países em desenvolvimento seja de 49%, enquanto que nos países desenvolvidos essa estimativa gira em torno de 59 a 69% (INCA, 2016). Estas variações são atribuídas pelas diferenças entre o tempo de desenvolvimento da doença quando diagnosticada e início de tratamento, como também, pela eficácia e diferenças na oferta de diagnóstico e tratamento entre os países (ALBUQUERQUE *et al.*, 2009).

O principal fator de risco para o desenvolvimento do câncer do colo do útero é a infecção pelo papiloma vírus humano – HPV (INCA, 2016), sendo que

95% dos casos de câncer do colo do útero são devidos a esta infecção (WHO, 2017). A associação entre o desenvolvimento do câncer do colo do útero e a infecção pelo HPV é tão intensa que esta correlação apresenta maiores riscos quando comparada ao hábito do tabagismo e a possibilidade de desenvolvimento do câncer de pulmão (RIBEIRO, 2008). Entre os mais de 100 tipos de HPV existentes, em torno de 13 tipos podem levar a infecções persistentes, bem como a lesões precursoras do câncer do colo do útero. Assim, estes tipos de HPV são considerados como oncogênicos (BRASIL, 2016). Outros fatores de risco também se tornam importantes para o surgimento do câncer do colo do útero, tais como: início precoce das atividades sexuais, multiplicidade de parceiros sexuais, tabagismo, baixa condição socioeconômica, imunossupressão, uso prolongado de contraceptivos orais, higiene íntima inadequada, multiparidade e história familiar (BRASIL, 2014, 2006d; RIBEIRO, 2008).

O câncer do colo do útero tem uma evolução lenta, uma vez que o seu desenvolvimento ocorre num período de 10 a 20 anos. Suas chances de cura são de quase 100% se detectado e tratado precocemente (BRASIL, 2011c). Vidal (2009) afirma que o desenvolvimento do câncer de colo de útero se dá de maneira progressiva, iniciando com lesões leves displásicas que evoluem para severas, e depois para carcinoma, e se não tratadas, para o câncer invasivo cervical escamoso. As lesões pré- invasivas são chamadas de Neoplasias Intraepiteliais Cervicais (NIC), que são classificadas em graus I, II e III, os quais refletem o seu comportamento biológico (INCA, 2016).

Nos estágios iniciais de anormalidades na diferenciação, as células de displasias, localizadas na superfície do epitélio, podem ser detectadas através da técnica do exame de Papanicolaou. Caso não haja intervenção, a displasia poderá estagnar ou mesmo regredir espontaneamente; entretanto, pode progredir dando origem à neoplasia localizada sem invasão dos tecidos adjacentes, o chamado carcinoma *in situ*. Neste estágio, ainda é fácil alcançar a cura completa pela destruição ou remoção cirúrgica do tecido anormal, pois as células alteradas ainda estão confinadas ao lado epitelial da lâmina basal. Porém, sem o tratamento adequado, as células displásicas ainda poderão estagnar ou regredir; mas cerca de 20% a 30% dos casos evoluirão num período de alguns anos, originando um carcinoma cervical invasor, cujas

células desprendem-se do epitélio, atravessam a lâmina basal e começam a invadir o tecido conectivo, e à medida que o crescimento invasivo se espalha, a cura passa a ser progressivamente mais difícil (LORENZATO, 2008).

Assim, os programas de rastreamento constituem uma importante estratégia dos serviços de saúde para a diminuição da incidência e mortalidade desta neoplasia, uma vez que permitem a identificação de lesões precursoras da doença vários anos antes da instalação do seu processo invasor (LORENZATO, 2008; SANKARANARAYANAN et al., 2008). Uma vez que a prevenção não foi possível, o tratamento farmacológico é feito com a cisplatina, carboplatina, doxorubicina, 5-fluoracil, bleomicina, hidroxiuréia e mitomicina, medicamentos utilizados em protocolos de alguns centros de quimioterapia ou como protocolos de pesquisa (POTTER et al., 2010). No INCA e na rede conveniada do SUS, os antineoplásicos de primeira linha são a cisplatina e carboplatina (INCA, 2016).

1.4. TUMOR WALKER-256

A indução de câncer em animais e o cultivo de células tumorais são abordagens importantes para investigar a dinâmica tumoral, bem como as alterações causadas no organismo portador de tumor. O tumor Walker-256 em ratos é geralmente utilizado em pesquisas experimentais de câncer por possuir baixa ocorrência de regressão tumoral, ser facilmente transplantado e ser espécie-específico para ratos (FISHER; FISHER, 1961).

O tumor Walker-256 se desenvolveu espontaneamente na região mamária de uma rata prenha albina em torno de dez meses de idade, em 1928, no Laboratório de George Walker, na *Johns Hopkins University School of Medicine*. O tumor observado por Walker exibia uma estrutura tumoral definida como adenocarcinoma (tecido glandular), por isso a sua origem mamária foi altamente suspeitada (FISHER & FISHER, 1961; AGOSTINO; CLIFFTON, 1968). A massa tumoral tinha o tamanho de uma noz, composta de um tecido granular firme com pequenos pontos de necrose, sem a presença de metástase. Seccionado, o tumor se apresentava com uma área central semi-sólida de cor branca amarelada, com material necrótico, circundado por uma zona firme de coloração branco brilhante. Em 1956, as células Walker-256 da massa tumoral foram transferidas para a forma ascítica, na qual podem ser

mantidas por passagens intraperitoneais sucessivas, sendo esta, uma variação do carcinoma (AGOSTINO & CLIFFTON, 1968).

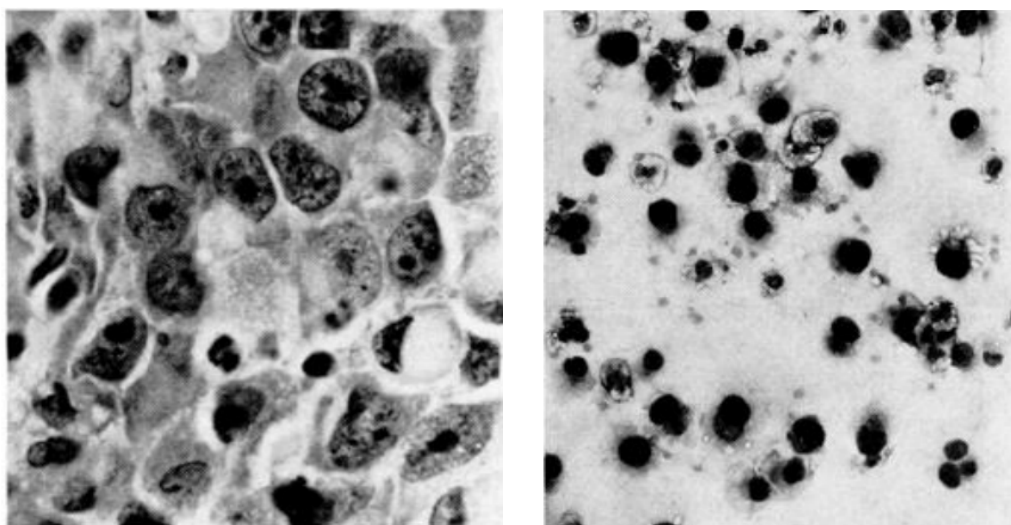


FIGURA 1. (A) Imagem de microscopia de luz da forma sólida do tumor Walker256 transplantada em ratos. (B) Imagem de microscopia de luz do fluido peritoneal de um rato portador de tumor ascítico Walker-256. FONTE: AGOSTINO & CLIFFTON (1968).

Estudos em microscopia eletrônica e de transmissão indicaram que as células de tumor Walker-256 de origem ascítica e sólida apresentam diferenças morfológicas (Fig. 1). As células de fluido ascítico apresentam uma população heterogênea, porém quando estas células são cultivadas em suspensão, um único tipo celular é predominante. A eficiência de induzir a formação de tumores sólidos a partir de células ascíticas é mais alta do que utilizar células provenientes de tumor sólido. As células provenientes do líquido ascítico são mais tumorigênicas do que quando são cultivadas em suspensão, sendo que mudanças nos antígenos de superfície dessas células provavelmente sejam responsáveis pela redução da tumorigenicidade primária (ARVELO *et al.*, 1984).

As células Walker-256 apresentam linhagens diferentes, denominadas como sensíveis (WS) e resistentes (WR) à cisplatina e clorambucil (SIMPIKINS *et al.*, 1991), além de duas variantes, denominadas como metastizante (A) e não metastizante (B) (GUAITANI *et al.*, 1983). Algumas vias de inoculação podem ser utilizadas para administração das células Walker-256, como: subcutânea, intramuscular, intraperitoneal, intracardíaca, arterial, venosa e em

tecido ósseo. Na inoculação subcutânea ocorre o desenvolvimento de tumores sólidos, firmes à palpação, encapsulados, podendo ocorrer infiltração da pele e da musculatura adjacente (GUIMARAES *et al.*, 2010). Devido à massa tumoral formada, o Walker-256 vem sendo utilizado como modelo para estudar o potencial antineoplásico de compostos naturais (MARTINS *et al.*, 2015; DREIFUSS *et al.*, 2013; STIPP *et al.*, 2017) e sintéticos (BASTOS-PEREIRA, 2009; GALUPPO *et al.*, 2016) por nosso grupo de pesquisa.

Este tumor é considerado um bom modelo para estudos envolvendo anorexia associada a câncer, pois induz significativas modificações orgânicas, representadas por alterações enzimáticas, imunológicas, inflamatórias e oxidativas. Portanto, o tumor Walker-256 é adequado para estudos farmacológicos, bioquímicos e patológicos relacionados a tumores sólidos (ACCO, BASTOS-PEREIRA, DREIFUSS, 2012).

1.5. ALVOS E PROCESSOS DE MORTE CELULAR

A distinção entre uma célula neoplásica e uma célula sadia, além das alterações morfológicas e metabólicas, é a sua proliferação descontrolada, possíveis alterações de função e um alto poder invasivo, podendo levar à metástase.

A perda do controle do ciclo celular é um dos eventos responsáveis pelo aparecimento de células tumorais. Estas células podem ser modificadas como consequência de uma alteração da função das ciclinas/CDKs, superexpressão de oncogenes, anormalidade na função de fatores de crescimento e devido a mutações dos genes supressores tumorais. Um dos principais supressores tumorais é a proteína p53, também chamada de “guardiã do genoma”. O supressor de tumor p53 tem uma importante função na resposta celular a diferentes sinais de estresse, como danos ao DNA, hipóxia ou ativação de oncogenes. Uma vez que um dano ao DNA é detectado, a proteína p53 é a responsável por promover uma parada no ciclo celular até que o reparo do dano esteja completo. Caso isso não ocorra, p53 desencadeia uma via de sinalização intracelular promotora de morte, geralmente a via apoptótica, para que esse dano ao DNA não seja conservado durante o processo de replicação celular (VOUSDEN *et al.*, 2006).

1.5.1 Mecanismos de Morte Celular

Uma das primeiras classificações para diferenciar os tipos de morte celular foi proposta por Schweichel e Merker que estabeleceram três classes: tipo I (ou heterofagia), tipo II (autofagia) e tipo III (morte celular sem digestão), sendo estes processos atualmente nomeados como apoptose, autofagia e necrose (SCHWEICH; MERKER, 1973; GALLUZZI *et al.*, 2012).

A morte celular por apoptose, por sua vez, pode ocorrer pelas denominadas vias extrínseca e intrínseca. A via extrínseca é desencadeada por sinais extracelulares, os quais sensibilizam receptores específicos na membrana plasmática que são responsáveis por propagar os sinais de morte. Os principais ligantes envolvidos na iniciação destes sinais através de receptores de morte são: Fas-L (ligante de Fas), TNF- α (fator de necrose tumoral α) e TRAIL (ligante indutor de apoptose relacionado ao TNF) (CIRCU; AW, 2010). Já a intrínseca pode ser desencadeada por danos ao DNA, estresse oxidativo, acúmulo de Ca^{2+} no citosol, aumento de proteínas mal enoveladas no retículo endoplasmático, entre outros fatores. Esta via se caracteriza pela participação direta das mitocôndrias e devido a isto muitos autores a denominam de via mitocondrial (INDRAN *et al.*, 2011). Alterações na permeabilidade mitocondrial são acompanhadas de: (i) dissipação do potencial de membrana mitocondrial ($\Delta\Psi$), (ii) liberação de proteínas mitocondriais para o citosol, como é o caso do citocromo c e fator indutor de apoptose (AIF), entre outras, e (iii) inibição da cadeia respiratória, agravando e amplificando os sinais de morte celular (KROEMER *et al.*, 2007). Em alguns casos de apoptose pela via intrínseca, observa-se a dependência do envolvimento de caspases, já em outros casos se observa eventos semelhantes aos citados acima, porém sem o envolvimento de caspases (GALLUZZI *et al.*, 2012).

A morte celular por necrose foi descrita, por muito tempo, como uma via de morte celular causada por situações extremas, sendo caracterizada como acidental e sem o envolvimento de sinalização ou vias de regulação, como ocorre na apoptose ou autofagia (KROEMER *et al.*, 2009). Esse conceito mudou e atualmente sabe-se que a necrose pode ocorrer de maneira regulada, sendo induzida por diferentes fatores, como por exemplo, danos ao DNA. O termo *necroptose* também vem sendo utilizado para descrever a via necrótica

regulada, a qual na maioria dos casos envolve a proteína quinase de interação ao receptor (RIP)-1 e/ou seu homólogo RIP-3 (GALLUZZI *et al.*, 2012).

Em relação à autofagia, embora o termo originalmente não caracterize um tipo de morte celular propriamente dito, esse conceito se modificou com base em diferentes estudos, como a observação (*in vivo*) de que este processo pode mediar a morte celular em certos organismos, como *Drosophila melanogaster* (NEZIS *et al.*, 2010). Também foram identificados marcadores bioquímicos que caracterizam a via (ex: AMBRA1, ATG5, ATG12 e Beclina 1), inibidores farmacológicos como a cloroquina, um antimalárico que inibe a formação do autolisofagossomo e, ainda, os indutores de autofagia, como a rapamicina (GALLUZZI *et al.*, 2012).

1.5.2 Radicais Livres e Espécies Reativas

Os radicais livres podem ser definidos como moléculas ou fragmentos moleculares contendo um ou mais elétrons desemparelhados. A presença de elétrons desemparelhados geralmente confere um considerável grau de reatividade aos radicais livres.

Dentre estas espécies podemos citar espécies radicalares derivadas do oxigênio, como o ânion radical superóxido ($O_2^{\bullet-}$), radical perhidroxila (HOO^{\bullet}), radical hidroxila (HO^{\bullet}), radical alcóxila (RO^{\bullet}), radical peróxila (ROO^{\bullet}) e radical ânion carbonato ($CO_3^{\bullet-}$); e também espécies não radicalares como o peróxido de hidrogênio (H_2O_2), ácido hipocloroso ($HOCl$), oxigênio singlete (1O_2) hidroperóxidos orgânicos ($ROOH$) e ozônio (O_3) (HALLIWELL; GUTTERIDGE, 2007). A Figura 2 ilustra a sobreposição das vias de geração destas espécies reativas (ER).

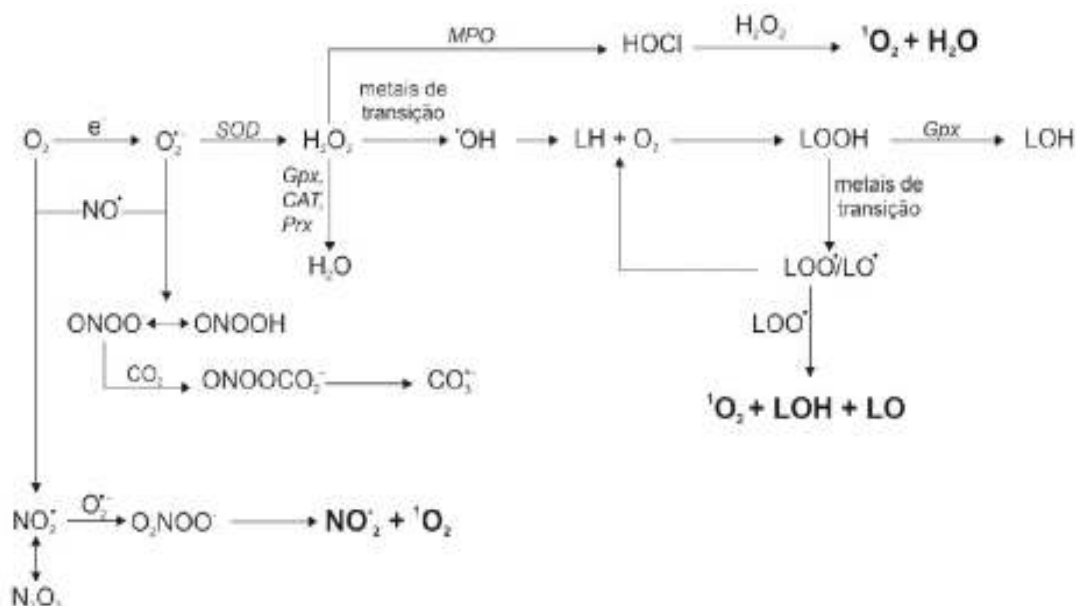


FIGURA 2. Principais vias de formação de espécies reativas de oxigênio/nitrogênio. SOD - superóxido dismutase; MPO - mieloperoxidase; CAT - catalase; GPX glutathiona peroxidase; LH – lipídios; LO - radical alcoxila; LOO - radical peroxila; LOH – álcool lipídico; $ONOOCO_2^{\bullet}$ - radical peroximonocarbonato; $HOCl$ - ácido hipocloroso e H_2O_2 - peróxido de hidrogênio.

Espécies reativas podem ser produzidas a partir de fontes endógenas e exógenas. Potenciais fontes endógenas incluem as mitocôndrias, a via metabólica do citocromo P450, peroxissomos, e ativação de células inflamatórias (VALKO *et al.*, 2006). Uma das principais fontes de espécies reativas é a cadeia de transporte de elétrons mitocondrial, pois durante a transferência de elétrons pelos complexos da cadeia respiratória, formas parcialmente reduzida de O_2 podem ser geradas. Acredita-se que cerca de 1-5% dos elétrons direcionados à cadeia de transporte sejam “perdidos” diretamente para o oxigênio (HALLIWELL *et al.*, 2007).

Espécies reativas são formadas constantemente em sistemas biológicos, para isso, os organismos desenvolveram defesas antioxidantes de forma a proteger-se dos possíveis danos causados por essas espécies. Por definição, pode ser denominado antioxidante qualquer molécula que inibe ou minimiza um processo de oxidação. Do ponto de vista biológico, um antioxidante protege biomoléculas ou estruturas celulares contra os efeitos deletérios de substâncias que promovem a oxidação (HALLIWELL; GUTTERIDGE, 2007).

Em condições fisiológicas normais existe um balanço extremamente controlado entre moléculas pró e antioxidantes. As principais fontes endógenas de EROs como radical superóxido, oxigênio singlete, peróxido de hidrogênio e radicais hidroxila são provenientes de alguns processos do metabolismo celular, como fosforilação oxidativa, reações catalisadas pelo sistema do citocromo P450, peroxissomos, NADPH oxidase, mieloperoxidase, xantina oxidase e inflamação (KUO, 2017). O controle da homeostase do estado redox celular é realizado principalmente por glutathione (GSH) e uma série de enzimas antioxidantes tais como: superóxido dismutase (SOD), catalase, glutathione redutase, glutathione peroxidase (GPx), tioredoxina (Trx), entre outras (LAU *et al.*, 2016). Apesar de vários sistemas de defesa estarem envolvidos na manutenção do estado redox celular, em algumas situações não são suficientes para deixá-lo em equilíbrio, sendo observado um quadro de estresse oxidativo, o qual pode trazer várias consequências para o organismo (LAU *et al.*, 2016).

Em geral podemos dizer que baixos níveis de EROs podem promover proliferação celular, já em níveis intermediários podem causar uma transiente ou uma permanente parada de ciclo celular, ou senescência (MARTINDALE; HOLBROOK, 2002). Em altos níveis de EROs ocorre a indução de morte celular por diferentes mecanismos (MARTINDALE; HOLBROOK, 2002). Mesmo que EROs apresentem um papel importante nos processos de morte celular via receptor de morte (WOO *et al.*, 2017) ou necroptose (SAINI *et al.*, 2017), o mecanismo apoptótico via mitocondrial é mais suscetível aos níveis de EROs (LAU *et al.*, 2016).

Foi descrito que EROs estão envolvidas na ativação de oncogenes, podendo levar à progressão tumoral e indução do processo de metástase de células tumorais (SAINI *et al.*, 2017), visto que existe uma correlação entre um elevado nível de EROs em células tumorais comparado à células normais (GLASAUER & CHANDEL, 2014; WOO *et al.*, 2017). Entretanto, EROs também estão envolvidas na indução de morte em células tumorais em abordagens terapêuticas que geram estresse oxidativo, como por exemplo: quimioterapia, radioterapia e terapia fotodinâmica (GLASAUER; CHANDEL, 2014). Devido aos diferentes papéis desempenhados por EROs no meio intracelular, tanto o uso de antioxidantes, com o objetivo de diminuir a

progressão tumoral causada por níveis elevados de EROs, bem como o uso de pró-oxidantes, que tem como objetivo induzir morte celular via estresse oxidativo, tem sido estratégias úteis na terapia contra o câncer (REUTER *et al.*, 2010; GLASAUER; CHANDEL, 2014).

Recentemente foi demonstrado que os níveis de expressão do mRNA das enzimas antioxidantes é regulado pelo complexo Nrf2-Keap1 (LEONARDUZZI *et al.*, 2010). Nrf2 é um fator transcricional sensível ao equilíbrio redox celular, sendo a interação de Nrf2 com a proteína Keap1 (*Kelch-like ECH-associated protein*) controlada pelos níveis de GSH/GSSG (JONES, 2006). Normalmente a proteína Nrf2 está ligada com a proteína Keap1, sendo direcionada para degradação proteossomal. Entretanto, quando é gerado um estresse oxidativo por EROs, o complexo Nrf2-Keap1 se dissocia e Nrf2 é translocada para o núcleo onde se liga ao DNA na região ARE (*antioxidant response element*) (OSBURN; KENSLER, 2008), ativando a transcrição de algumas enzimas antioxidantes, como superóxido dismutases, glutatona S-transferase e catalase (ANTELMANN; HELMANN, 2011). Diante de tais efeitos, Nrf2 tem surgido como um alvo farmacológico em células tumorais. Porém, sua *up-regulation* tem sido questionada em termos terapêuticos, pois poderia proteger as células tumorais contra o estresse oxidativo, aumentando a viabilidade destas células (MILKOVIC *et al.*, 2017).

1.6. METABOLISMO DE CÉLULAS TUMORAIS

1.6.1. O Efeito Warburg

Desde as últimas duas décadas, o estudo de diversos tipos de células proliferativas tem permitido aumentar o conhecimento de seu metabolismo, que difere das células quiescentes pela alta taxa de glicólise, produção de lactato, biossíntese de lipídeos e outras macromoléculas (KIM, 2016). Em contraste com células normais diferenciadas, que majoritariamente realizam a fosforilação oxidativa, células tumorais utilizam a glicólise para a produção de ATP. Tal fenômeno também é conhecido como “efeito Warburg” em homenagem ao bioquímico/fisiologista alemão que o descreveu, Otto Warburg (WARBURG, 1925; WARBURG, 1956).

Na presença de oxigênio, tecidos não proliferativos (diferenciados), oxidam totalmente a glicose para produção de ATP. Otto Warburg observou

que em células tumorais, o produto final da glicólise é o lactato mesmo na presença de oxigênio (glicólise aeróbica). As mitocôndrias permanecem funcionais e a fosforilação oxidativa continua acontecendo tanto nos tecidos proliferativos quanto nos tumorais (VANDER HEIDEN *et al.*, 2009). Acredita-se que a acentuada atividade da via glicolítica proporciona diversas vantagens para as células tumorais. Se o fluxo glicolítico é alto o suficiente, como acontece no processo canceroso, o consumo da glicose para a produção de ATP, mesmo possuindo um baixo rendimento por molécula de glicose, resulta em uma porcentagem final de ATP que pode exceder à produzida pela fosforilação oxidativa (KIM, 2016). Desta maneira, o efeito Warburg beneficiaria tanto a necessidade bioenergética quanto biossintética das células. Além disso, em contraste com a respiração mitocondrial, a geração de energia pela via glicolítica ocorre independentemente da oferta de oxigênio e permite às células tumorais sobreviverem e migrarem para regiões em hipóxia (KIM, 2016). A observação de que células derivadas de tumores hipóxicos cultivadas em condições de normóxia ainda mantêm o fenótipo glicolítico, sugere que a maior atividade da glicólise não é uma simples adaptação metabólica às condições de falta de oxigênio e que, ao contrário, mecanismos genéticos promovem a ativação desta via nos tumores (DE BERARDINIS; CHENG, 2010).

A adaptação metabólica pode estar relacionada com a agressividade do tumor, sugerindo que o fenótipo glicolítico confere uma vantagem proliferativa às células tumorais, podendo ser um componente crucial do fenótipo maligno (WOO, 2016). A contribuição da fosforilação oxidativa (OXPHOS) frente à glicólise aeróbica difere na produção de ATP em diferentes tipos celulares e condições patológicas (PLECITA-HLAVATA, *et al.*, 2015).

Considerando que as células tumorais promovem alterações na sua bioenergética, aumentando as concentrações de lactato provenientes do efeito Warburg, e diminuindo as concentrações de piruvato, resultando em resistência à apoptose, esta regulação metabólica pode ser interessante terapeuticamente, explorando-se novos alvos farmacológicos. Esta via também foi em parte estudada neste trabalho.

1.7. QUIMIOTERAPIA

1.7.1. Química Inorgânica Medicinal

A química inorgânica medicinal estuda as aplicações de íons inorgânicos e seus complexos em sistemas fisiológicos, correlacionando a atividade biológica com as características estruturais e eletrônicas. Os dois principais focos desta área de pesquisa são os estudos dos metais com ocorrência natural em sistemas biológicos e a introdução de metais em sistemas biológicos, através da utilização de metalofármacos (MONGE *et al.*, 2000; FARRELL, 2002).

Os elementos inorgânicos desempenham um papel essencial nos processos biológicos e participam efetivamente na constituição de várias proteínas. Estas proteínas altamente elaboradas são denominadas de metaloproteínas e contêm um ou mais íons metálicos em sua estrutura. Dentre as funções que desempenham estão o transporte de oxigênio no processo (HOLM *et al.*, 1996) respiratório, o transporte de elétrons e função estrutural. Com o auxílio de técnicas avançadas de cristalografia - métodos teóricos e experimentais - é possível estudar a estrutura das metaloproteínas e investigar suas interações e sítios de ligação.

Os metais, em particular os metais de transição, oferecem vantagens em relação aos fármacos à base de compostos orgânicos, incluindo uma grande variedade de números de coordenação e geometrias, estados de oxidação acessíveis, capacidade de troca de ligantes no meio fisiológico e uma grande diversidade estrutural (RIJT *et al.*, 2009). A química inorgânica medicinal é uma área de investigação crescente que foi inicialmente alimentada pela descoberta da cisplatina há cerca de 40 anos. Atualmente, existem no comércio alguns metalofármacos e candidatos a fármacos em fase de testes clínicos (BARRY; SADLER, 2013).

1.7.2. Cisplatina

A pesquisa por complexos metálicos atuando como agentes quimioterápicos iniciou com a descoberta da ação antitumoral da cis-diaminodicloroplatina (II), ou cisplatina, que foi descrita pela primeira vez em 1844 por Reisner e em 1845 por Peyrone, sendo que Peyrone sintetizou um complexo diferente de Reiset, mas de mesma fórmula molecular. Algumas

décadas depois, em 1893, Werner propôs que estes complexos de platina de mesma fórmula molecular eram isômeros, sendo o de Reiset a forma *trans* e o de Peyrone a forma *cis* (Fig. 3).

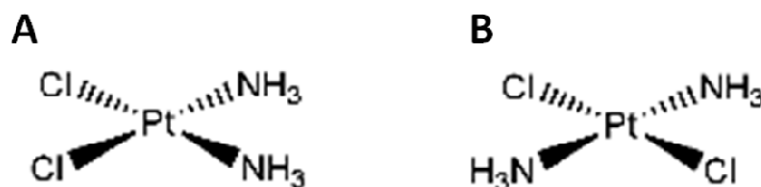


FIGURA 3. Estrutura da (A) cisplatina e (B) transplatina representada em forma estrutural espacial.

Em seguida, Rosenberg deu início a estudos em camundongos, portadores de sarcoma-180 e leucemia L1210 (ROSENBERG *et al.*, 1969). Foram testados tanto o complexo transplatina como a cisplatina, mas apenas o isômero *cis* provocou a regressão completa do tumor em poucos dias (BOULIKAS; VOUGIOUKA, 2003).

Devido aos excelentes resultados, a cisplatina foi introduzida nos estudos de testes clínicos em 1971, sendo aprovada sua comercialização pelo *Food and Drug Administration* (FDA) em 1978 nos EUA, com o nome de *Platinol*, inicialmente para o tratamento de câncer de testículo e ovário, tornando-se um dos medicamentos mais utilizados no tratamento de câncer em todo o mundo (SUGIYAMA *et al.*, 2016). Posteriormente a aplicação da cisplatina foi ampliada para outros cânceres, sendo atualmente utilizada para tumor testicular (GHEZZI *et al.*, 2016), de ovário (SUGIYAMA *et al.*, 2016), bexiga (HSIEH *et al.*, 2016), fígado (CRIPPA *et al.*, 2016), cérvix (RADES *et al.*, 2016), cabeça e pescoço (BANERJEE *et al.*, 2014), entre outros.

Nos 40 anos após a aprovação da cisplatina, 23 outros complexos de platina tiveram seus ensaios clínicos iniciados, sendo que apenas dois destes complexos, a carboplatina e a oxaliplatina, ganharam aprovação pelo FDA para serem comercializados mundialmente. Outros três compostos, a nedaplatina, a lobaplatina e a heptaplatina, tiveram a sua aprovação no Japão, China e Coreia, respectivamente (ZHU *et al.*, 2017). Efeitos adversos graves decorrentes do uso do quimioterápico cisplatina, como a ototoxicidade,

náuseas, nefrotoxicidade, neurotoxicidade, disfunção gastrointestinal e mielossupressão, (ZHU *et al.*, 2017), bem como resistência a essa droga (GO; ADJEI, 1999), foram observados.

Os efeitos colaterais e a resistência adquirida à cisplatina pelas células tumorais impulsionaram o desenvolvimento de complexos análogos que apresentassem efeitos mais toleráveis e com capacidade de atuar nas células resistentes à cisplatina, além da busca por complexos mais estáveis e solúveis no meio extracelular. Devido a isto, tem sido avaliado o potencial terapêutico de outros elementos da família dos metais de transição (a mesma família da cisplatina), tais como o Paládio (Pd), Rutênio (Ru), Irídio (Ir), Ródio (Rh) e o Ósmio (Os) (AM *et al.*, 2015).

1.7.3. Complexos de Rutênio

Os complexos de rutênio podem ser uma alternativa promissora aos complexos de platina (CLARKE, 2002). Um número expressivo de complexos de rutênio foram sintetizados e testados em células tumorais, sendo que dois deles se destacaram: NAMI-A (SAVA *et al.*, 1999) e KP1019 (HARTINGER *et al.*, 2008). Os primeiros complexos de Ru (III) sintetizados e testados para a atividade antitumoral, NAMI-A, ([Him] [trans- RuCl₄ (DMSO) (im)]), im = imidazol), KP1019, ([Hind] - [trans- [RuCl₄ (ind) 2], ind = indazol), e o seu análogo de potássio (Na⁺) (KP1339) apresentaram efeito semelhante ao da cisplatina e seletividade para células tumorais (ALESSIO, 2004; FISCHER, 2014). Acredita-se que a citotoxicidade destes compostos, como no caso da cisplatina, relaciona-se à formação de adutos com o DNA celular, que inibem a transcrição e replicação, além de interações com biomoléculas tumorais levando à morte celular (SCHLUGA, 2006; GROESSL, 2010; GROESSL, 2011).

Estudos sugerem que NAMI e KP1019 atuam como pró-fármacos, sendo "ativados por redução" à Ru (II) em células tumorais através de redutores biológicos, tais como a glutatona, ácido ascórbico, cisteína e citocromo c (JAKUPEC, 2005; REISNER, 2005; SANTOS, 2013). Reforçando estes estudos, experimentos eletroquímicos demonstraram que esta redução é favorecida em tecido tumoral em relação ao tecido saudável, devido à baixa concentração de oxigênio e pH mais ácido (FRASCA, CLARKE, 1999).

O complexo de rutênio, segundo a nomenclatura IUPAC denominado $\text{cis-[Ru(1,10-fenantrolina)}_2\text{(imidazol)}_2\text{]}^{2+}$ ou RuC (Fig. 4) - abreviação utilizada neste trabalho – foi sintetizado e gentilmente doado, pelo grupo da Prof.^a Dr.^a. Rose Maria Carlos, do Departamento de Química da Universidade Federal de São Carlos. O complexo foi planejado de forma a atuar da mesma maneira que a cisplatina, ou seja, como um pró-fármaco que ao ser ativado pela dissociação de um ligante e/ou redução do centro metálico, leva à formação de uma espécie mais reativa, capaz de interagir com o DNA de forma a promover a morte celular.

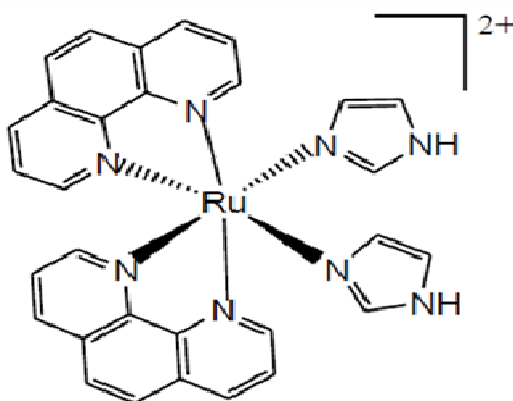


FIGURA 4. Estrutura química do $\text{(cis-[Ru(1,10-fenantrolina)}_2\text{(imidazol)}_2\text{]}^{2+})$, onde 1,10-fenantrolina (phen) e imidazol (ImH), sendo denominado RuphenImH ou RuC neste trabalho (CARDOSO et al., 2014).

O complexo de rutênio (II) apresenta o centro metálico que permite a coordenação de até seis ligantes monodentados (ligantes que se coordenam através de um átomo). O ligante fenantrolina foi escolhido para aumentar a estabilidade e rigidez e fornecer a lipofilicidade necessária para uma rápida absorção celular; já o ligante imidazol coordenado ao centro metálico tem a função de trazer uma região hidrofílica ao complexo, aumentando sua solubilidade e, ainda, possibilitar interações do tipo ligação de hidrogênio com os alvos biológicos. Ligantes imidazólicos também estão presentes em compostos que apresentam atividades antitumoral, antiviral (como antiHIV), antiprotozoário, entre outras (NARASIMHAN *et al.*, 2011).

A síntese e caracterização do RuC foi descrita por CAMILO e colaboradores (2014) e CARDOSO e colaboradores (2014), respectivamente.

Cardoso et al. (2014) observaram que o RuC induziu a inibição do ciclo celular em células HCT116 p53^{+/+} (câncer de colorretal) e HCT116 p53^{-/-} (câncer colorretal com ausência do gene p53) na fase G1 em ambas as células, porém, o aumento da população celular na fase G1 foi mais acentuada nas células HCT116 p53^{+/+}.

Considerando o potencial antineoplásico do RuC e a ausência de dados sobre este composto, a hipótese deste trabalho é que o RuC apresenta atividade antitumoral contra diferentes linhagens celulares tumorais. Para tanto, duas linhagens humanas (HeLa e HepG2) e uma linhagem murina (Walker-256) foram usadas como ferramentas para testar nossa hipótese.

2. OBJETIVO

2.1. Objetivo Geral

O presente trabalho teve como objetivo geral investigar a atividade antineoplásica do complexo de rutênio (RuC) em modelos *in vitro* com as células HepG2 e HeLa, e *in vivo* frente ao modelo de carcinossarcoma Walker-256 em ratos.

2.2. Objetivos Específicos

In vitro:

2.2.1. Estabelecer o perfil de citotoxicidade, proliferação e crescimento celular do composto RuC em linhagens de células tumorais através dos métodos MTT, Cristal Violeta e Vermelho Neutro em células HepG2 e HeLa;

2.2.2. Mensurar a respiração celular na cadeia respiratória íntegra e os níveis de piruvato e lactato de células HepG2 e HeLa;

2.2.3. Determinar a recuperação celular após exposição das células HepG2 e HeLa ao RuC;

In vivo:

2.2.4. Avaliar o crescimento tumoral em ratos tratados e não tratados com RuC e acompanhar o peso ponderal dos animais;

2.2.5. Investigar possíveis mecanismos de ação envolvidos na atividade antitumoral, como estresse oxidativo, apoptose e necrose;

2.2.6. Mensurar a respiração das células Walker-256 na forma ascítica;

2.2.7. Avaliar se o tratamento com RuC diante do tumor altera parâmetros de função hepática, renal e metabólica, através de bioquímica plasmática e parâmetros de estresse oxidativo em fígado e rins;

2.2.10. Avaliar a toxicidade do RuC *per se* em animais sem a indução do tumor Walker-256, e compará-la à toxicidade da cisplatina.

3. PRIMEIRO ARTIGO CIENTÍFICO

Antineoplastic activity of a ruthenium complex against human hepatocellular carcinoma (HepG2) and human cervix adenocarcinoma (HeLa) cells

Carlos Eduardo Alves de Souza¹, Carolina Riverin Cardoso³, Rose Maria Carlos³, Sílvia Maria Suter Correia Cadena² and Alexandra Acco^{1*}

¹Department of Pharmacology, Federal University of Parana, Curitiba, Brazil

²Department of Biochemistry and Molecular Biology, Federal University of Parana, Curitiba, Brazil

³Department of Chemistry, Federal São Carlos University, São Carlos, Brazil

*** Corresponding author:**

Alexandra Acco, Federal University of Paraná (UFPR), Biological Science Sector, Department of Pharmacology, Anexo I, Centro Politécnico, Cx. P. 19031, Curitiba – Paraná – Brazil, Zip Code 81531-980

Phone: +55 (41) 3361-1742; Fax: +55 (41) 3266-2042

E-mail: aleacco@ufpr.br

3.1. ABSTRACT

Novel metal complexes have received great attention in the last decades due to their potential anticancer activity. Notably, ruthenium-based complexes have emerged as good alternative to the currently used platinum-based drugs for cancer therapy, providing less toxicity and side effects to patients. The beneficial properties of Ru, which make it a highly promising therapeutic agent, include its variable oxidation states, low toxicity, and high selectivity for cancer cells. In this work, we evaluated the cytotoxicity effect of a ruthenium complex namely RuC ($\text{cis-}[\text{Ru}(\text{1,10-phenanthroline})_2(\text{imidazole})_2]^{2+}$) on human hepatocellular carcinoma (HepG2) and human cervix adenocarcinoma (HeLa) cells, associated with metabolic parameters analysis. RuC reduced HepG2 and HeLa viability in all tested concentrations (10, 50 and 100 nmol/L) at 48h of incubation through MTT, crystal violet and neutral red assays. The cell proliferation of HepG2 was not recovery, while HeLa recovery partially after RuC treatment. RuC also inhibited all states of cell respiration, and increased the levels of the metabolites pyruvate and lactate in both cell lineages. The cytotoxicity of RuC was higher than that observed for cisplatin (10 nmol/L), used as positive control, in both lineages. These results show that RuC affects metabolic functions related to energy provision and viability of HepG2 and HeLa cells, being a promising candidate for further investigations in models of human cervix adenocarcinoma and mainly of hepatocellular carcinoma.

Keywords: hepatocellular carcinoma, ruthenium complexes, RuC, metabolism, HepG2 cells, HeLa cells.

3.2. INTRODUCTION

Nowadays cancer ranges among the principal causes of morbidity and mortality worldwide. The World Health Organization projects an increase of 70% in the number of new cases over the next two decades (STØVING *et al.*, 2015). Cisplatin has been the most frequent choice for the treatment of a wide range of cancers, e.g. ovarian, testicular, in head and neck, bladder and lung cancers (DASARI *et al.*, 2014). However, the efficiency of cisplatin is limited by acquired or intrinsic resistance and by severe side effects such as ototoxicity, peripheral neuropathy, myelosuppression and nephrotoxicity (GALUZZI *et al.*, 2016). Consequently, novel anti-cancer compounds have been synthesized aiming to find a more efficient drug with lesser side effects.

In this sense, ruthenium organometallic complexes have been synthesized as an alternative to cisplatin treatment. . These complexes are considered as pro-drugs since they are only effective against the tumor cells after the reduction of Ru(III) to Ru(II) by biological reducing agents (JAKUPEC *et al.*, 2005; REISNER, 2004; REISNER, 2005; SANTOS, 2013). Electrochemical experiments have shown that this reduction is favored in solid tumors in comparison to healthy tissue because of the low oxygen concentration (i.e., hypoxia) and acid pH in the tumor microenvironment (CLARKE, 1996; HARTMANN, 1998, FRASCA, 1999).

The compound of ruthenium ($\text{cis-[Ru(phen)}_2\text{(ImH)}_2\text{]}^{2+}$) referred as RuphenImH or RuC (Fig. 1), has shown an important cytotoxic effect, compared to cisplatin, on colorectal adenocarcinoma HT116 cells ($\text{p53}^{-/-}$) and HT116 cells ($\text{p53}^{+/+}$). RuC promoted a cell cycle arrest in G1 phase, which was more pronounced in HT116 cells ($\text{p53}^{+/+}$) (CARDOSO *et al.*, 2014). Also in HT116 cells ($\text{p53}^{+/+}$), RuC was not able to induce the cleavage of caspase 3 and PARP, suggesting that apoptosis was not involved in the inhibition of cells proliferation.

Recently we show that RuC was effective against the Walker-256 tumor in rats through the modulation of oxidative stress and impairment of oxidative phosphorylation, causing necrosis instead of apoptosis in these tumor cells (ALVES-DE-SOUZA *et al.*, 2017). Additionally, no clinical signs of toxicity or death were observed in rats that were treated with RuC (ALVES-DE-SOUZA *et al.*, 2017).

Cancer cells have their metabolism changed to maintain the fast growth and proliferation. They depend on the synthesis of ATP by glycolysis rather than oxidative phosphorylation, a phenomenon known as Warburg effect (WARBURG, 1956). This effect was firstly attributed to mitochondrial dysfunction, but this mechanism has been reevaluated (TSAI CH *et al.*, 2017). In fact, in mitochondria from cancer cells anaplerotic and cataplerotic reactions work together to provide sufficient biosynthetic precursors, supporting cell proliferation. Thus, in contrast to Warburg's earliest observations, the maintenance of functional mitochondria appears to be essential for the survival and proliferation of cancer cells (WALLACE, 2016).

In this work we investigated the cytotoxic effect of the RuC on human hepatocellular carcinoma cells (HepG2) and human cervix adenocarcinoma (HeLa), human glioblastoma (U87MG), human breast adenocarcinoma (NDAmb234) and murine melanoma cells (B16F10) cells associated with changes on metabolic parameters. These cells were selected from an initial toxicity screening also including human glioblastoma (U87MG), human breast adenocarcinoma (NDAmb234), non-tumor human embryonic kidney (HEK293), and murine melanoma cells (B16F10). The significant toxicity of RuC on HepG2 and HeLa cells, related to the inhibition of respiration and the activation of anaerobic glycolysis, became RuC a promisor alternative for the treatment of HCC and cervix adenocarcinoma, with the advantage of minimizing the adverse effects caused by other transition metals.

3.3. MATERIALS AND METHODS

3.3.1. Chemicals

High-glucose Dulbecco's modified Eagle's medium (DMEM HG) and Minimum Essential Medium Eagle (MEM) mediums were obtained from Cultilab (Campinas, Brazil) and fetal bovine serum (FBS) was purchased from Cripion Biothecnology (Andradina, SP, Brazil). Dimethylsulfoxide (DMSO) was obtained from Merck (São Paulo, SP, Brazil). Bovine serum albumin (BSA), 3-(4,5-dimethylthiazol-2-yl)-2,5-diphenyltetrazolium bromide (MTT), 4-(2-hydroxyethyl)-1-piperazine ethanesulfonic acid (HEPES) and Trypan Blue were purchased from Sigma. The *cis*-diamineplatinum(II) dichloride (cisplatin) was obtained from

Sigma Aldrich with $\geq 99.9\%$ trace metals basis. The ruthenium complex (cis-(Ru[phen]₂[ImH]₂)²⁺, also called RuphenImH or RuC (Fig. 1), was synthesized by the Department of Chemistry of the Federal University of São Carlos, São Paulo, Brazil, and its structure was confirmed by ¹H NMR, ¹³C NMR and mass spectrometry (CARDOSO *et al.*, 2014). For this study, the compound was dissolved in DMSO and then further diluted with the assay medium. Controls with DMSO (0.1%, v/v) were carried out in each assay. All other reagents were commercial products of the highest available purity grade.

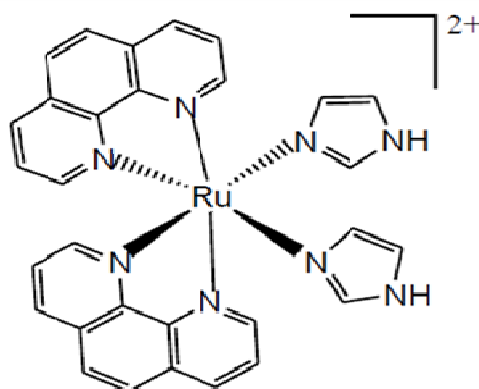


FIGURE 1. Chemical structure of RuC, according to IUPAC nomenclature, cis-[Ru(1,10-phen)₂(ImH)₂]²⁺, which *phen* refers to 1,10-phenanthroline and *ImH* refers to imidazole. Source: Cardoso *et al.*, 2014.

METHODS

3.3.2. Cell culture

The human hepatocarcinoma (HepG2), human glioblastoma (U87MG) and human breast adenocarcinoma (NDAmb234) were maintained in high-glucose DMEM (DMEM HG), cervix adenocarcinoma (HeLa) was maintained in MEM, and human embryonic kidney (HEK293) and murine melanoma cells (B16F10) were maintained in RPMI medium. All cell lines were obtained from the American Type Culture Collection — ATCC. The culture media were supplemented with 10% FBS, 100 UI/mL penicillin G and 100 µg/mL streptomycin, 20 mmol/L 4-(2-hydroxyethyl)-1-piperazine ethanesulfonic acid (HEPES), adjusted to pH 7.4 with 1 mol/L sodium bicarbonate. HepG2 cells were grown in poly-L-lysine-coated flasks at 37°C, 5% CO₂ under controlled

humidity. Sub-culturing was performed at approximately 48 h intervals, and cells growth was monitored with an Olympus inverted microscope.

3.3.3. Toxicity screening of the RuC

In order to establish the range of RuC concentration, the sensitivity of cell lines and time of treatment, assays of toxicity were performed with RuC in a concentration range of 10 nmol/L to 1 μ mol/L, in several tumor cell lines (HeLa, HepG2, B16F10, U87MG and NDAmb234), and in the immortalized kidney cell HEK293. The cells were treated with RuC by 24, 48 and 72 hours and then the cell viability was evaluated by the MTT method, as described in the next section. For comparison, cells were also treated with cisplatin (1 to 20 μ mol/L) or DMSO (0.1%, v/v) in each assay, as positive and negative control, respectively.

3.3.4. Cellular viability assays

3.3.4.1. MTT

Briefly, the cells were seeded at a density of 1×10^4 cells/well into 96-well culture plates and after 24 h (confluent state of ~70%) were treated with cisplatin and RuC at concentrations from 1 to 20 μ mol/L and 10 nmol/L to 1 μ mol/L, respectively, for 24, 48 and 72 hours. After the treatment, 200 μ L of 3-(4,5-dimethylthiazol-2-yl)-2,5-diphenyltetrazolium bromide (MTT) solution (0.5 mg/mL) were added to each well and incubated for 3 h at 37°C. The culture medium was discarded and 200 μ L of a DMSO solution was added into each well and mixed by gently until complete homogenization (MOSSMAN *et al.*, 1983; PIRES *et al.*, 2013). The formazan absorbance was determined at 570 nm and the results were expressed as a percentage of viable cells in comparison to the control (taken as 100%).

3.3.4.2. Crystal violet

The crystal violet assay was performed according to Gillies *et al.*, (1986). After the treatment with Cisplatin (5 and 10 μ mol/L) or RuC (10, 50 and 100 nmol/L), HepG2 and HeLa cells monolayer were washed with pre-warmed PBS

and fixed with 100 μL of cold absolute methanol for 10 min. Then, the cells were stained with crystal violet dye solution (0.2% crystal violet, 2% ethanol) for 3 min and successive washings with PBS were performed for the removal of dye excess. The remained dye was solubilized using crystal violet destaining solution (50% ethanol, 0.05 M sodium citrate) and the absorbance was measured by reading at 540 nm in a microplate reader (TECAN® Infinite Reader, Austria).

3.3.4.3. *Neutral red*

Cells (HepG2 and HeLa) were plated on 96-well plates at a density of 1×10^4 cells per well in a final volume of 200 μL . After 24 h the cells were treated with cisplatin at concentrations of 5 and 10 $\mu\text{mol/L}$ or RuC at concentrations of 10, 50 and 100 nmol/L for 48 hours, in a final volume of 200 μL . After 24 h incubation, the medium was removed and the cells washed twice with 150 μL per well of PBS solution heated at 37°C. Then neutral red assay was performed according to Borenfreund and Puerner method (1984). The cells were flooded with 100 μL of neutral red solution (50 $\mu\text{g/mL}$ neutral red in the culture medium) and incubated for 4 h at 37°C in an atmosphere of 5% CO_2 . Then, neutral red solution was discarded, the cells were washed twice with 150 μL PBS and 150 μL of fixative solution (1% formaldehyde, 1% calcium chloride) for 2 min. Plates were then rapidly drained, followed by addition of 200 μL of extraction buffer (1% acetic acid and 50% ethanol) and left in the dark for 20 min at room temperature. Absorbance of extracted dye was measured using a microplate reader (TECAN® Infinite Reader, Austria) at a wavelength of 570 nm.

3.3.5. Cellular proliferation

HepG2 and HeLa cells were plated on 96 well plates at a density of 1×10^4 cells per well at 200 μL of final volume. Then, the cell proliferation at time of 24, 48 and 72 h were determined by MTT method as described above.

3.3.6. Cellular respiration

The HepG2 and HeLa cells were grown on 60 mm plate and treated with cisplatin at concentrations of 5 and 10 $\mu\text{mol/L}$ or RuC at concentrations of 10, 50 and 100 nmol/L for 48 hours. After treatment, the cells were removed with

trypsin and resuspended in DMEM HG or MEM for HepG2 and HeLa cells, respectively, and cell viability was assessed by the trypan blue dye exclusion assay (STROBER *et al.*, 2015) in a Neubauer chamber. Cell respiration was then measured by high-resolution respirometry using an Oxygraph-2k device (Oroboros Instruments, Innsbruck, Austria) in two chambers at 37°C under gentle agitation. The cells respiration (10^6 cells/ chamber) was monitored in DMEM HG or MEM, for HepG2 or HeLa cells, respectively. Oxygen flux was determined in the different states of respiration as previously described (GNAIGER *et al.*, 2001; HUTTER *et al.*, 2006; RENNER *et al.*, 2003; GNAIGER *et al.*, 2009). These states were defined as: *basal* (oxygen consumption in the absence of inhibitors or uncouplers), *leak* (respiration in the presence of 2 µg/mL oligomycin, which results of the reentry of protons into the mitochondrial matrix and represents respiration that is not coupled to ATP synthesis), and *uncoupled* (oxygen consumption in the presence of 0.5 µmol/L FCCP, which corresponds to the maximal respiratory capacity to restore the dissipated proton gradient due to the presence of the uncoupling agent). The oxygen flow in these states was corrected by subtracting non-mitochondrial respiration, which was obtained after the addition of rotenone (0.5 µmol/L) and antimycin (3 µg/mL). The results were analyzed using DataLab4 software and are expressed as the mean \pm standard error of the mean (SEM) of cells oxygen flow ($\text{pmol} \cdot [\text{seg} \times 1 \times 10^6 \text{ cells}]^{-1}$).

3.3.7. Determination of lactate and pyruvate released by cultured cells

HepG2 and HeLa cells were cultured in DMEM HG and MEM, respectively, and treated for 48 h with cisplatin (5 and 10 µmol/L) and RuC (10, 50 and 100 nmol/L). Then, the supernatant was collected and centrifuged at 1500 rpm for 5 min. Finally, the concentrations of lactate and pyruvate in the supernatant were measured as previously described (CZOC *et al.*, 1974; GUTMANN *et al.*, 1974).

3.3.8. Proliferation recovery curve of HepG2 and HeLa cells

Cells proliferation recovery curves were performed for both cell lines, which were seeded in 6-well plates at density of 1.5×10^4 in a final volume of 1 mL. After 24 hours of plating, the number of cells was determined (day 1) and

another set of plates were treated with cisplatin (100 nmol/L, 5 and 10 μ mol/L) or RuC (10, 50 and 100 nmol/L) for 48 h (day 3). After this time, the treatment was removed and the wells were washed with 500 μ l of PBS and the culture medium was replaced every 2 days. Cell viability was determined by the trypan blue method every 2 days for 9 days (day 5 to day 9).

3.3.9. Protein determination

The cells protein concentrations were determined using the method described by Bradford with BSA as the standard (BRADFORD, 1976), and used when necessary to normalize the amount of protein in assays with cultured cells.

3.3.10. Statistical analysis

The statistical analysis was performed by Shapiro-Wilk normality test and then analysis of variance (one-way ANOVA) and Tukey as *posthoc* test or two-way ANOVA followed by the Bonferroni test when comparing cellular proliferation curves for average comparison. The results were expressed as mean \pm SEM. For all comparisons *p* values lower than 0.05 were considered statistically significant.

3.4. RESULTS

3.4.1. RuC toxicity screening in cell lines

The ruthenium complex, at range from 10 nmol/L to 1 μ mol/L, reduced the viability of all cell lines from 24h to the maximum time of 72h of treatment (data not shown). As exemplified in figure 2, RuC (100 nmol/L) was more cytotoxic for HepG2 and HeLa cells, reducing the cells viability at 65 and 58% after 48h of treatment, respectively (Fig. 2B). Interestingly, the non-tumor cell line HEK293 was lesser affected in comparison to tumor cell lines, in particular for 24 and 48h of treatment, with a slightly reduction of 8 and 13%, respectively. Considering these results, the RuC concentration of 10, 50 and 100 nmol/L and the time of treatment of 48h were fixed for the course of the next experiments. In the subsequent assays it was also included cisplatin (5 and 10 μ mol/L),

aiming to compare the effects of different transition metals on HepG2 and HeLa cells.

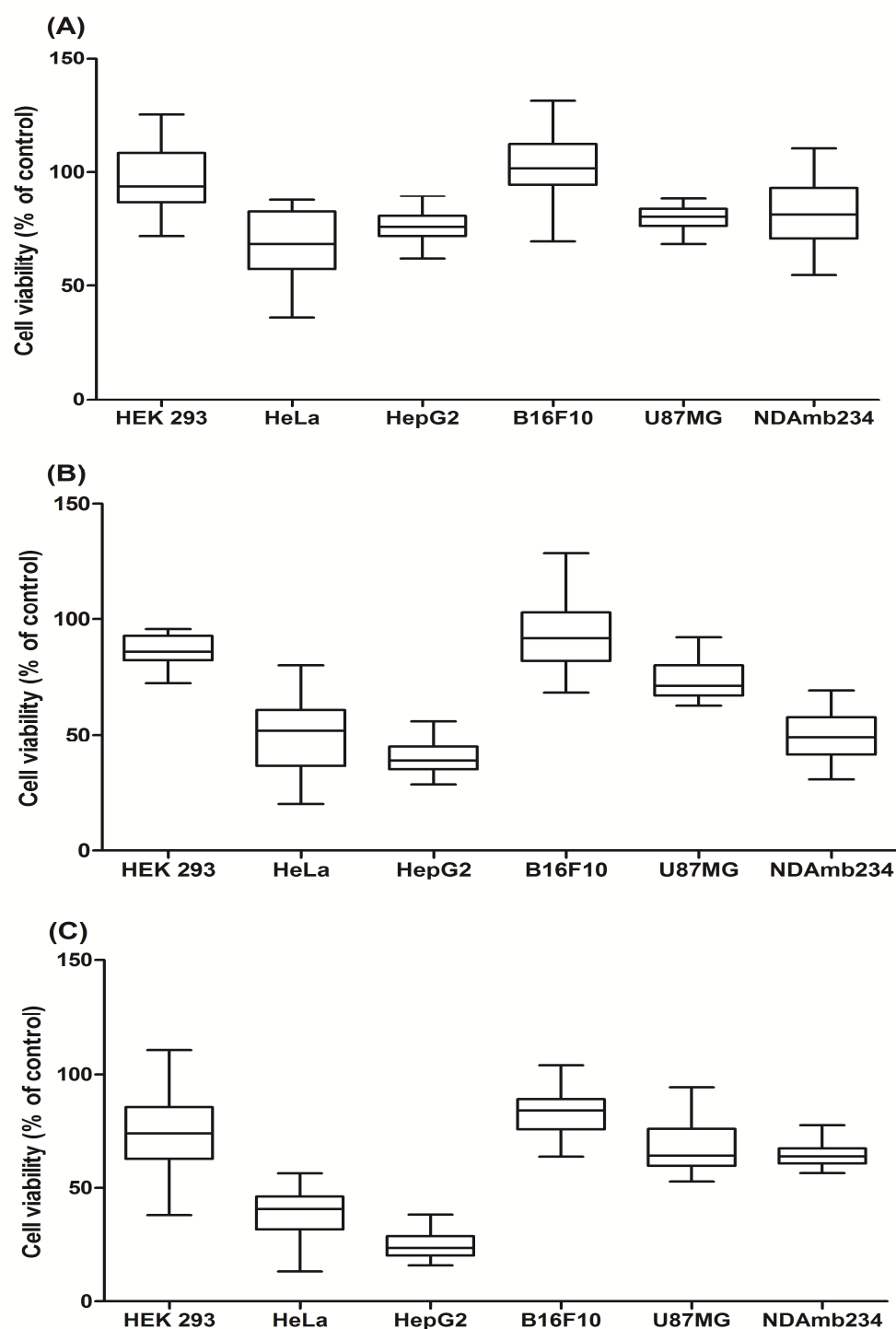


FIGURE 2. Toxicity of RuC complex on cell lines. Different cell lines were treated with RuC at concentration of 100 nmol/L for **(A)** 24, **(B)** 48 and **(C)** 72 hours. The experimental conditions are described in the Materials and Methods. Briefly, the cells (10^4 cell/ well) were seeded in 96-well plates with RuC at 100 nmol/L and treatment with RuC for 24, 48 and 72 hours and cell viability was evaluated by MTT. The values represent the mean \pm SEM of four experiments.

3.4.2. RuC is toxic for HepG2 and HeLa cells

RuC complex (10, 50 and 100 nmol/L) and cisplatin (5 and 10 μ mol/L) were toxic for both cell lines after 48h of treatment. The viability evaluated by the MTT was decreased by 38% and 42% for HepG2 cells, and 63% and 28% for HeLa cells at the highest concentration of RuC (100 nmol/L) and cisplatin (10 μ mol/L), respectively (Fig. 3A,B). As MTT method is based on the activity of cellular dehydrogenases, we also performed viability assays using violet crystal and neutral red to confirm the results. The crystal violet stains the nucleus of fixed cells, which are considered viable. In turn, neutral red stains acidic vesicles into the cells in process of cell death. Determination of viability by crystal violet stain showed reductions of viability for HepG2 by 60% and 28%, and for HeLa cells by 33% and 51% at the highest concentration of RuC (100 nmol/L) and cisplatin (10 μ mol/L), respectively (Fig. 3C,D). The same effect was observed by neutral red assay, on which RuC and cisplatin at the same concentrations, reduced the HepG2 viability by 48% and 74%, and reduced 38% and 58% the viability of HeLa cells (Fig. 3E,F).

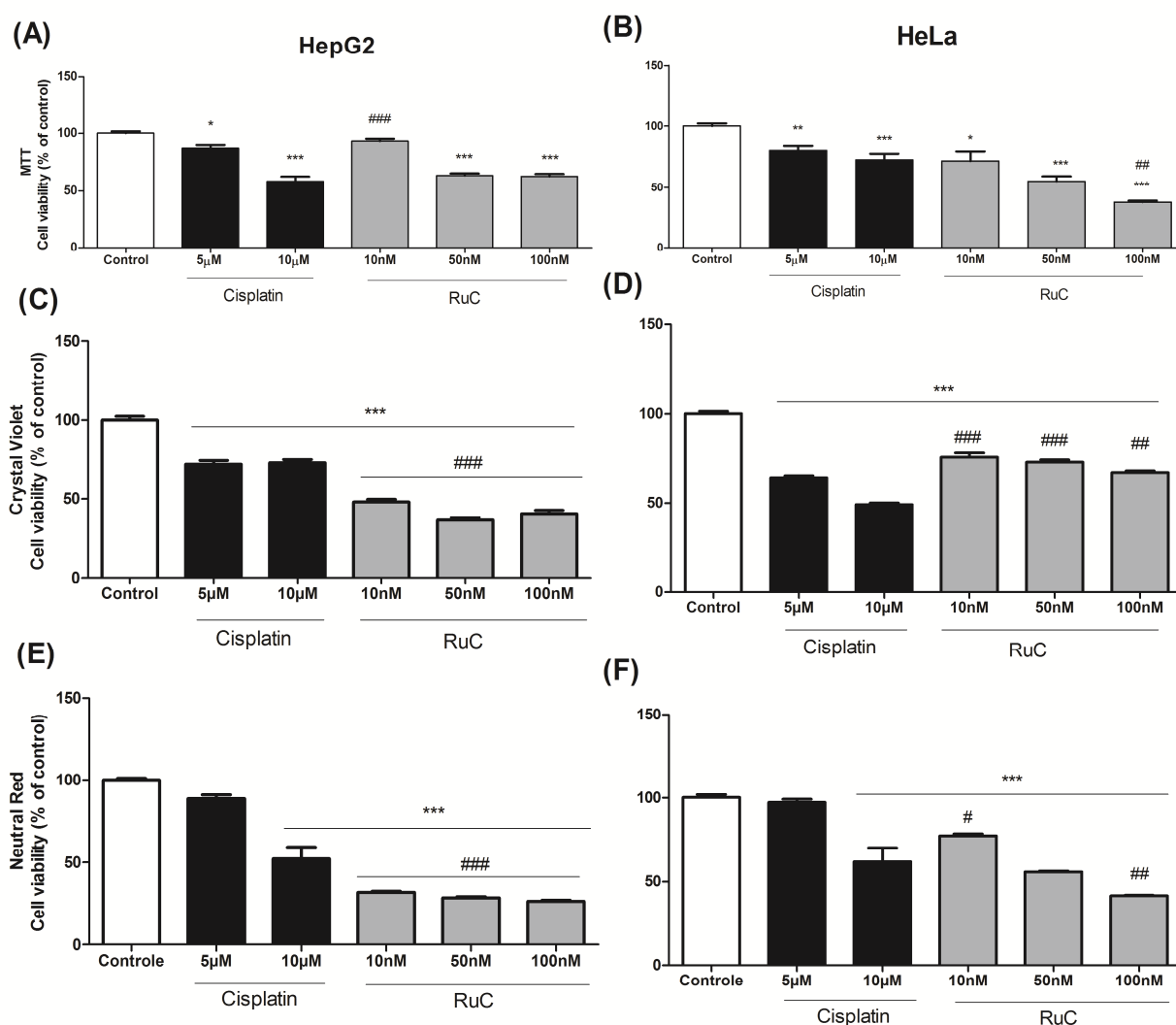


FIGURE 3. Cytotoxicity of cisplatin and RuC on HepG2 and HeLa cells. **(A and B)** MTT assay, **(C and D)** crystal violet, and **(E and F)** neutral red assay. The experimental conditions are described in the Materials and Methods. Briefly, the cells (10^4 cell/ well) were seeded in 96-well plates with cisplatin (5 and 10 $\mu\text{mol/L}$) or RuC (10, 50 and 100 nmol/L) for 48 h. The values represent the mean \pm SEM of six experiments. The results are expressed as % of control (DMSO 0.1%). Symbols: * significantly different from the control; # significantly different from cisplatin 10 $\mu\text{mol/L}$; one, two, and three symbols refer to $p < 0.05$, $p < 0.01$, and $p < 0.001$, respectively.

3.4.3. RuC affects HepG2 and HeLa proliferation

MTT data were used to plot a cell proliferation curve measuring the activity of cellular dehydrogenases at 24, 48 and 72 h. A gradual reduction in cells proliferation was observed after 48h and 72h of treatment, except for the control condition. The cell proliferation showed a time-course decline with the highest concentrations of cisplatin (10 $\mu\text{mol/L}$) and RuC (50 and 100 nmol/L) in both HepG2 (Fig. 4A) and HeLa (Fig. 4B) cells.

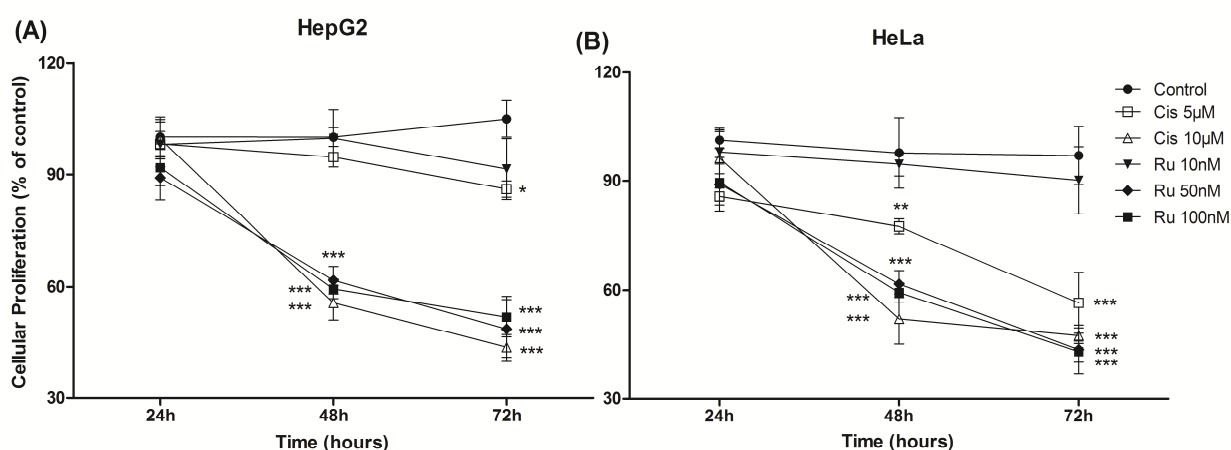


FIGURE 4. Effect of RuC and cisplatin on proliferation of HepG2 **(A)** and HeLa cells **(B)**. The experimental conditions are described in the Materials and Methods. The cells were cultured by 48 hours prior the addition of cisplatin (100 nmol/L, 5 and 10 $\mu\text{mol/L}$) or RuC (10, 50 and 100 nmol/L). The values represent the mean \pm SEM of six experiments. The results obtained by MTT test are expressed as % of control (DMSO 0.1% in 24h.). Symbols: * significantly different from the control in the same time of treatment; one, two, and three symbols refer to $p < 0.05$, $p < 0.01$, and $p < 0.001$, respectively.

3.4.4. RuC affects the respiration of HepG2 and HeLa cells

Considering the significant reduction of the cell viability and proliferation, we evaluated the effects of RuC and cisplatin on respiration of HepG2 and

HeLa cells. These assays were performed using non-permeabilized cells in attempt to approximate the experimental to physiological conditions. Figure 5 shows the cells respiration after 48 h of treatment with the drugs. In HepG 2 cells, RuC decreased the respiration rate in the highest concentration, reaching this inhibition to 77% for basal (Fig. 5A), 62% for leak (Fig. 5C), and 86% for uncoupled states (Fig. 5E), respectively. Curiously, both concentrations of cisplatin (5 and 10 $\mu\text{mol/L}$) did not alter the respiration of these cells.

Differently, in HeLa cells the basal and uncoupled states were inhibited by both drugs (Fig. 5B,F). The basal state was inhibited by 5 and 10 $\mu\text{mol/L}$ cisplatin (62% and -72%), while the presence of RuC inhibited this state at 84%, 85% and 91% at concentrations of 10, 50 and 100 nmol/L, respectively. (Fig. 5B). On leak state only the treatment with the highest concentration of RuC (100 nmol/L) promoted an inhibition of 61% (Fig. 5D). The uncoupled state was inhibited by 91% in all concentrations of cisplatin and RuC (Fig. 5E,F).

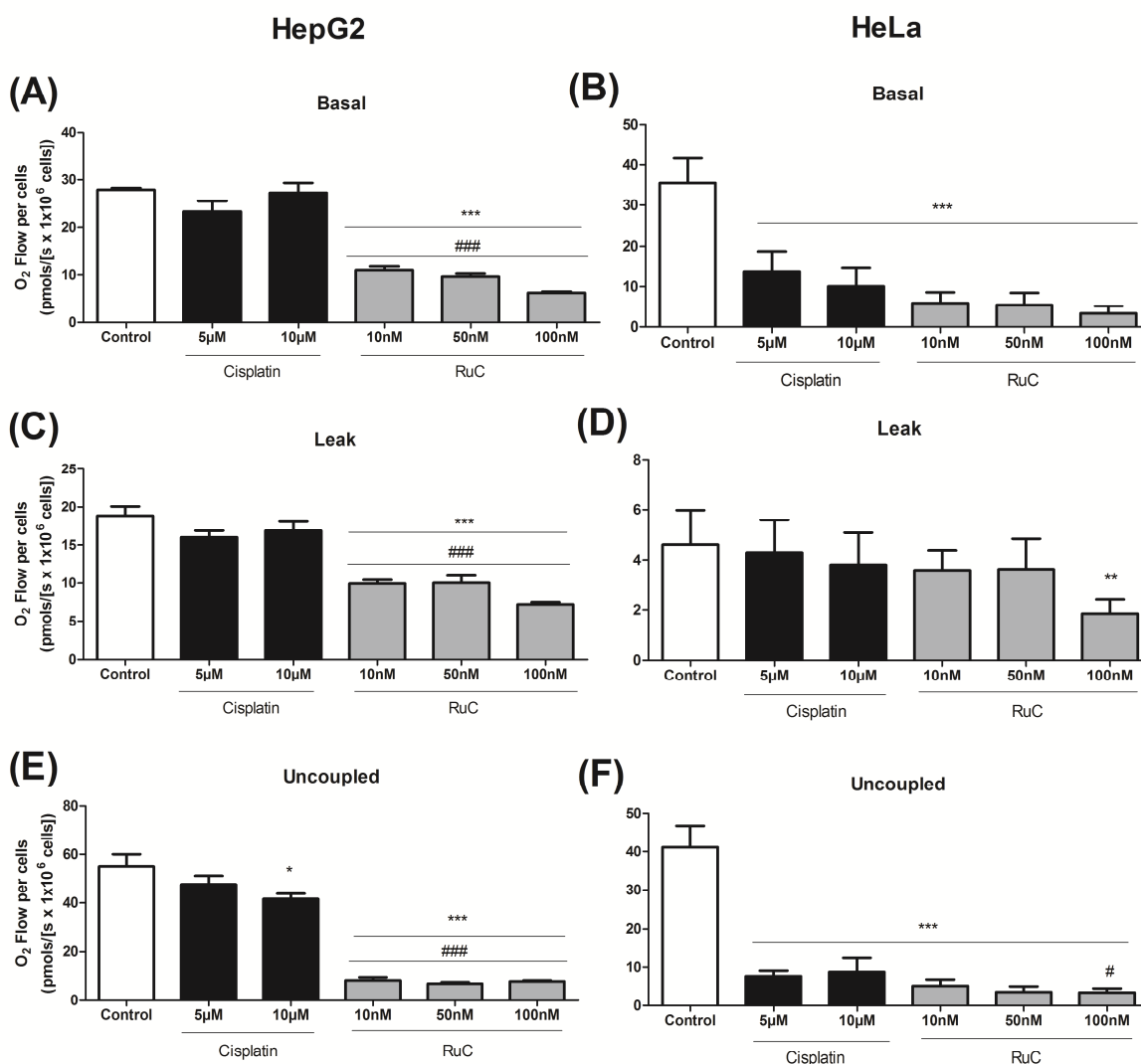


FIGURE 5. Effect of cisplatin and RuC in the respiration of HepG2 cells (**A, C** and **E**) and HeLa cells (**B, D** and **F**). The experimental conditions are described in the Materials and Methods. Briefly, cells (10^6 cell/ well) were seeded in 60 mm plates for 48h, treated and transferred to the Oroboros 2-K oxygraph chambers, where the oxygen consumption was determined in the absence of inhibitors or uncouplers (basal state), in the presence of oligomycin (leak state) and in the presence of FCCP (uncoupled state). The results were expressed as respiration ($\text{pmolO}_2/1 \times 10^6 \text{ cells}$) relatively to the control. Values represent the mean \pm SEM of four independent experiments. Symbols: * significantly different from the control (DMSO 0.1% - vehicle); # significantly different from cisplatin 10 $\mu\text{mol/L}$; one, two, and three symbols refer to $p < 0.05$, $p < 0.01$, and $p < 0.001$, respectively.

3.4.5. RuC increases the levels of pyruvate and lactate

Considering that significant inhibition of respiration may result in the activation of glycolytic pathway, the levels of pyruvate and lactate released by HepG2 and HeLa cells were also measured. Cisplatin did not alter the levels of pyruvate or lactate in HeLa cells, while RuC increased the levels of these metabolites only at the highest concentration (100 nmol/L). In HepG2 cells, cisplatin (10 nmol/L) was able to increase the pyruvate levels (55%); however, it did not affect the lactate concentration. In turn, the effects of RuC (100 nmol/L) were more pronounced, increasing the levels of both metabolites, pyruvate (116% and 72%) and lactate (60% and 42%) in HepG2 and HeLa, respectively (Figure 6).

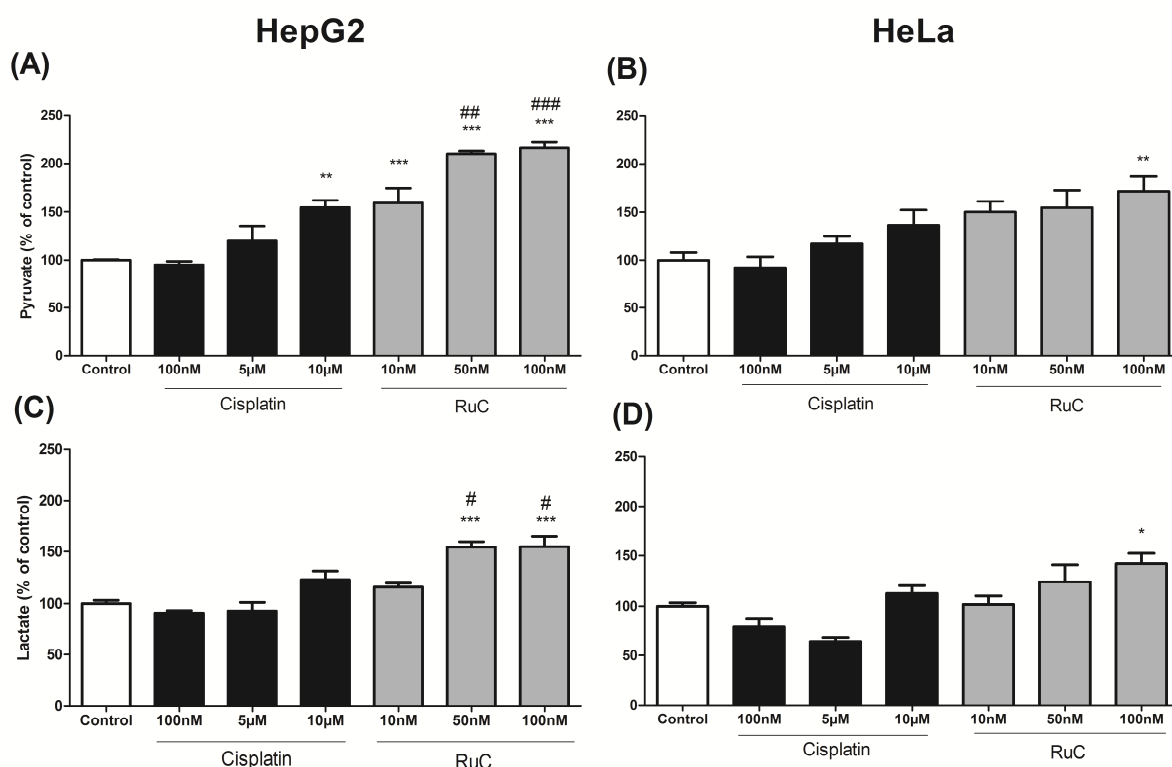


FIGURE 6. Levels of pyruvate (**A** and **B**) and lactate (**C** and **D**) released by HepG2 and HeLa cells treated with Cisplatin or RuC. The experimental conditions are described in the Materials and Methods. The cells (10^6 cell/ well) were seeded in 60 mm plates and treated with cisplatin (5 and 10 $\mu\text{mol/L}$) and RuC (10, 50 and 100 nmol/L) for 48 h. The pyruvate and lactate concentrations were measured in the culture medium. The results are expressed as the mean \pm SEM of four independent experiments. Symbols: * significantly different from the control (DMSO 0.1% - Vehicle); # significantly different from cisplatin 10 $\mu\text{mol/L}$; one, two, and three symbols refer to $p < 0.05$, $p < 0.01$, and $p < 0.001$, respectively.

3.4.6. Recovery curve of HepG2 and HeLa cells

HepG2 cells were not able to recover their proliferation capacity after treatments with the highest concentration of cisplatin and RuC during 9-days of culture in standard culture media (Fig. 7A). Similarly, the proliferation of HeLa cells was also impaired after cisplatin treatment. Differently, after the treatment with RuC these cells partially recover this capacity; however, the number of cells was lower than that observed in the absence of the compound (control) (Fig. 7B). It is also important to observe that 100 nmol/L cisplatin, corresponding to the highest concentration of RuC, did not inhibit the cells growth (Fig. 7A,B).

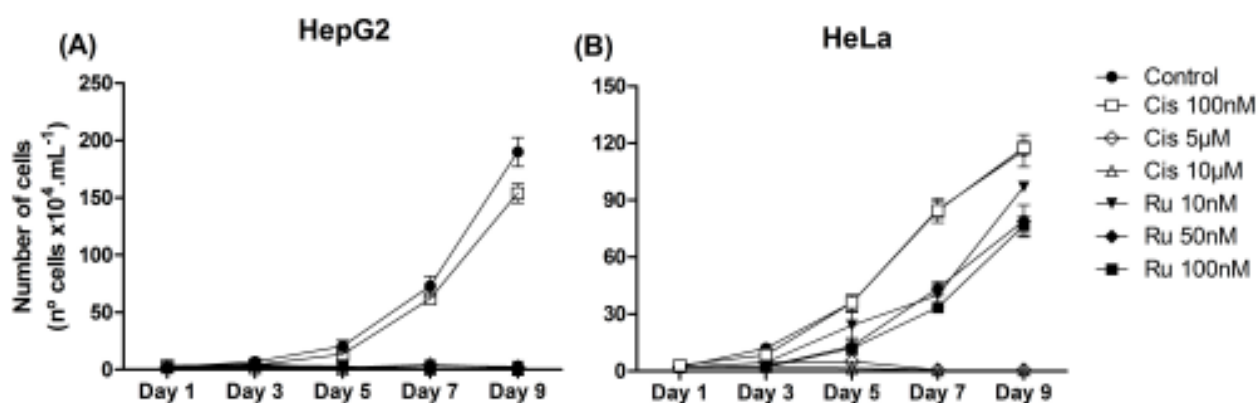


FIGURE 7. Recovery proliferation curve of HepG2 (**A**) and HeLa (**B**) cells. The experimental conditions are described in the Materials and Methods. The cells (10^6 cell/well) were plated in 6-well plate with a cell density of 1.5×10^4 cell and treated with cisplatin or RuC during the first 48h of the experiment protocol. After the treatment the proliferation of the cells were monitored during 9 days. The results are expressed as the numbers of cells ($10^4 \text{ cells} \times 10^4/\text{mL}$) of four independent experiments.

3.5. DISCUSSION

Innovative anticancer drugs with new molecular mechanisms of action are essential in chemotherapeutic treatment against specific cancer types, in order to overcome the toxic effects and the chemoresistance of the current compounds. In this context the organometallic compound RuC (Fig. 1) is a potential candidate for assays aiming a novel therapy for the treatment of HCC and cervix adenocarcinoma. In the toxicity screening of the RuC, HepG2 and HeLa were the most sensitive cells lineages over 24, 48 and 72 hours of exposure (Fig. 2). Therefore, as a model for the anticancer activity we performed the present *in vitro* study with the human liver cancer (HepG2) and cervix adenocarcinoma cancer (HeLa) cell lines. In all experiments, the cisplatin, a metallic chemotherapeutic agent, was used as a positive control, since this drug is used for treating HCC (KIM *et al.*, 2017; OGAWA *et al.*, 2017) and cervix tumors (DATTA *et al.*, 2017; SMALL *et al.*, 2017). After 48h of drug exposure the cell viability was evaluated using three assays (MTT, crystal violet, and neutral red), which evidenced that RuC was cytotoxic to HepG2 and HeLa cells at nanomolar concentration, while cisplatin promoted a similar effect at micromolar (μM) range (Fig. 3). Therefore, indicating the higher *in vitro* potency of RuC against HepG2 and HeLa cells in comparison to cisplatin. Interestingly, in the *in vivo* study with Walker-256 tumor-bearing rats, the cisplatin presented antitumor effect at lower dose (2 mg/kg i.p.) than RuC (10 mg/kg i.p.) (ALVES-DE-SOUZA *et al.*, 2017). These results confirm that different cancer cells have distinct sensitivities to chemotherapies, justifying studies that have been aimed in the comprehension of each cell response and/or resistance to anticancer treatments (WEISS *et al.*, 2017).

The effects of RuC in both cell lines may be associated with the reduced cell proliferation observed at the highest concentration of this compounds (Fig. 4). The higher cytotoxicity of RuC in comparison to cisplatin may result of the metal released from the complex, which is favored by the acidic environment of tumor cells. Thus, we evaluated the influence of RuC in the rates of lactate and pyruvate, which can reduce the cell pH. The results showed that RuC was able to increase the levels of pyruvate and lactate in both cells lines, while cisplatin increases only the pyruvate levels at the highest concentration (10 μM) in HepG2 cells. The increased levels of lactate and pyruvate in HepG2 cells

treated with RuC, more than lower the cell pH, also suggest an activation of glycolysis, probably a compensation of the strong inhibition of oxidative phosphorylation by the compound. These results are in agreement with the respiration assays, in which the effects of RuC were more pronounced than those of cisplatin on both cells lines. However, RuC at intermediate concentrations (10 and 50 nM) deeply inhibited the leak state only in HepG2 cells. Since the oxygen consumption during the leak state depends on the integrity of the inner mitochondrial membrane, it is possible suggest that RuC affects the membrane permeability of distinct ways in HepG2 and HeLa cells. These results suggest that the impairment of oxidative phosphorylation by RuC may be involved in its pronounced cytotoxicity. These results are in accordance with our previous data in Walker-256 tumor cells, in which RuC also promoted inhibition of the respiratory chain (ALVES-DE-SOUZA *et al.*, 2017).

Activation of mitochondrial signaling pathways and modulation of mitochondrial physiology may circumvent the drug-resistant phenotype of cancer cells (LYAKHOVICH; LLEONART, 2016; ESNER *et al.*, 2017). In this sense, a number of experimental drugs have also been reported to act primarily on mitochondria and then induce cancer cell death (LYAKHOVICH; GRAIFER, 2015; TAN *et al.*, 2015). In this sense, it is known that the modulation of key enzymes of the energetic metabolism of cancer, such as lactate dehydrogenase (LDH) (LU *et al.*, 2017), hexokinase II (HK-II) and 6-phosphofructo-1-kinase (PFK-1) (ZHU *et al.*, 2016), may compromise cellular bioenergetics leading to loss of membrane integrity, apoptosis or necrosis, and loss of recovery capacity leading to death (MALLEPALLY *et al.*, 2017). It is possible that cells under RuC effects have modified LDH activity, as we evidenced with the increased levels of its products (lactate and pyruvate), and then could induce cell necrosis, which was already reported in Walker-256 cells in tumor-bearing rats treated with RuC (ALVES-DE-SOUZA *et al.*, 2017).

Interestingly, the severity of RuC toxicity on hepatocarcinoma cells (HepG2) did not permit the recovery of these cells (Fig. 7), what was not observed for HeLa cells at the same concentration of the compound (100 nM). Over again, HepG2 cells were more affected by RuC than HeLa cells. This result may be related with resistance mechanisms of HeLa, which involved the

increased expression of certain proteins, such as Herpud1, a mammalian ubiquitin domain protein strongly induced by the unfolded protein response (UPR) (YANG *et al.*, 2017). The function of Herpud1 is not fully understood, but evidences suggest that it has an essential role in ER-membrane-associated protein degradation (ERAD) (SCHULZE *et al.*, 2005; OKUDA-SHIMIZU *et al.*, 2007). Herpud1 seems to have a cytoprotective function acting in endoplasmic reticulum stress (PAREDES *et al.*, 2015), autophagy by inducing the degradation of beclin-1 (QUIROGA *et al.*, 2013), and in oxidative stress of cancer cells (YANG *et al.*, 2017), conferring resistance to HeLa cells. Cervix adenocarcinoma remains the most lethal gynecological malignancy (SIEGEL *et al.*, 2013), and acquired resistance to the chemotherapy with platinum is considered the major factor in disease relapse (LIU *et al.*, 2015).

The current standard of care of cervix adenocarcinoma consists of radical surgery and platinum-based chemotherapy. The average 5-year survival rate of cervical cancer has reached 66% in developed countries, yet less than half patients from developing countries could live longer than 5 years (PISANI *et al.*, 1999; FRANCO, SCHLECHT, SASLOW, 2003; CHANG & GUO, 2017). In turn, the traditional therapies for HCC, such as resection, transplantation, or transarterial interventions, have limited efficacy and the available drugs may also affect non-tumor cells, promoting many serious side effects (MASUZAKI, 2008; BAFFY, 2015). In this context, our results show that RuC is more effective than cisplatin for both cell lines, HepG2 and HeLa, particularly on the first. This antineoplastic effect is related with the impairment of oxidative phosphorylation and the apparent activation of the glycolysis pathway. The fail of the hepatocarcinoma cells recovery reinforces the drastic toxicity of the RuC in these cells and encourage further investigations *in vitro* and *in vivo* models, aiming to evaluate the potential of this complex mainly for hepatocarcinoma treatment.

3.6. CONFLICT OF INTEREST

The authors have no conflicts of interest to declare.

3.7. ACKNOWLEDGMENTS

This work was supported by Conselho Nacional de Desenvolvimento Científico e Tecnológico (CNPq). CEAS and CRC are recipients of a graduate fellowship from Coordenação de Aperfeiçoamento de Pessoal de Nível Superior (CAPES). AA and SMSCC are recipients of a research fellowship (PQ 2) from CNPq.

3.8. REFERENCES

- ALAVIAN, K.N.; BEUTNER, G.; LAZROVE, E.; SACCHETTI, S.; PARK, H.A.; LICZNERSKI, P. *et al.* An uncoupling channel within the c-subunit ring of the F1FO ATP synthase is the mitochondrial permeability transition pore. **Proc Natl Acad Sci USA**. 111; 10580–10585; 2014.
- ALVES-DE-SOUZA, C.E.; ALVES DE SOUZA H.M.; STIPP, M.C.; CORSO C R.; GALINDO, C.; CARDOSO, C.R.; DITTRICH, R.L.; CAVALIERI, E.A.S.R.; KLASSEN, G.; CARLOS, R.M.; CADENA, S.M.S.C.; ACCO A. Ruthenium complex exerts antineoplastic effects that are mediated by oxidative stress without inducing toxicity in Walker-256 tumor-bearing rats. **Free Radical Biology & Medicine**. Accepted on June 16, 2017.
- APPAIX, F. MINATCHY, M.; RIVA-LAVIEILLE, C.; OLIVARES, J.; ANTONSSON, B.; SAKS, V.A. **Biochimica et Biophysica Acta**. 1456;75–181; 2000.
- BAFFY, G. Decoding multifocal hepatocellular carcinoma: an opportune pursuit, Hepatobiliary Surg. **Nutr**. 4; 206e210; 2015.
- BASRI, A.M.; LORD, R.M.; ALLISON, S.J.; RODRÍGUEZ-BÁRZANO, A.; LUCAS, S.J.; JANEWAY, F.D.; SHEPHERD, H.J.; PASK, C.M.; PHILLIPS, R.M.; MCGOWAN, P.C. Bis-picolinamide Ruthenium(III) Dihalide Complexes: Dichloride-to-Diiodide Exchange Generates Single trans Isomers with High Potency and Cancer Cell Selectivity. **Chemistry**. 22; 2017.
- BERNARDI, P.; DI LISA, F. The mitochondrial permeability transition pore: molecular nature and role as a target in cardioprotection. **J Mol Cell Cardiol**. 78C:100–106; 2015.
- BERNARDI, P.; KRAUSKOPF, A.; BASSO, E.; PETRONILLI, V.; BLACHLY-DYSON, E.; DI, L.F. The mitochondrial permeability transition from in vitro artifact to disease target. **FEBS J**. 273; 2077–2099; 2006.

BONORA, M.; BONONI, A.; DE, M.E.; GIORGI, C.; LEBIEDZINSKA, M.; MARCHI, S. *et al.* Role of the c subunit of the FO ATP synthase in mitochondrial permeability transition. **Cell Cycle**. 12; 674–683; 2013.

BONORA, M.; WIECKOWSK, M;R.; CHINOPOULOS, C.; KEPP, O.; KROEMER, G.; GALLUZZI, L. *et al.* Molecular mechanisms of cell death: central implication of ATP synthase in mitochondrial permeability transition. **Oncogene**. 34: 1608; 2015.

BORENFREUND, E.; PUERNER, J. A simple quantitative procedure using monolayer cultures for cytotoxicity assays (HTD/NR-90). **J Tissue Culture Methods**. 9:7–9; 1984.

BRADFORD, M. **Analytical Biochemistry**. 72 ;248–254; 1976.

CARDOSO, R. C.; LIMA, M. V. S.; CHELESK, J.; PETERSON, E. J.; VENÂNCIO, T.; FARRELL, N. P.; CARLOS, R .M. Luminescent Ruthenium Complexes for Theranostic Applications. **J. Med. Chem**. 57:4906-4915; 2014.

CHAN, S.L.; FU, W.; ZHANG, P.; CHENG, A.; LEE, J.; KOKAME, K.; MATTSON, M.P. Herp stabilizes neuronal Ca²⁺ homeostasis and mitochondrial function during endoplasmic reticulum stress. **J Biol Chem**. 279:28733–28743; 2004.

CHANG, L.; GUO, R. Comparison of the efficacy among multiple chemotherapeutic interventions combined with radiation therapy for patients with cervix cancer after surgery: A network meta-analysis. *Oncotarget*, 2017, Vol. 8, (No. 30), pp: 49515-49533. doi: 10.18632/**oncotarget**.17259.

CHENG, J.W.; LV, Y. New progress of non-surgical treatments for hepatocellular carcinoma. **Med Oncol**. 30:381; 2013.

CHEUNG, C.S.; CHUNG, K.K.; LUI, J.C.; LAU, C.P.; HON, P.M.; CHAN, J.Y. *et al.* Leachianone A as a potential anticancer drug by induction of apoptosis in human hepatoma HepG2 cells. **Cancer Lett**. 2007; 253:224– 35.

CHOU, T.C. Theoretical basis, experimental design, and computerized simulation of synergism and antagonism in drug combination studies. **Pharmacol Rev**. 58: 621-681; 2006.

CLARKE, M. J.; BAILEY, V. M.; DOAN, P. E.; HILLER, C. D.; LACHANCE-GALANG, K. J.; DAGHLIAN, H.; MANDAL, S.; BASTOS, C. M.; LANG, D. 1H NMR, EPR, UV-vis, and electrochemical studies of imidazole complexes of Ru(III). Crystal Structures of cis-[(Im)₂(NH₃)₄Ru(III)]Br₃ and [(1MeIm)₆Ru(III)]Cl₂·2H₂O. **Inorg. Chem**. 35:4896-4903; 1996.

CZOC, R. Pyruvate, Phosphoenolpyruvate and D-glycerate-2-phosphate Methods Enzym. **Anal, Weinheim**. 1446e1451;1974.

DASARI, S.; TCHOUNWOU, P.B. Cisplatin in cancer therapy: molecular mechanisms of action. **Eur J Pharmacol.** 5;740:364-78. 2014.

DATTA, N.R.; STUTZ, E.; LIU, M.; ROGERS, S.; KLINGBIEL, D.; SIEBENHÜNER, A.; SINGH, S.; BODIS, S. Concurrent chemoradiotherapy vs. radiotherapy alone in locally advanced **cervix** cancer: A systematic review and meta-analysis. **Gynecol Oncol.** 2017 May;145(2):374-385. doi: 10.1016/j.ygyno.2017.01.033.

ESNER, M.; GRAIFER, D.; LLEONART, M.E.; LYAKHOVICH, A. Targeting cancer cells through antibiotics-induced mitochondrial dysfunction requires autophagy inhibition. **Cancer Lett.** 1;384;60-69; 2017.

FRANCO, E.L.; SCHLECHT, N.F.; SASLOW, D. The epidemiology of cervical cancer. **Cancer J.** 2003; 9:348–59.

FRANKEN, N.A.; RODERMOND, H.M.; STAP, J.; HAVEMAN, J.; VAN BREE, C.; Clonogenic assay of cells in vitro. **Nat. Protoc.** 1;2315–2319; 2006.

FRASCA, D. R.; CLARKE, M. J. Alterations in the binding of $[\text{Cl}(\text{NH}_3)_5\text{RuIII}]^{2+}$ to DNA by glutathione: Reduction, autoxidation, coordination, and decomposition. **J. Am. Chem. Soc.** 121:8523-32; 1999.

GALLUZZI, L.; SENOVILLA, L.; VITALE, I.; MICHELS, J.; MARTINS, I.; KEPP, O.; CASTEDO, M.; KROEMER, G. Molecular mechanisms of cisplatin resistance. **Oncogene.** 12;3:1869-83; 2012.

GILLIES, R.J.; DIDIER, N.; DENTON, M. Determination of cell number in monolayer cultures. **Analytical Biochemistry.** 159; 109–113; 1986.

GIORGIO, V.; VON, S.S.; ANTONIEL, M.; FABBRO, A.; FOGOLARI, F.; FORTE, M. *et al.* Dimers of mitochondrial ATP synthase form the permeability transition pore. **Proc Natl Acad Sci USA.** 110; 5887–5892; 2013.

GNAIGER E. Bioenergetics at low oxygen: dependence of respiration and phosphorylation on oxygen and adenosine diphosphate supply. **Respir. Physiol.** 128; 277e297; 2001.

GNAIGER, E. Capacity of oxidative phosphorylation in human skeletal muscle: new perspectives of mitochondrial physiology. **Int. J. Biochem. Cell Biol.** 41; 1837e1845; 2009.

GUTMANN, I.; W.A.W., L-(p)-Lactate Determination with Lactate Dehydrogenase and NAD. **Methods Enzym. Anal, Weinheim.** 1464e1469; 1974.

HALESTRAP, A.P.; CLARKE, S.J.; JAVADOV, S.A. Mitochondrial permeability transition pore opening during myocardial reperfusion a target for cardioprotection. **Cardiovasc Res.** 61: 372–385; 2004.

HALESTRAP, A.P.; PASDOIS, P. The role of the mitochondrial permeability transition pore in heart disease. **Biochim Biophys Acta.**;1787;1402–1415; 2009.

HARTMANN, M.; LIPPONER, K. G.; KEPPLER, B. K. Imidazole release from the antitumor-active ruthenium complex imidazolium transtetrachlorobis (imidazole) ruthenate(III) by biologically occurring nucleophiles. **Inorg. Chem. Acta.** 267:137-141; 1998.

HORI, O.; ICHINODA, F.; YAMAGUCHI, A.; TAMATANI, T.; TANIGUCHI, M.; KOYAMA, Y.; KATAYAMA, T.; TOHYAMA, M.; STERN, D.M.; OZAWA, K.; KITAO, Y.; OGAWA, S. Role of Herp in the endoplasmic reticulum stress response. **Genes Cells.** 9:457–469; 2004.

HUTTER E., *et al.*, High-resolution respirometry a modern tool in aging research. **Exp. Gerontol.** 41; 103e109; 2006.

ISLAM, M.M.; BANERJEE, T.; PACKARD, C.Z.; KOTIAN, S.; SELVENDIRAN, K.; COHN, D.E.; PARVIN, J.D. HDAC10 as a potential therapeutic target in ovarian cancer. **Gynecologic Oncology.** 2017.

JAKUPEC, M. A.; REISNER, E.; EICHINGER, A.; PONGRATZ, M.; ARION, V. B.; GALANSKI, M.; HARTINGER, C. G.; KEPPLER, B. K. Redox-active antineoplastic ruthenium complexes with indazole: Correlation of in vitro potency and reduction potential. **J. Med. Chem.** 48:2831-2837; 2005.

KIM, J.K.; KIM, J.W.; LEE, I.J.; JOO, S.M.; LEE, K.H.; CHO, E.S.; YU, J.S.; JEON, T.J.; KIM, Y.; LEE, J.I.; LEE, K.S. Factors affecting survival after concurrent chemoradiation therapy for advanced hepatocellular carcinoma: a retrospective study. **Radiat Oncol.** 2017 Aug 15;12(1):133. doi: 10.1186/s13014-017-0873-1.

KOHLER, B.A.; SHERMAN, R.L.; HOWLADER, N.; JEMAL, A.; RYERSON, A.B.; HENRY, K.A.; BOSCOE, F.P.; CRONIN, K.A.; LAKE, A.; NOONE, A.M.; HENLEY, S.J.; EHEMAN, C.R.; ANDERSON, R.N.; PENBERTHY, L. Annual report to the nation on the status of cancer, 1975–2011, featuring incidence of breast cancer subtypes by race/ethnicity, poverty and state. **J. Natl. Cancer Inst.** 107; djv048; 2015.

LEE, J.M.; PARK, J.W.; CHOI, B.I. KLCSG-NCC Korea Practice Guidelines for the management of hepatocellular carcinoma: HCC diagnostic algorithm. **Dig. Dis.** 32; 764e777; 2014.

LIU, G.; YANG, D.; RUPAIMOOLE, R.; PECOT, C.V.; SUN, Y.; MANGALA, L.S.; LI, X.; JI, P.; COGDELL, D.; HU, L.; WANG, Y.; RODRIGUEZ-AGUAYO,

C.; LOPEZ-BERESTEIN, G.; SHMULEVICH, I.; DE CECCO, L.; CHEN, K.; MEZZANZANICA, D.; XUE, F.; SOOD, A.K.; ZHANG, W. Augmentation of response to chemotherapy by microRNA-506 through regulation of RAD51 in serous ovarian cancers. **J Natl Cancer Inst.** 20;107;7. 2015.

LU, Y.; KWINTKIEWICZ, J.; LIU, Y.; TECH, K.; FRADY, L.N.; SU, Y.T.; BAUTISTA, W.; MOON, S.I.; MACDONALD, J.; EWEND, M.G.; GILBERT, M.R.; YANG, C.; WU, J. Chemosensitivity of IDH1-Mutated Gliomas Due to an Impairment in PARP1-Mediated DNA Repair. **Cancer Res.** 1; 77; 1709-1718; 2017.

LYAKHOVICH, A.; LLEONART, M.E. Bypassing Mechanisms of Mitochondria-Mediated Cancer Stem Cells Resistance to Chemo- and Radiotherapy. **Oxid Med Cell Longev.** 1716341; 2016.

MALLEPALLY, R.R.; CHINTAKUNTALA, N.; PUTTA, V.R.; K, N.; VURADI, R.K.; P, M.; S, S.S.; CHITUMALLA, R.; JANG, J.; PENUMAKA, N.; SIRASANI, S. Synthesis, Spectral Properties and DFT Calculations of new Ruthenium (II) Polypyridyl Complexes; DNA Binding Affinity and in Vitro Cytotoxicity Activity. **J Fluoresc.** 22; 2017. doi: 10.1007/s10895-017-2091-5.

MASUZAKI, R.; OMATA, M. Treatment of hepatocellular carcinoma, Indian J. **Gastroenterol.** 27; 113e122; 2008.

MOSSMAN, T. Rapid colorimetric assay for cellular growth and survival: application to proliferation and cytotoxicity assays. **J Immunol Methods.** 65:55–63; 1983.

OGAWA, K.; KAMIMURA, K.; WATANABE, Y.; MOTAI, Y.; KUMAKI, D.; SEKI, R.; SAKAMAKI, A.; ABE, S.; KAWAI, H.; SUDA, T.; YAMAGIWA, S.; TERA, S. Effect of double platinum agents, combination of miriplatin-transarterial oily chemoembolization and cisplatin-hepatic arterial infusion chemotherapy, in patients with hepatocellular carcinoma: Report of two cases. **World J Clin Cases.** 2017 Jun 16;5(6):238-246. doi: 10.12998/wjcc.v5.i6.238.

OKUDA-SHIMIZU, Y.; HENDERSHOT, L.M. Characterization of an ERAD pathway for nonglycosylated BiP substrates, which require Herp. **Mol Cell.** 28:544–54; 2007. <https://doi.org/10.1016/j.molcel.2007.09.012>.

PADHYA, K.T.; MARRERO, J.A.; SINGAL, A.G. Recent advances in the treatment of hepatocellular carcinoma. **Curr Opin Gastroenterol.** 29:285–92; 2013.

PAREDES, F.; PARR, A. V.; TORREALBA, N.; NAVARRO-MARQUEZ, M.; GATICA, D.; BRAVO-SAGUA, R. *et al.* HERPUD1 protects against oxidative stress-induced apoptosis through downregulation of the inositol 1,4,5-

trisphosphate receptor. **Free Radic Biol Med.** 90:206–18; 2016;. <https://doi.org/10.1016/j.freeradbiomed.2015.11.024>.

PAREDES, F.; PARRA, V.; TORREALBA, N.; NAVARRO-MARQUEZ, M.; GATICA, D.; BRAVO-SAGUA, R.; TRONCOSO, R.; PENNANEN, C.; QUIROGA, C.; CHIONG, M.; CAESAR, C.; TAYLOR, W.R.; MOLGÓ, J.; SAN MARTIN, A.; JAIMOVICH, E.; LAVANDERO, S. HERPUD1 protects against oxidative stress-induced apoptosis through downregulation of the inositol 1,4,5-trisphosphate receptor. **Free Radic Biol Med.** 90: 206–218; 2016.

PIOT, C.; CROISILLE, P.; STAAT, P.; THIBAUT, H.; RIOUFOL, G.; MEWTON, N. *et al.* Effect of cyclosporine on reperfusion injury in acute myocardial infarction. **N Engl J Med.** 359; 473–481; 2008.

PISANI, P.; PARKIN, D.M.; BRAY, F.; FERLAY, J. Estimates of the worldwide mortality from 25 cancers in 1990. *Int J Cancer.* 1999; 83:18–29. 6. Franco EL, Schlecht NF, Saslow D. The epidemiology of cervical cancer. **Cancer J.** 2003; 9:348–59.

PIRES, A.D.R.A.; RUTHES, A.C.; CADENA, S.M.; ACCO, A.; GORIN, P.A.; IACOMINI, M. Cytotoxic effect of *Agaricus bisporus* and *Lactarius rufus* β -D-glucans on HepG2 cells. **Int J Biol Macromol.** 58:95-103; 2013.

QUIROGA, C.; GATICA, D.; PAREDES, F.; BRAVO, R.; TRONCOSO, R.; PEDROZO, Z.; RODRIGUEZ, A.E.; *et al.* Herp depletion protects from protein aggregation by upregulating autophagy. **Biochim Biophys Acta.** 1833; 3295–3305; 2013.

RAHA, S.; ROBINSON, B. H. Mitochondria, oxygen free radicals, disease and ageing. **Trends Biochem. Sci.** 25, 502- 508; 2000.

REATAZA, M.; IMAGAWA, D.K. Advances in managing hepatocellular carcinoma. **Front. Med.** 8; 175e189; 2014.

REISNER, E.; ARION, V. B.; DA SILVA, M. F. C. G.; LICHTENECKER, R.; EICHINGER, A.; KEPPLER, B. K.; KUKUSHKIN, V. Y.; POMBEIRO, A. J. L. Tuning of redox potentials for the design of ruthenium anticancer drugs - an electrochemical study of [trans-RuCl₄L(DMSO)]⁻ and [trans-RuCl₄L₂]⁻ complexes, where L = imidazole, 1,2,4-triazole, indazole. **Inorg. Chem.** 43:7083-7093; 2004.

REISNER, E.; ARION, V. B.; EICHINGER, A.; KANDLER, N.; GIESTER, G.; POMBEIRO, A. J. L.; KEPPLER, B. K. Tuning of redox properties for the design of ruthenium anticancer drugs: Part 2. Syntheses, crystal structures, and electrochemistry of potentially antitumor [RuIII/IICl₆-n(azole)_n]^z (n = 3, 4, 6) complexes. **Inorg. Chem.** 44:6704-6716; 2005.

RENNER, K. AMBERGER, A.; KONWALINKA, G.; KOFLER, R.; GNAIGER, E. Changes of mitochondrial respiration, mitochondrial content and cell size after

induction of apoptosis in leukemia cells. **Biochim. Biophys. Acta.** 1642; 115e123; 2003.

RÍOS-LUCI, C.; LEÓN, L.G.; MENA-CRUZ, A.; PÉREZ-ROTH, E.; LORENZO-LUIS, P.; ROMEROSA, A.; PADRÓN, J.M. Antiproliferative activity of dmoPTA-Ru(II) complexes against human solid tumor cells. **Bioorg Med Chem Lett.** 1;21; 15:4568-71;2011.

SANTOS, R. L. S. R.; VAN ELDIK, R.; DE OLIVEIRA SILVA, D. Kinetic and mechanistic studies on reactions of diruthenium(II,III) with biologically relevant reducing agents. **Dalton. Trans.** 42:16796-805; 2013.

SCANDURRA, F.M.; GNAIGER, E.; Cell respiration under hypoxia: facts and artefacts in mitochondrial oxygen kinetics. **Adv. Exp. Med. Biol.** 662; 7e25; 2010.

SCHLUGA, P.; HARTINGER, C. G.; EGGER, A. REISNER, E.; GALANSKI, M.; JAKUPEC, M.A.; KEPPLER, B.K. Redox behavior of tumor-inhibiting ruthenium(III) complexes and effects of physiological reductants on their binding to GMP. **Dalton. Trans.** 14:1796-1802; 2006.

SCHULZE, A.; STANDERA, S.; BUERGER, E.; KIKKERT, M.; VAN VOORDEN, S.; WIERTZ, E.; KONING, F.; KLOETZEL, P.M.; SEEGER, M. The ubiquitin-domain protein HERP forms a complex with components of the endoplasmic reticulum associated degradation pathway. **J Mol Biol.** 354; 1021–7; 2005. <https://doi.org/10.1016/j.jmb.2005.10.020>.

SEIDLMAYER, L.K.; JUETTNER, V.V.; KETTLEWELL, S.; PAVLOV, E.V.; BLATTER, L.A.; DEDKOVA, E.N. Distinct mPTP activation mechanisms in ischaemia–reperfusion: contributions of Ca²⁺, ROS, pH, and inorganic polyphosphate. **Cardiovascular Research.** 106; 237–248; 2015.

SIEGEL, R.; NAISHADHAM, D.; JEMAL, A. Cancer statistics, 2013. **CA Cancer J Clin.** 63;1:11–30; 2013.

SRIRAMAN, S.K.; SALZANO, G.; SARISOZEN, C.; TORCHILIN V. Anti-cancer activity of doxorubicin-loaded liposomes co-modified with transferrin and folic acid. **European Journal of Pharmaceutics and Biopharmaceutics.** 105; 40–49; 2016.

STØVING, D.C.; ALEJO, P.H.S; TSOLAKOU, T.; ALEXANDER, S.C.; GAMMELGAARD, B.; YELLOL, G.S.; RUIZ, J.; LAMBERT, I.H., STÜRUP, S. In vitro characterization of a novel C,N-cyclometalated benzimidazole Ru(II) arene complex: stability, intracellular distribution and binding, effects on organic osmolyte homeostasis and induction of apoptosis. **Metallomics.** 7;5:885-95; 2015.

STROBER, W. Current protocols in immunology trypan blue exclusion test of cell viability. **Curr. Protoc. Immunol.** 2; 1-3; 2015.

TAI, X.; CAI, X.; ZHANG, Z.; WEI, R. Antitumor study of combined dihydroartemisinin and doxorubicin treatment. **Oncology letters**. 12: 3701-3706; 2016.

TAN, A.S.; BATY, J.W.; DONG, L.F.; BEZAWORK-GELETA, A.; ENDAYA, B.; GOODWIN, J.; BAJZIKOVA, M.; KOVAROVA, J.; PETERKA, M.; YAN, B.; PESDAR, E.A.; SOBOL, M. et al. Mitochondrial genome acquisition restores respiratory function and tumorigenic potential of cancer cells without mitochondrial DNA. **Cell Metab**. 6;21; 81-94; 2015.

TSAI, C.H.; HUNG, A.C.; CHEN, Y.Y.; CHIU, Y.W.; HSIEH, P.W.; LEE, Y.C.; SU, Y.H.; CHANG, P.C.; HU, S.C.; YUAN S.F. 3'-hydroxy-4'-methoxy- β -methyl- β -nitrostyrene inhibits tumor- igenesis in colorectal cancer cells through ROS-mediated DNA damage and mitochondrial dysfunction. **Oncotarget**. 2; 2017. doi: 10.18632/oncotarget.14996.

UHL, P.; FRICKER, G.; HABERKORN, U.; MIER, W. Current status in the therapy of liver diseases. **Int J Mol Sci**. 15:7500–12; 2014.

WALLACE, D.C. Genetics: Mitochondrial DNA in evolution and disease. **Nature**. 28; 535; 7613:498-500; 2016.

WARBURG, O. On the origin of cancer cells. **Science**. 123:309-314; 1956.
WEISS, G.R.; SHAFFER, D.W.; DEMOOR, C.; RINALDI, D.A.; RODRIGUEZ, G.I.; ECKARDT, J.R.; STEPHENS, C.; VON HOFF, D.D. A randomized phase I study of oral etoposide with or without granulocyte-macrophage colony-stimulating factor for the treatment of patients with advanced cancer. **Anticancer Drugs**. 7;402-9; 1996.

WOO, H.Y.; HEO, J. New perspectives on the management of hepatocellular carcinoma with portal vein thrombosis. **Clin. Mol. Hepatol**. 21; 115e121; 2015.

YAN, L.; LIU, W.; ZHANG, H.; LIU, C.; SHANG, Y.; YE, Y.; ZHANG, X.; LI, W. Ube2g2-gp78-mediated HERP polyubiquitylation is involved in ER stress recovery. **J Cell Sci**. 127:1417–1427; 2014.

YANG, L.; MU, Y.; CUI, H.; LIANG, Y.; SU, X. MiR-9-3p augments apoptosis induced by H₂O₂ through down regulation of Herpud1 in glioma. **PLoS One**. 21;12; e0174839; 2017. doi: 10.1371/journal.pone.0174839.

ZHU, W.; YE, L.; ZHANG, J.; YU, P.; WANG, H.; YE, Z.; TIAN, J. PFK15, a Small Molecule Inhibitor of PFKFB3, Induces Cell Cycle Arrest, Apoptosis and Inhibits Invasion in Gastric Cancer. **PLoS One**. 26;11; e0163768; 2016.

4. SEGUNDO ARTIGO CIENTÍFICO

Artigo aceito pela revista *Free Radical Biology & Medicine* (ISSN: 0891-5849) em 16 de junho de 2017.

Ruthenium complex exerts antineoplastic effects that are mediated by oxidative stress without inducing toxicity in Walker-256 tumor-bearing rats

Carlos Eduardo Alves de Souza¹, Helen de Moraes Alves de Souza¹, Maria Carolina Stipp¹, Claudia Rita Corso¹, Claudia Martins Galindo¹, Carolina Riverin Cardoso², Rosangela Locatelli Dittrich³, Edneia Amancio de Souza Ramos Cavalieri⁴, Giseli Klassen⁴, Rose Maria Carlos², Sílvia Maria Suter Correia Cadena⁵, Alexandra Acco^{1*}

¹Department of Pharmacology, Federal University of Parana, Curitiba, Brazil

²Department of Chemistry, Federal São Carlos University, São Carlos, Brazil

³Department of Veterinary Medicine, Federal University of Parana, Curitiba, Brazil

⁴Department of Basic Pathology, Federal University of Parana, Curitiba, Brazil

⁵Department of Biochemical and Molecular Biology, Federal University of Parana, Curitiba, Brazil

*** Corresponding author:**

Alexandra Acco, Federal University of Paraná (UFPR), Biological Science Sector, Department of Pharmacology, Anexo I, Centro Politécnico, Cx. P. 19031, Curitiba – Paraná – Brazil, Zip Code 81531-980

Phone: +55 (41) 3361-1742; Fax: +55 (41) 3266-2042

E-mail: aleacco@ufpr.br

4.1. ABSTRACT

The present study evaluated the *in vivo* antitumor effects and toxicity of a new Ru(II) compound, cis-(Ru[phen]₂[ImH]₂)²⁺ (also called RuphenImH [RuC]), against Walker-256 carcinosarcoma in rats. After subcutaneous inoculation of Walker-256 cells in the right pelvic limb, male Wistar rats received 5 or 10 mg·kg⁻¹ RuC orally or intraperitoneally (i.p.) every 3 days for 13 days. A positive control group (2 mg·kg⁻¹ cisplatin) and negative control group (vehicle) were also used. Tumor progression was checked daily. After treatment, tumor weight, plasma biochemistry, hematology, oxidative stress, histology, and tumor cell respiration were evaluated. RuC was effective against tumors when administered i.p. but not orally. The highest i.p. dose of RuC (10 mg.kg⁻¹) significantly reduced tumor volume and weight, induced oxidative stress in tumor tissue, reduced the respiration of tumor cells, and induced necrosis but did not induce apoptosis in the tumor. No clinical signs of toxicity or death were observed in tumor-bearing or healthy rats that were treated with RuC. These results suggest that RuC has antitumor activity through the modulation of oxidative stress and impairment of oxidative phosphorylation, thus promoting Walker-256 cell death without causing systemic toxicity. These effects make RuC a promising anticancer drug for clinical evaluation.

Keywords: tumor, rats, Walker-256, ruthenium, RuphenImH, oxidative stress

4.2. INTRODUCTION

The increasing incidence of neoplastic diseases shows that more effective chemotherapeutic agents with lower toxicity are needed to improve patients' well-being and adherence to treatment. Cisplatin (cis-diaminedichloroplatinum II) is a chemotherapeutic drug that is used to treat solid tumors of the ovaries, cervix, testis, lungs, head, and neck [1,2]. However, cisplatin treatment is accompanied by adverse dose-limiting effects, such as nephrotoxicity, ototoxicity, neurotoxicity, gastrointestinal toxicity, and bone marrow toxicity [3,4]. Significant side effects and drug resistance limit the clinical applications of cisplatin and have stimulated the development of non-platinum metal-based therapies [5-7]. Based on the chemical structure of cisplatin, ruthenium (Ru)III complexes have been shown to have important antitumor properties in numerous *in vitro* and *in vivo* tumor models and lower systemic toxicity than platinum(II) compounds [8,9].

The Ru(III) complexes NAMI-A ([Him][trans-RuCl₄(DMSO)(im)], im = imidazole), KP1019 ([Hind]-[trans-(RuCl₄[ind]₂), ind = indazole), and its Na⁺ analogue KP1339 have been shown to have therapeutic effects that are similar to cisplatin but are more selective for tumor cells [10-12]. The biological targets of NAMI-A and KP1019 have not yet been thoroughly elucidated. Both of these compounds are able to target DNA and proteins, suggesting multiple pathways or pathways that are different from those of cisplatin [13-15]. NAMI-A [16] is selective for metastatic cells, whereas KP1019 [17] acts only on primary tumors. Both of these compounds exhibit excellent activity against colorectal tumor cells [18]. Previous studies suggested that both Ru(III) complexes act as pro-drugs. In biological media, their actions against tumor cells are activated by the

reduction to Ru(II) by biological reducing agents, such as glutathione, ascorbic acid, cysteine, and cytochrome c [19-23]. Ru(II) interacts with DNA, proteins, and other biomolecules to disturb the function of tumor cells [24]. Electrochemical experiments have shown that this reduction is favored in tumor tissue compared with healthy tissue because of the low oxygen concentration (i.e., hypoxia) and acid pH that are caused by the intense production of lactic acid in solid tumors [25-27].

Cancer cells must rewire cellular metabolism to satisfy the demands of tumor cell growth and proliferation. Most tumor cells rely on adenosine triphosphate synthesis by glycolysis rather than oxidative phosphorylation, a phenomenon known as the Warburg effect [28]. This process was initially attributed to mitochondrial dysfunction, but this mechanism is now being reevaluated because of the important role of this organelle in cancer. In fact, in cancerous states, anaplerotic and cataplerotic mitochondrial reactions work together to provide sufficient biosynthetic precursors to sustain cell growth and proliferation. Thus, in contrast to Warburg's first observations, the maintenance of functional mitochondria appears to be a key process for cancer cell survival and proliferation [29,30]. Consequently, intense mitochondrial energy metabolism becomes an important source of reactive oxygen species (ROS) [31], such as superoxide anion ($O_2^{\cdot-}$) [32,33], nitric oxide (NO^{\cdot}) [34], protonated superoxide (HO_2^{\cdot}), hydrogen peroxide (H_2O_2), peroxynitrite ($ONOO^-$) [35,36] and hydroxyl (HO^{\cdot}), all of which are extremely reactive. Cisplatin acts in tumor cells through the production of ROS. Similarly, the activation of Ru(II) by the oxidation of Ru(III) in tumor cells plays a crucial role in the oxidative process and electron transport in the respiratory chain. These findings encouraged us to

study the antitumor activity, oxidative balance, mitochondrial activity, and toxicity of a novel Ru(II) compound: (cis-[Ru(L-L)2(L)2]²⁺), in which L-L is 1,10-phenanthroline (phen) and L is imidazole (ImH). Hereinafter, this compound is referred to as RuphenImH or RuC [37]. We performed *in vivo* and *in vitro* studies using a Walker-256 carcinosarcoma cell model. This tumor grows fast, induces cachexia and oxidative stress, and has high metabolic demands.

4.3. MATERIAL AND METHODS

4.3.1. Chemicals

D-Mannitol, HEPES, rotenone, FCCP, oligomycin, L-glutamine, sodium bicarbonate, penicillin, streptomycin, and Roswell Park Memorial Institute (RPMI) 1640 medium were purchased from Sigma Chemical Co. (St. Louis, MO, USA). All of the other chemicals were of the highest commercially available purity. Cisplatin (cis-diaminedichloroplatinum II [CDDP]) was obtained commercially (Platinil, Quiral Química, Juiz de Fora, Brazil). The ruthenium complex (RuphenImH [RuC]; IUPAC nomenclature: cis-[Ru(1,10-phenanthroline)₂(imidazole)₂]²⁺) was synthesized by the laboratory of Dr. Rose Maria Carlos (Department of Chemistry, Federal University of São Carlos, São Carlos, SP, Brazil) and kindly donated for the execution of this work. The RuC complex (Fig. 1A) was synthesized through the reaction of imidazole with cis-(Ru[phen]₂Cl₂) in H₂O/ETOH (1:1). The removal of solvent and addition of hexafluorophosphate induced precipitation of the complex as a dark red powder. The composition and molecular structure of the complex was confirmed by CHN analyses and NMR spectroscopy as described by Cardoso *et al.* [37].

4.3.2. Methods

4.3.2.1. *Animal Handling and Ethical Issues*

Male Wistar rats, weighing 180-220 g, were obtained from the Central Animal House of the Federal University of Paraná (Curitiba, Brazil). The animals were housed in plastic cages (41 cm × 32 cm × 16.5 cm) with four rats per cage and food (Nuvital®) and water available *ad libitum*. They were maintained in a temperature-controlled room (22°C ± 2°C) under a 12 h/12 h light/dark cycle (lights on at 7 AM). All of the experimental protocols that involved animals were performed in accordance with the recommendations of Brazilian laws for the scientific management of animals and the Principles of Laboratory Animal Care (NIH Publication no. 85-23, revised 1985). The Institutional Animal Ethics Committee of the Federal University of Paraná revised and approved all of the procedures in the present study (certificate no. 822).

4.3.2.2. *Handling and Inoculation of Walker-256 Tumor Cells*

The maintenance of Walker-256 cells in Wistar male rats was performed by weekly passages (4 or 5) through intraperitoneal (i.p.) inoculation according to Vicentino *et al.* [38]. After 5-7 days, the animals developed ascites. The rats were then euthanized, and ascitic fluid was collected and centrifuged at 1126 × *g* for 10 min at 4°C. The supernatant was discarded, and the precipitate was resuspended in 1 ml of phosphate-buffered saline (PBS; 16.5 mM phosphate, 137 mM NaCl, and 2.7 mM KCl). The viability of tumor cells was assessed by the Trypan blue exclusion method in a Neubauer chamber. Approximately 10⁷ Walker-256 cells were injected subcutaneously in the right pelvic limb in each rat for preclinical trials using the solid tumor model.

4.3.2.3. *Experimental Design and Sample Collection*

Treatment began 1 day after the subcutaneous inoculation of tumor cells and continued for 13 days. Ruthenium complex was dissolved in PBS that contained 2% Tween 80. Cisplatin was dissolved in PBS. Both compounds were used in a maximum volume of 0.3 ml per rat. The selected doses for RuC were 5 and 10 mg·kg⁻¹, administered orally by gavage (p.o.) or i.p. (RuC p.o. and RuC i.p. groups, respectively). Cisplatin was administered only i.p. (2 mg·kg⁻¹). The treatments were performed every 3 days to reduce toxicity. The control group received a similar volume of vehicle. For some of the parameters, a baseline group was added, which consisted of non-tumor-bearing rats that received vehicle during the experiment. The number of rats (*n*) in each group was 6-8. Following day 13 of treatment, all of the animals were anesthetized with an i.p. injection of 60 mg·kg⁻¹ ketamine (Quetamina, Vetnil, Louveira, Brazil) and 7.5 mg·kg⁻¹ xylazine (Kensol, König, Santana de Parnaíba, Brazil). Blood samples from the inferior cava vein were obtained for biochemical and hematological assays. The animals were euthanized, and the tumor, liver, lungs, kidneys, and spleen were removed and weighed, and tumor, liver and kidney tissues were stored at -80°C for further analyses.

4.3.2.4. *Biophysical Measurements*

During treatment, the tumor volume was calculated by measuring its diameter using a pachymeter according to Mizuno *et al.* [39]:

$$V (cm^3) = \frac{4\pi \cdot a^2 \cdot (b)}{3 \cdot 2}$$

where a is the smallest diameter, and b is the largest diameter (in centimeters). We also assessed the inhibitory effect, when appropriate, using the following formula:

$$\text{Tumor Suppression (\%)} = (1 - T/C)$$

where T is the average volume in the experimental group, and C is the average volume in the control group. The animals' body weight was daily checked. After recording the weight, we determined weight gain as the following:

$$\text{Weight Gain} = W_{\text{end}} - W_{\text{initial}}$$

where W_{end} is the body weight on the day of euthanasia, minus the tumor weight.

4.3.2.5. Plasma Biochemistry and Hematological Assays

Plasma samples were obtained after blood centrifugation at $3000 \times g$ for 10 min at 4°C . These samples were used to determine plasma urea, creatinine, alanine aminotransferase/serum glutamic pyruvic transaminase (ALT/SGPT), aspartate aminotransferase/serum glutamic oxaloacetic transaminase (AST/SGOT), and alkaline phosphatase (AP) using commercial kits (Kovalent, Reagelabor, São Paulo, Brazil) and an automated device (Cobas Mira, Roche Diagnostics, Germany). Hematological parameters were investigated using whole blood and a BC2800-Vet automated device (Mindray, Shenzhen, China).

4.3.2.6. Tumor Gene Expression

Tumor samples were homogenized in TRIzol reagent (Life Technologies, Carlsbad, USA) to extract RNA. Complementary cDNA was prepared from 500 ng RNA in a 20 µl reaction volume that contained 0.5 mmol deoxyribonucleotide triphosphate, 1 µmol oligodT, 10 U RNasin (Promega, Madison, USA), and a high-capacity polymerase enzyme kit (Life Technologies). The negative control consisted of adding all of the products that were needed for cDNA synthesis except the reverse transcriptase. Quantitative polymerase chain reaction was performed using a Step One Plus thermocycler with the 1x Syber Green PCR Master Mix Kit (Applied Biosystems, Life Technologies). The primers were prepared (Invitrogen, São Paulo, Brazil) with the following sequences: internal control (600 nM) *Gapdh* (forward: 5'-AAGGACCCCTTCATTGAC-3'; reverse: 5'-TCCACGACATACTCAC-3') and the apoptotic markers (200 nM) *Bcl-2* (forward: 5'-GACTGAGTACCTGAACCGGC-3'; reverse: 5'-AGTTCCACAAAGGCATCCAG-3'), *Bax* (forward: 5'-AAACTGGTGCTCAAGGCCC-3'; reverse: 5'-GGGTCGCGAAGTAGGAAAGG-3'), *p53* (forward: 5'-AGCGACTACAGTTAGGGGGTA-3'; reverse: 5'-ACAGTTATCCAGTCTTCAGGGG-3'), *caspase 3* (forward: 5'-GGTATTGAGACAGACAGTGG-3'; reverse: 5'-CATGGGATCTGTTTCTTTGC-3'), *Vegf* (forward: 5'-AGAAACCCAATGAAGTGGTG-3'; reverse: 5'-ACTCCAGGGCTTCATCATTG-3'), *Cat* (forward: 5'-TTCTACACTGAAGATGGTAACTG-3'; reverse: 5'-GAAAGTAACCTGATGGAGAGAC-3'), and *Nrf2* (forward: 5'-ATGTCACCAGCTCAAGGGCACAGTGC-3'; reverse: 5'-

CCATCCTCCCCGAACCTAGTT-3'). Relative expression levels were calculated as described previously [40].

4.3.2.7. *In vitro Free Radical-Scavenging Activity of RuC*

The reactivity of RuC and cisplatin with the stable free radical 2,2-diphenyl-1-picrylhydrazyl (DPPH) was measured using an adaptation of the method of Chen *et al.* [41]. The system consisted of 250 μl of a methanolic solution of DPPH (1 mg in 25 ml), which was then combined with 750 μl of six ascending test solutions of each product (1-300 $\mu\text{g}\cdot\text{mL}^{-1}$). The decrease in absorbance was measured after 5 min. A solution of the reducing agent ascorbic acid (50 $\mu\text{g}\cdot\text{mL}^{-1}$) was used as the positive control, and distilled water was used as the negative control. Considering possible color shifts in the solutions that occur because of naturally occurring pigments in the test substances, we included measurements of the absorbance of each solution prior to the addition of DPPH, which were subtracted from the final values. Absorbance was measured at 517 nm using a microplate reader (BioTek Synergy HT, BioTek Instruments, Winooski, USA).

4.3.2.8. *In vivo Oxidative Stress Parameter Assays*

4.3.2.8.1. *Lipid peroxidation rate.* The lipid peroxidation (LPO) rate was measured by the FOX-2 method [42]. This technique determines lipid hydroperoxide synthesis during peroxidation. Tumor, liver, and kidney samples were homogenized at 25000 rotations per minute and then dissolved in methanol (1:2 ratio). They were then centrifuged at $5000 \times g$ for 5 min at 4°C .

Absorbance of the supernatant was measured at 560 nm using a microplate reader. The results are expressed as $\text{nmol}\cdot\text{mg protein}^{-1}$.

4.3.2.8.2. *Catalase, superoxide dismutase, and glutathione-S-transferase activity.* For the biochemical analyses of these enzymes, liver, tumor, and kidney samples were homogenized in phosphate buffer, pH 6.5. Catalase (Cat) activity was measured according to Aebi [43]. The reaction was performed in a microplate reader and examined at 240 nm, and activity is expressed as $\text{nmol}\cdot\text{mg protein}^{-1}$. Superoxide dismutase (SOD) activity was measured as the ability of this enzyme to inhibit pyrogallol auto-oxidation according to the method of Gao *et al.* [44]. The reaction was performed in a 96-well microplate and examined at 440 nm. The amount of enzyme that inhibited the reaction by 50% (IC_{50}) was defined as one unit of SOD, and enzyme activity is expressed as Units of SOD $\cdot\text{mg protein}^{-1}$. The activity of glutathione-S-transferase (GST) was measured according to the method of Habig *et al.* [45], which is based on the ability of this enzyme to conjugate the substrate 2,4-dinitrochlorobenzene (DNCB) with reduced glutathione, forming a tioether that can be measured as an increase in absorbance at 340 nm. Glutathione-S-transferase levels are expressed as $\text{nmol}\cdot\text{min}^{-1}\cdot\text{mg protein}^{-1}$.

4.3.2.8.3. *Reduced glutathione levels.* Reduced glutathione (GSH) levels were measured according to the method of Sedlak and Lindsay [46] using tissue that was homogenized with trichloroacetic acid. After centrifugation at $13750 \times g$ for 10 min at 4°C, the absorbance of the reaction with 5,5'-dithiobis-(2-nitrobenzoic acid) in methanol was measured at 415 nm in a microplate reader. The individual values were interpolated into a standard curve of GSH and are expressed as $\mu\text{g}\cdot\text{g tissue}^{-1}$.

4.3.2.9. *Quantification of Tissue Proteins*

The quantification of proteins in organs and tumor samples was performed according to the method of Bradford [47]. The reaction was examined at 595 nm in a microplate reader using bovine serum albumin as the protein standard in the concentration curve. The amount of protein was used to calculate the oxidative stress parameters (Cat, SOD, GST, and LPO).

4.3.2.10. *Tumor and Organ Histology*

Fragments from tumor, kidney, and liver tissues were fixed in buffered 10% formalin at room temperature. After fixation, the samples were dehydrated in ethanol, cleared with xylol, and embedded in paraffin. Thin sections (4 mm) were then processed for histology. Tissues were stained with hematoxylin and eosin, and the resulting slides were evaluated by optic microscopy in a blinded fashion. The following parameters were evaluated in tumor tissue: necrosis, tumor infiltration, and apoptosis. The following Ehrlich tumor classification was used [48]: 0 (lesions within < 5% of tissue), 1 (lesions within 5-25% of tissue), 2 (lesions within 26-50% of tissue), 3 (lesions within 51-75% of tissue), and 4 (lesions within > 75% of tissue). The livers and kidneys were checked for lymphocytic infiltrates, cell tumefaction, edema, necrosis, and cytological characteristics. The lesions were classified according to intensity: negative (–), mild (+), moderate (++), and pronounced (+++).

4.3.2.11. *Oxygen Uptake of Walker-256 Ascitic Cells*

After four weekly passages of Walker-256 cells through i.p. inoculation [38], Wistar rats were euthanized, and ascitic fluid was collected and centrifuged at $570 \times g$ for 15 min at 4°C. The supernatant was discarded, and the precipitate was resuspended in 3.0 ml of $1.5 \text{ mmol} \cdot \text{L}^{-1}$ NaCl and incubated for 2 min to lyse the erythrocytes. Washing and lysis were performed until the complete removal of erythrocytes. The Walker-256 cells were resuspended in RPMI, and cell viability was assessed by the Trypan blue exclusion method in a Neubauer chamber. Cell respiration was then measured by high-resolution respirometry using an Oxygraph-2k device (Oroboros Instruments, Innsbruck, Austria) and two chambers at 37°C under gentle agitation. The oxygen uptake of 10^6 cells/chamber was monitored in RPMI immediately (time 0) and 10 min after incubation with RuC (10, 50, and 100 nmol^{-1}) or cisplatin (5 and $10 \text{ } \mu\text{mol}^{-1}$). The concentrations were based on our previous experiments, in which the IC_{50} values for cisplatin and RuC were 10 and 100 nmol^{-1} , respectively, within 48 h for HeLa and HepG2 cells (unpublished data). Oxygen consumption was determined in the different states of respiration as described previously [48-52]. The states of oxygen consumption were defined as the following: basal (oxygen consumption in the absence of inhibitors or uncouplers), leak (respiration in the presence of $2 \text{ } \mu\text{g} \cdot \text{ml}^{-1}$ oligomycin, which results in the reentry of protons into the mitochondrial matrix and represents respiration that is not coupled to ATP synthesis), and uncoupled (oxygen consumption in the presence of $0.5 \text{ } \mu\text{mol}^{-1}$ FCCP, which corresponds to the maximal respiratory capacity to restore the dissipated proton gradient due to the presence of the uncoupling agent). The oxygen flow in these states was corrected by subtracting non-mitochondrial

respiration, which was obtained after the addition of rotenone ($0.5 \mu\text{mol}^{-1}$) and antimycin ($3 \mu\text{g}\cdot\text{ml}^{-1}$). The results were analyzed using DataLab4 software and are expressed as the mean \pm standard error of the mean (SEM) oxygen flow of the cells by second ($\text{pmol}\cdot[\text{s} \times 1 \times 10^6 \text{ cells}]^{-1}$).

4.3.2.12. Statistical Analysis

Mean differences were determined by one-way analysis of variance (ANOVA) followed by the Bonferroni or Tukey *post hoc* test or two-way ANOVA followed by the Bonferroni test when comparing tumor growth curves. The data are expressed as mean \pm SEM. All of the analyses were performed using Prism 5.0 software (GraphPad, San Diego, USA). For all of the comparisons, values of $p < 0.05$ were considered statistically significant.

4.4. RESULTS

4.4.1. Biophysical Parameters

The tumor volume was measured daily beginning on day 5 (when it became palpable) until day 13. The groups that were treated with 5 and 10 $\text{mg}\cdot\text{kg}^{-1}$ RuC, p.o., and 5 $\text{mg}\cdot\text{kg}^{-1}$ RuC, i.p., did not differ from the control group (Fig. 1A). The groups that were treated with 10 $\text{mg}\cdot\text{kg}^{-1}$ RuC, i.p., and 2 $\text{mg}\cdot\text{kg}^{-1}$ cisplatin, i.p., presented 72% and 91% reductions of tumor volume, respectively, compared with the control group (Fig. 1B). Similarly, the 5 and 10 $\text{mg}\cdot\text{kg}^{-1}$ RuC, i.p., and cisplatin groups presented significant 60%, 89%, and 91% reductions of tumor weight, respectively (Fig. 1C). The cisplatin group exhibited significant weight loss during treatment, unlike the groups that received 5 $\text{mg}\cdot\text{kg}^{-1}$ RuC, p.o., and 5 and 10 $\text{mg}\cdot\text{kg}^{-1}$ RuC, i.p., which presented

similar weight recovery as the basal group, which surpassed the weight gain of the control group (Fig. 1D).

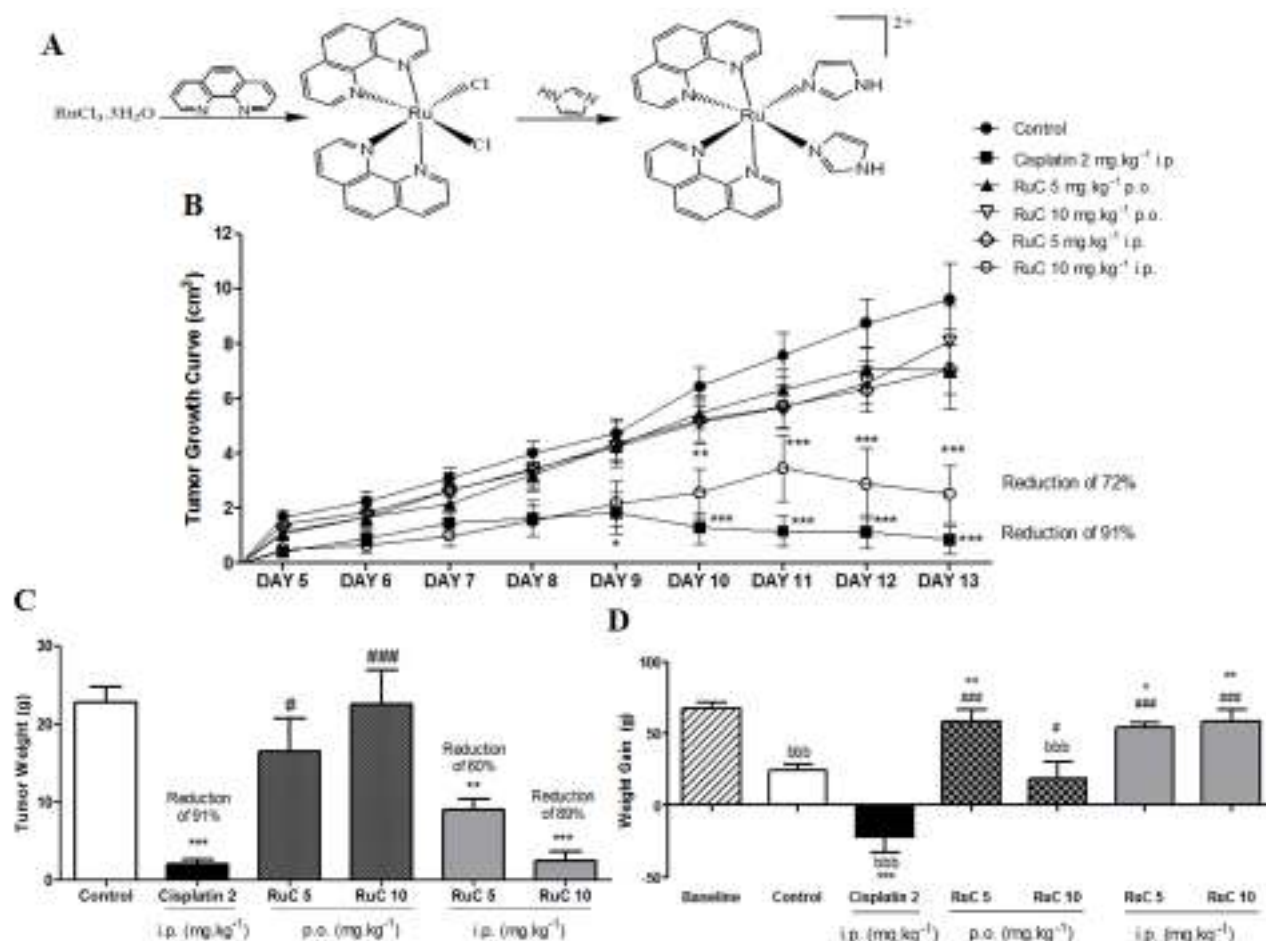


FIGURE 1. Synthetic route and chemical structure of ruthenium complex (RuphenImH [RuC]) (A), tumor growth curve (cm^3) (B), tumor weight (g) (C), and weight gain (D) in healthy (baseline) and tumor-bearing rats that were treated with RuC, cisplatin, and vehicle (control) for 13 days. The data are expressed as mean \pm SEM. The statistical analyses were performed using two-way (B) or one-way (C, D) ANOVA followed by the Bonferroni test. ^b, ^{*}, [#]Significant difference from baseline, control, and cisplatin groups, respectively (one, two, and three symbols refer to $p < 0.05$, $p < 0.01$, and $p < 0.001$, respectively).

The relative organ weight is presented as a percentage of body weight (Fig. 2). The relative weight of the kidney (Fig. 2A) decreased in animals that received cisplatin, similar to the $10 \text{ mg kg}^{-1} \text{ RuC, p.o.,}$ group. The weight of the

spleen (Fig. 2C) was increased by ~33% in most of the tumor groups, with the exception of the group that was treated with 10 mg·kg⁻¹ RuC, i.p.. The weights of the liver (Fig. 2B) and lungs (Fig. 2D) were not different among groups.

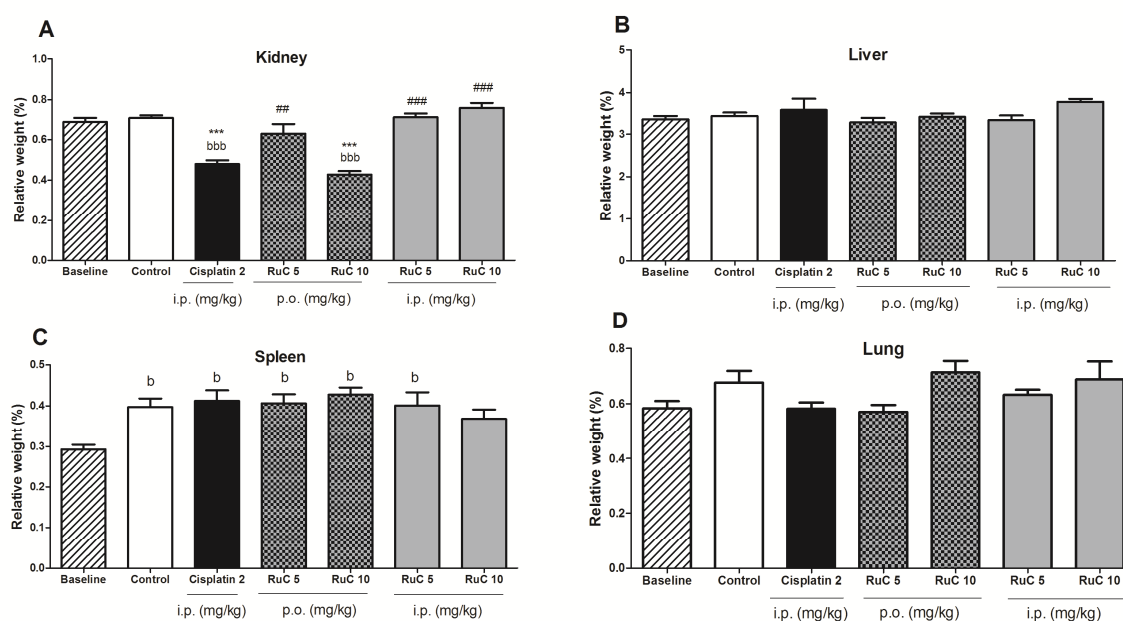


FIGURE 2. Relative weight (%) of the kidney (A), liver (B), spleen (C), and lung (D) in the healthy (baseline) group and tumor-bearing control, cisplatin, and RuC groups. The data are expressed as mean \pm SEM. The statistical analyses were performed using one-way ANOVA followed by the Bonferroni test. ^b, ^{*}, [#]Significant difference from baseline, control, and cisplatin groups, respectively (one, two, and three symbols refer to $p < 0.05$, $p < 0.01$, and $p < 0.001$, respectively).

4.4.2. Plasma Biochemistry and Hematology

The presence of the tumor (control) caused blood alterations compared with baseline values, including an increase in plasma creatinine, decrease in ALT, decrease in AP, and decrease in the number of lymphocytes. Cisplatin treatment accentuated these alterations, increasing the levels of urea and creatinine, decreasing AP, and decreasing granulocyte and monocyte counts, indicating some degree of toxicity. RuC treatment normalized most of these hematological alterations, with only a slight decrease in granulocyte and lymphocyte counts in rats that were treated with 10 mg·kg⁻¹ RuC, i.p. (Table 1).

TABLE 1. Plasma biochemistry and hematological parameters in Walker-256 tumor-bearing rats that were treated for 13 days with vehicle (control), cisplatin (2 mg·kg⁻¹), and RuC (5 and 10 mg·kg⁻¹) p.o. or i.p.

Experimental Group							
Parameter	Baseline	Control	Cisplatin 2 mg·kg ⁻¹ (i.p.)	RuC 5 mg·kg ⁻¹ (p.o.)	RuC 10 mg·kg ⁻¹ (p.o.)	RuC 5 mg·kg ⁻¹ (i.p.)	RuC 10 mg·kg ⁻¹ (i.p.)
Plasma Biochemistry							
Creatinine (mg/dL)	0.56 ± 0.1 ^{###}	0.63 ± 0.2 ^{b,###}	0.93 ± 0.1 ^{bbb,***}	0.50 ± 0.1 ^{###}	0.53 ± 1.0 ^{###}	0.51 ± 0.2 ^{###}	0.66 ± 0.4 ^{###}
Urea (mg/dL)	58.4 ± 4.7 ^{###}	54.8 ± 9.0 ^{###}	88.4 ± 4.8 ^{bbb,***}	63.7 ± 7.3 ^{##}	65.9 ± 10.1 ^{##}	60.4 ± 9.1 ^{##}	64.4 ± 5.3 ^{##}
ALT (U/L)	79.4 ± 53.4	47.5 ± 10.7 ^{bbb}	52.6 ± 13.5 ^{bb}	51.4 ± 14.8 ^{bb}	47.2 ± 20.2 ^{bbb}	52.0 ± 13.9 ^{bb}	58.2 ± 15.1 ^{bb}
AST (U/L)	123.1 ± 18.8	140.8 ± 36.4	82.5 ± 9.6 ^{bb,**}	137.6 ± 41.0 ^{##}	147.5 ± 42.6 ^{##}	140.5 ± 40.0 ^{##}	150.5 ± 34.5 ^{###}
AP (U/L)	222.0 ± 40.4	158.9 ± 39.0 ^{bb}	84.3 ± 44.6 ^{**}	171.5 ± 32.0	200.5 ± 81.8	166.2 ± 28.9	155.1 ± 57.2 [#]
Hematology							
Lymphocyte (1 × 10 ³ /μl)	11.07 ± 1.9	9.39 ± 2.0 ^{bbb}	6.88 ± 1.4 [*]	9.38 ± 2.2	8.66 ± 1.8	10.13 ± 1.7	10.03 ± 1.5 [#]
Monocytes (1 × 10 ³ /μl)	0.41 ± 0.1	0.55 ± 0.3	0.22 ± 0.4 [*]	0.71 ± 0.3	0.71 ± 0.2	0.55 ± 0.3	0.56 ± 0.2
Granulocyte (1 × 10 ³ /μl)	2.98 ± 0.6	5.36 ± 2.76	2.68 ± 0.5 ^{**}	5.93 ± 2.6	6.42 ± 2.3	4.65 ± 2.0	4.42 ± 1.9 [*]

The data are expressed as mean ± SEM. The statistical analyses were performed using one-way ANOVA followed by the Bonferroni test. ^{b, *, #} Significant difference from baseline, control, and cisplatin groups, respectively (one, two, and three symbols refer to $p < 0.05$, $p < 0.01$, and $p < 0.001$, respectively).

4.4.3. Tumor Gene Expression

As shown in Fig. 1, the highest i.p. dose of RuC exerted a significant antitumor effect. Thus, we investigated the effects of the treatments on the expression of genes that are related to apoptosis, angiogenesis, and oxidative stress. We observed upregulation of the expression of *p53* (Fig. 3A), *Bax* (Fig. 3B), and *caspase 3* (Fig. 3D) and no changes in the expression of *Vegf* (data not shown) in tumors from animals that were treated with cisplatin. RuC treatment did not alter the expression of nuclear factor E2-related (*Nrf2*; Fig. 3F) or apoptosis- and angiogenesis-related genes, but it reduced the expression of catalase (*Cat*) compared with the cisplatin group (Fig. 3E).

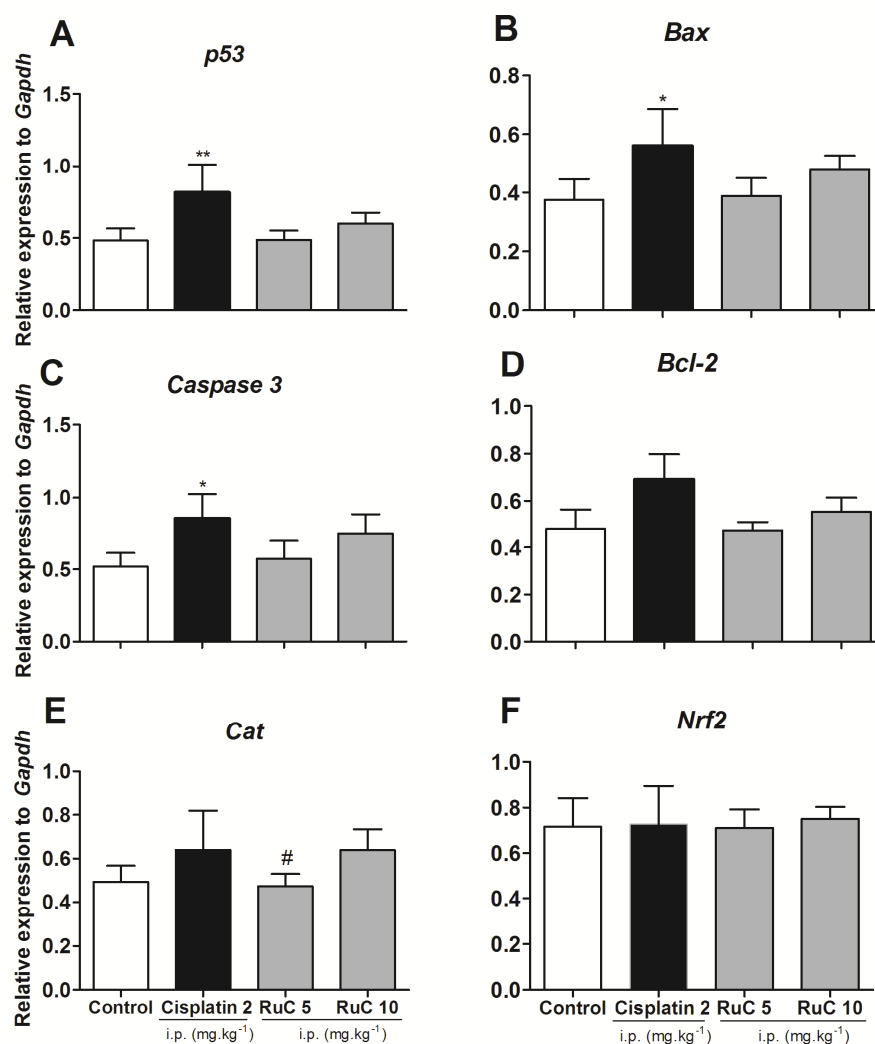


FIGURE 3. Gene expression of *p53* (A), *Bax* (B), *Bcl-2* (C), *caspase 3* (D), *catalase* (E), and *Nrf2* (F) in tumor tissue from animals that were treated i.p. with vehicle, cisplatin ($2 \text{ mg}\cdot\text{kg}^{-1}$), or RuC ($10 \text{ mg}\cdot\text{kg}^{-1}$) for 13 days at 3 days intervals. The data are expressed as mean \pm SEM and were analyzed by one-way ANOVA followed by the Bonferroni test. $*p < 0.05$, $**p < 0.01$, significant difference from control group; $^{\#}p < 0.05$, $^{\#\#}p < 0.01$, significant difference from cisplatin group.

4.4.4. *In vitro* Free Radical-Scavenging Activity

The antioxidant effect of RuC was evaluated *in vitro*, free from biological interference. Antioxidant activity was observed at all RuC concentrations ($1\text{--}300 \text{ }\mu\text{g}\cdot\text{mL}^{-1}$; Fig. 4A), indicating activity that was similar to the positive control (ascorbic acid). Cisplatin had antioxidant properties only at the highest concentrations (Fig. 4B).

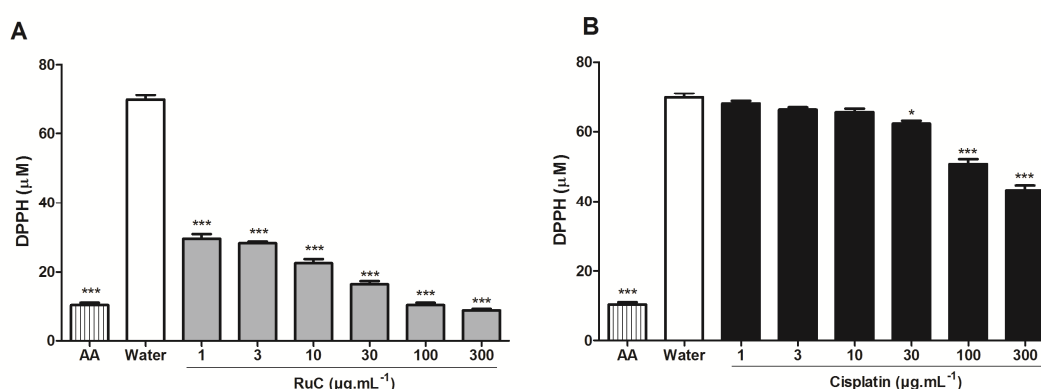


FIGURE 4. DPPH free radical-scavenging activity of RuC (A) and cisplatin (B) at various concentrations ($1\text{--}300 \text{ }\mu\text{g}\cdot\text{mL}^{-1}$). The negative control was distilled water. The positive control was ascorbic acid (AA, $50 \text{ }\mu\text{g}\cdot\text{mL}^{-1}$). The data are expressed as mean \pm SEM and were analyzed by one-way ANOVA followed by the Bonferroni test. $*p < 0.05$, and $***p < 0.001$, compared with negative control.

4.4.5. *In vivo* Oxidative Stress Parameters

We observed *in vitro* antioxidant effects of RuC. We then measured oxidative stress parameters in tumor, hepatic, and kidney tissues. RuC, mainly at the highest i.p. dose, induced significant changes in tumor tissue compared with the control group, reflected by decreases in SOD (-50%) and Cat (-45%)

activity and increases in GSH (43%) and LPO (27%) levels (Fig. 5A,D,J,M). The changes that were induced by cisplatin were less pronounced, in which it reduced SOD and Cat activities (Fig. 5A,D) and the LPO rate (Fig. 5M). The presence of Walker-256 tumors also caused systemic alterations, reflected by oxidative stress parameters in the liver (Fig. 5B, E, H, K, N) and kidney (Fig. 5C,F,I,L,O). The tumor elevated SOD activity, reduced Cat and GST activity, reduced GSH levels, and elevated LPO rates in both organs compared with the baseline group. These alterations were attenuated by RuC treatment but not cisplatin. RuC elevated GST activity and GSH and LPO levels in both organs and increased Cat activity in the kidneys. All of these parameters reached values that were similar to the baseline group.

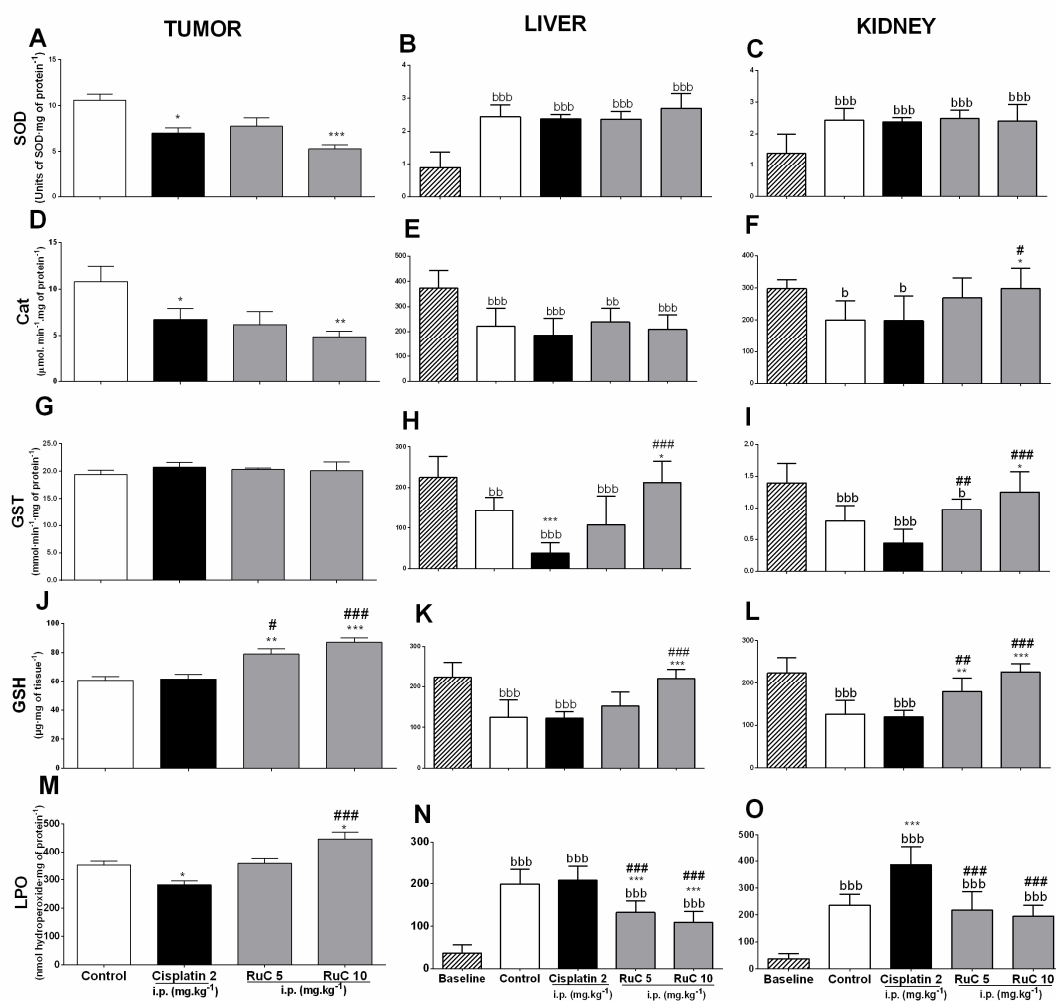


FIGURE 5. Oxidative stress parameters in Walker-256 tumor-bearing rats that were treated with vehicle, cisplatin ($2 \text{ mg} \cdot \text{kg}^{-1}$), and RuC (5 and $10 \text{ mg} \cdot \text{kg}^{-1}$) for 13 days. The following parameters were analyzed in tumor tissue (1st column), liver tissue (2nd column), and kidney tissue (3rd column): SOD activity (A-C), Cat activity (D-F), GST activity (G-I), GSH rate (J-L), and LPO rate (M-O). The data are expressed as mean \pm SEM and were analyzed by one-way ANOVA followed by the Bonferroni test. ^b, *, #Significant difference from baseline, control, and cisplatin groups, respectively (one, two, and three symbols refer to $p < 0.05$, $p < 0.01$, and $p < 0.001$, respectively).

4.4.6. Walker-256 Tumor Histology

Tumors in the control and RuC groups presented a high degree of necrosis and mononuclear infiltration, which were more intense (grade 4) with the dose of $10 \text{ mg} \cdot \text{kg}^{-1}$ RuC. Lymphocytes and plasmocytes were the predominant infiltrated cells. These features were different from cisplatin-treated rats, which presented a low degree of necrosis and cell infiltration in the tumors (grades 0 and 1, respectively). However, cell contraction, cytoplasmic eosinophilia, pycnosis, and cariorexis were observed, which are indicative of apoptosis (Fig. 6).

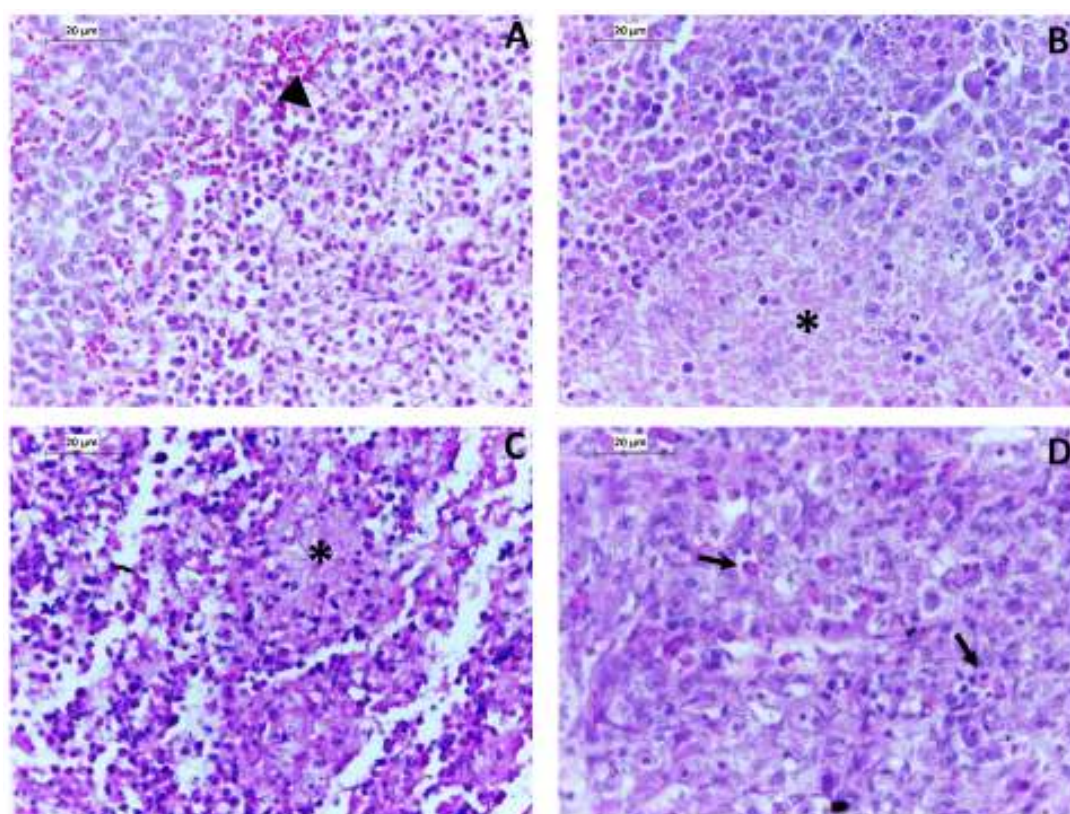


FIGURE 6. Walker-256 tumor histology in rats that were treated with vehicle (A), 5 mg.kg⁻¹ RuC (B), 10 mg.kg⁻¹ RuC (C), or cisplatin (D) for 13 days. Moderate (A-B) to severe (C) necrosis (*) was observed, accompanied by diffuse mononuclear infiltration (arrowhead). Cell contraction and cytoplasmic eosinophilia with pyknosis and cariorexis (arrows) were intensely observed in D.

4.4.7. Walker-256 Cell Respiration

We observed effects of RuC on oxidative processes *in vivo*. We then evaluated the direct actions of RuC on the respiration of Walker-256 cells that were collected from ascitic tumors. This assay was performed using non-permeabilized cells in an attempt to approximate the experimental physiological conditions. Figure 7 shows cell respiration immediately and 10 min after the addition of RuC and cisplatin. The rate of basal respiration (i.e., in the absence of inhibitors or uncouplers) was significantly decreased by both compounds and conditions. Cisplatin at the highest concentration (10 μ M) inhibited respiration immediately (40% reduction) and after 10 min of incubation (53% reduction). RuC at 100 nM inhibited respiration by 56% and 47% under the same conditions, respectively. In the leak state (i.e., in the presence of oligomycin), no differences were observed immediately in incubation. After 10 min of incubation cisplatin (10 μ mol⁻¹) and RuC (100 nmol⁻¹) inhibited respiration by 55% and 62%, respectively, compared with the control. In the presence of FCCP (uncoupled state), cisplatin and RuC also decreased oxygen flow similarly to the basal state (Fig. 7E, F).

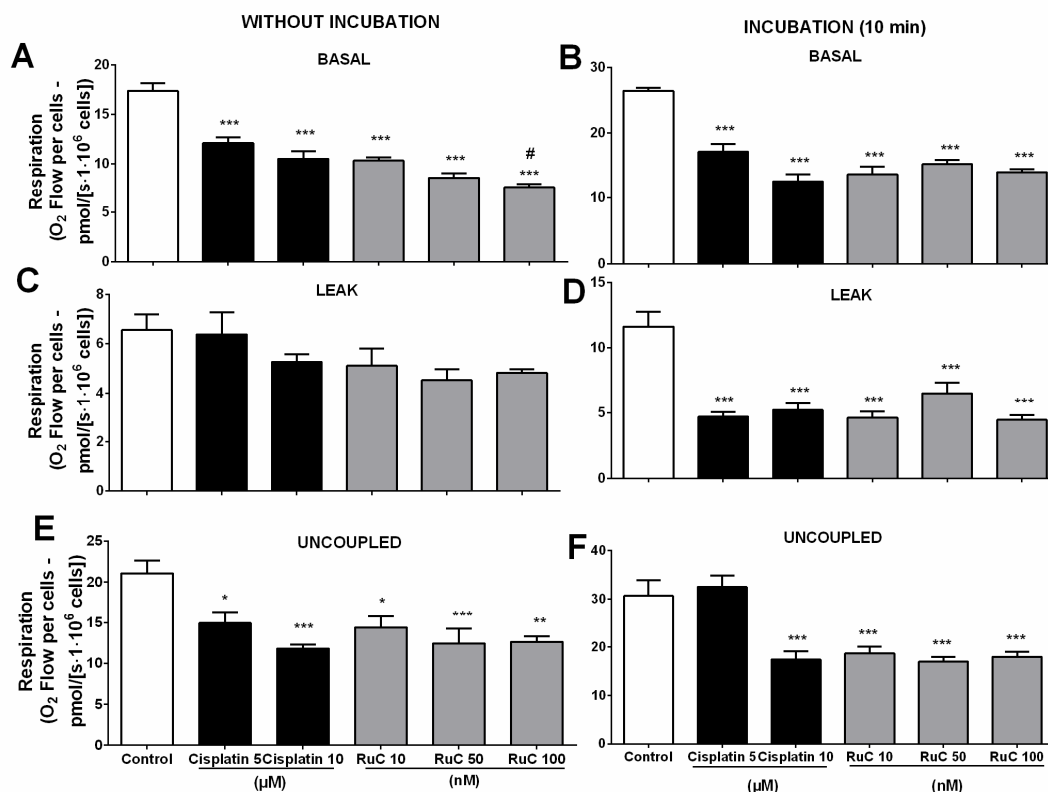


FIGURE 7. Effects of RuC and cisplatin on Walker-256 cell respiration. Oxygen consumption was determined immediately (1st column) or 10 min after (2nd column) the addition of compounds. Oxygen flow was determined by an Oroboros 2-K device in the absence of inhibitors or uncouplers (basal state) (A, B), in the presence of oligomycin (leak state) (C, D), and in the presence of FCCP (uncoupled state) (E, F). The data are expressed as the mean \pm SEM of six independent experiments. The data were analyzed by one-way ANOVA followed by the Tukey test. *, #Significant difference from control and cisplatin groups, respectively (one, two, and three symbols refer to $p < 0.05$, $p < 0.01$, and $p < 0.001$, respectively).

4.4.8. Toxicity Parameters in Healthy Rats

Cisplatin is a cytotoxic drug [37]. We compared the toxicity of RuC and cisplatin by evaluating toxicological parameters in healthy (non-tumor) rats that were treated for 13 days with 10 mg.kg⁻¹ RuC (i.p.) or 2 mg.kg⁻¹ cisplatin (i.p.), which exerted antitumor effects in Walker-256 tumor-bearing rats. The relative weights of the liver, spleen, and lung were not significantly different among groups (Fig. 8A-C). Significant weight loss (-141%) and an increase in kidney

weight (55%) were observed in the group that was treated with $2 \text{ mg} \cdot \text{kg}^{-1}$ cisplatin (i.p.) compared with the baseline group (Fig. 8E). These results were confirmed by histological analysis of the kidney and liver (Supplementary Fig. 1S). Only rats that were treated with cisplatin exhibited renal alterations (Fig. 8F), reflected by slight to moderate tumefaction of the tubular epithelium, predominantly in the internal cortex and external medullar regions, and occasional pycnosis and cariorexis, both indicative of cell death. No such changes were observed in the group that was treated with $10 \text{ mg} \cdot \text{kg}^{-1}$ RuC, i.p. (Fig. 8D, E). These results suggest low toxicity of RuC, which is consistent with the data from tumor-bearing rats (Table 1, Fig. 1D, 2, 5-liver and kidney).

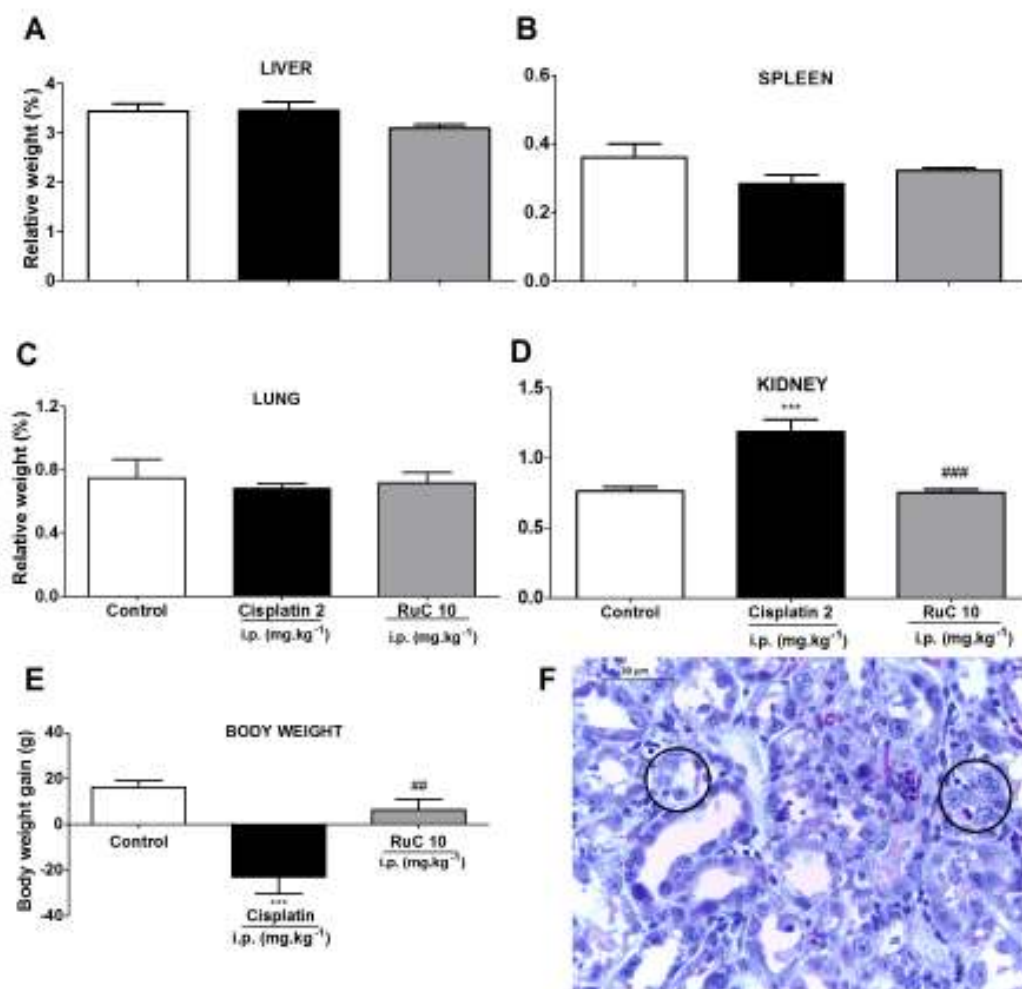


FIGURE 8. Relative weights of the liver (A), spleen (B), lung (C), and kidney (D) and body weight gain (E) in non-tumor-bearing rats that were treated with vehicle, cisplatin ($2 \text{ mg}\cdot\text{kg}^{-1}$), and RuC ($10 \text{ mg}\cdot\text{kg}^{-1}$), i.p., for 13 days at 3 day intervals. (F) Representative section of the kidney after cisplatin treatment (hematoxylin and eosin staining). Black circles indicate discrete to moderate tumefaction of the tubular epithelium. The data are expressed as mean \pm SEM and were analyzed by one-way ANOVA followed by the Bonferroni test. $**p < 0.01$, $***p < 0.001$, significant difference from control group; $^\#p < 0.01$, $^\#\#p < 0.001$, significant difference from cisplatin group.

4.5. DISCUSSION

The RuphenImH compound (RuC) exerted significant antitumor effects against Walker-256 carcinoma *in vivo*. We found that RuC inhibited tumor growth similarly to cisplatin (Fig. 1) but had less toxicity and did not cause weight loss. Toxicity and weight loss are common side effects of cisplatin treatment. The effectiveness of cisplatin as an anticancer agent has stimulated the search for cytotoxic compounds that contain heavy metals other than platinum and have lower systemic toxicity and greater efficacy. Many ruthenium complexes have been studied as antineoplastic compounds because of their actions in the tumor microenvironment [7], including $\text{cis-(Ru[1,10-phenanthroline]}_2\text{[imidazole]}_2\text{)}^{2+}$, which was used *in vivo* in the present study and previously in cell lineages [37]. Interestingly, our results clearly demonstrated that only i.p. administration of RuC had antitumor effects. Oral administration (5 and $10 \text{ mg}\cdot\text{kg}^{-1}$) did not produce such effects. These results suggest the following: (1) RuC may be hydrolyzed by gastric acids, (2) RuC may be poorly absorbed in the intestine, or (3) RuC may be first-pass biotransformed into inactive metabolites in the liver, thus losing its antineoplastic activity. To better understand the behavior of RuC in the gastrointestinal system, pharmacokinetic studies are necessary. The protein binding of Ru(III) complexes, particularly transferrin and albumin [54], likely impacts its biodistribution, pharmacokinetics,

and mechanism of action [55]. Thus, systemic injections may be the best mode of RuC treatment, similar to the cisplatin that is administered intravenously in chemotherapeutic protocols.

Considering the suppression of tumor growth by 89% that was induced by $10 \text{ mg} \cdot \text{kg}^{-1}$ RuC, which was similar to the 91% suppression that was exerted by $2 \text{ mg} \cdot \text{kg}^{-1}$ cisplatin, we investigated several parameters of the antineoplastic mechanism of action of RuC. We investigated the effects of RuC on protein genes that are related to cell apoptosis in tumor tissue. RuC did not alter the gene expression of key apoptosis-related genes, namely *p53*, *Bax*, *Bcl-2*, and *caspase 3* (Fig. 3), suggesting that apoptosis may not be involved in its antitumor activity against Walker-256 carcinoma. An *in vitro* experiment with RuC also reported the absence of caspase-3 cleavage in HCT116 $p53^{+/+}$ cells, indicating that apoptosis is not the pathway by which RuC promotes cell death [37]. Tumor histology corroborated these results (Fig. 6B,C), in which extensive areas of necrosis were observed, with no evidence of apoptosis. These results were clearly different for cisplatin, which induced the expression of the pro-apoptotic genes *p53*, *Bax*, and *caspase 3*, which is consistent with previous studies [56,57] and the histological features of apoptosis in tumors (Fig. 6D).

Considering the important modulation of oxidative stress in carcinogenesis, we performed assays to evaluate the antioxidant capacity of RuC. RuC prevented the oxidation of DPPH (Fig. 4), corroborating a previous study of Mohanraj *et al.* [58] that reported strong radical-scavenging properties of Ru(II) complexes. This activity was also confirmed locally in the tumor *in vivo* and systemically in kidney and liver tissues (Fig. 5). The modulation of oxidative stress in tumors may be related to the antitumor effect of RuC in rats, although

this compound did not alter the gene expression of *Nrf2* and *Cat* compared with the control group. These results may indicate that the modulation of oxidative stress by RuC does not occur at the genetic level but rather occurs posttranscriptionally and is related to the regulation of enzymatic activity (e.g., SOD and Cat). The non-influence of regulation of *Nrf2* expression by RuC is interesting because recent studies reported a contradictory role for this factor in cancer, which can suppress or promote oncogenesis [59,60]. Previous studies found evidence that the transient activation of *Nrf2* by inducing factors plays a protective role against cancer initiation in normal cells [59]. However, the upregulation of *Nrf2* can lead to the activation of cytoprotective genes, thus helping malignant cells withstand high levels of ROS and avoid apoptosis, eventually making them resistant to conventional anticancer therapy [60].

Reactive oxygen species play different roles in tumors than in healthy tissue because of variations in pH, hypoxia, and an increase in transferrin carriers in the tumor microenvironment. These factors can modulate the redox state and bioavailability of ruthenium in target tissue [61]. The reduction of Ru is facilitated by the presence of reducing conditions, such as hypoxia and GSH; both of these factors were influenced by RuC in Walker-256 cells. RuC treatment significantly increased GSH levels in tumor tissue (Fig. 5J). Tumors rapidly utilize oxygen and other nutrients, and the development of new blood vessels (i.e., angiogenesis) often fails to keep pace with tumor growth; therefore, there is usually lower O₂ content in tumor cells [61-63]. RuC apparently promotes inhibition of the respiratory chain, which could lead to more pronounced hypoxia (Fig. 7). Consequently, tumor cells would depend more on glycolysis for energy and may generate excess lactic acid, which lowers pH in

the tumor microenvironment. Lactic acid leads Ru(II) to maintain a redox state, thus promoting longer cytotoxic actions [64,65].

The presence of Walker-256 tumors also creates systemic oxidative conditions [65], with metabolic damage in several organs. In addition to the tumor, the modulation of oxidative stress by RuC also occurred systemically, demonstrated by oxidative stress that was observed in kidney and liver tissues (Fig. 5). RuC treatment improved several parameters, such as GSH, GST, and LPO in both kidney and liver tissue and Cat in kidney. These results may be related to the low toxicity of RuC in tumor-bearing (Fig. 1,2) and healthy (Fig. 8) rats compared with animals that were treated with cisplatin. In the present study, the animals that received cisplatin presented considerable body weight loss, which is consistent with previous studies. High-dose cisplatin ($20 \text{ mg} \cdot \text{kg}^{-1}$, i.p.) also caused body weight loss, functional and structural alterations of the kidney and liver (i.e., renohepatic toxicity), and mortality [66]. In the present study, Walker-256 tumor-bearing rats that were treated with low-dose cisplatin ($2 \text{ mg} \cdot \text{kg}^{-1}$, i.p.) presented a decrease in kidney weight, increase in plasma creatinine and urea levels, and lympho-, mono-, and granulocytopenia. Renal lesions were also observed in tumor-free rats that were treated with cisplatin, reflected by an increase in organ weight, tumefaction of the tubular epithelium, pycnosis, and cariorexis. These lesions represent acute and sublethal alterations, characterized by cell edema and changes in the cytoplasm/nucleus ratio. Macroscopically, these lesions were reflected by increases in organ weight and pallor, depending of the degree of cell tumefaction and vascular compression. Our findings corroborate the nephrotoxic effect of cisplatin in tubular cells by necrosis or apoptosis [68]. The loss of plasma membrane

integrity and cytosolic edema are early indications of necrosis, whereas the retraction and loss of cell adhesion are features of apoptosis [69]. Additionally, high-dose cisplatin ($10 \text{ mg}\cdot\text{kg}^{-1}$, i.p.) resulted in mortality in an entire group of Walker-256 tumor-bearing rats within a few days (data not shown). Altogether, these results demonstrate the systemic toxicity, mainly nephrotoxicity, of cisplatin in rats. Nephrotoxicity is a well-known adverse effect of this drug [70,71,61], which involves increases in oxidative stress, inflammation, and apoptosis and activation of the mitogen-activated protein kinase pathway [72]. Cisplatin elicits oxidative stress in mitochondria in the proximal tubule and endothelial cells, followed by the generation of a secondary wave of reactive oxygen/nitrogen species, the deterioration of mitochondrial structure and function, and renal damage [73]. The present study showed that cisplatin caused renal oxidative damage, manifested by an increase in LPO levels and depletion of the antioxidant molecules GSH, SOD, and Cat in the kidneys compared with the baseline group (Fig. 5). As cisplatin accumulated in kidney tissue, it covalently bound with the proteins that in turn impacted antioxidant enzymes [74]. Consequently, tissue damage occurred, and renal markers (i.e., creatinine and urea) were released into the circulatory system. RuC at a dose that exerted antitumor effects ($10 \text{ mg}\cdot\text{kg}^{-1}$, i.p.) did not induce these adverse effects, which may be attributable to the antioxidant, antiproliferative, and antitumor features of this ruthenium complex [75,76]. Rats that were treated with RuC presented baseline values of creatinine, urea, AST, ALT, AP, lymphocytes, monocytes, and granulocytes and no changes in body or organ weight. Therefore, our results demonstrate the antineoplastic and non-cytotoxic effects of RuC for the treatment of solid tumors. These features are desirable

for the treatment of cancer patients with cachexia, a syndrome that decreases quality of life and increases mortality [77].

In conclusion, the present results suggest that RuC exerts antitumor activity by modulating oxidative stress, impairing oxidative phosphorylation, and thus promoting Walker-256 cells death, with no systemic toxicity in rats under the present conditions. These effects of RuC make it a promising anticancer drug that should be evaluated in further pharmacokinetic and pharmacodynamic studies and possibly clinical trials.

4.6. CONFLICT OF INTEREST

The authors have no conflicts of interest to declare.

4.7. ACKNOWLEDGMENTS

This work was supported by Conselho Nacional de Desenvolvimento Científico e Tecnológico (CNPq). AA, SMSCC and GK are recipients of a research fellowship from CNPq. CEAS, HMAS, MCS, CRC and CMG are recipients of a graduate fellowship from Coordenação de Aperfeiçoamento de Pessoal de Nível Superior (CAPES). The authors are thanks to Larissa Favaretto Galuppo and Flavia Caroline Collere for the inestimable help in the experiments.

4.8. AUTHOR CONTRIBUTIONS

CEAS, HMAS, and MCS performed the *in vivo* experiments. CR Corso and CMG performed the histological analysis; RMC and CR Cardoso produced the RuC compound. RLD performed the hematological and biochemistry assays. EASRC and GK performed the PCR assays. CEAS and SMSCC

performed the *in vitro* analysis. CEAS, SMSCC, and AA wrote the manuscript. AA was the researcher responsible for the project.

4.9. REFERENCES

- [1] Qu, K.; Lin, T.; Wei, J.; Meng, F.; Wang, Z.; Huang, Z.; Wan, Y.; Song, S.; Liu, S.; Chang, H.; Dong, Y.; Liu, C. Cisplatin induces cell cycle arrest and senescence via upregulating P53 and P21 expression in HepG2 cells. *J. South. Med. Univ.* 33:1253-1259; 2013.
- [2] Zhao, J. L.; Zhao, J.; Jiao, H. Synergistic Growth-Suppressive Effects of Quercetin and Cisplatin on HepG2 Human Hepatocellular Carcinoma Cells. *Appl. Biochem. Biotechnol.* 172:784-791; 2014.
- [3] Saleh, S.; El-Demerdash, E. Protective effects of L-arginine against cisplatin-induced renal oxidative stress and toxicity: role of nitric oxide. *Basic. Clin. Pharmacol. Toxicol.* 97:91-97; 2005.
- [4] Im, G. J.; Chang, J.; Lee, S.; Choi, J.; Jung, H. H.; Lee, H. M.; Ryu, S. H.; Park, S. K.; Kim, J. H.; Kim, H. J. Protective role of edaravone against cisplatin-induced ototoxicity in an auditory cell line. *Hear. Res.* 330:113-118; 2015.
- [5] Zhang, C. X.; Lippard, S. J. New metal complexes as potential therapeutics. *Curr. Opin. Chem. Biol.* 7:481-489; 2003.
- [6] Liu, H. K.; Berners-Price, S. J.; Wang, F. Y.; Parkinson, J. A.; Xu, J.; Bella, J.; Sadler, P. J. Diversity in G-selective DNA binding modes for an organometallic ruthenium arene complex. *Angew Chem. Int.* 45:8153-8156; 2006.
- [7] Li, L. L.; Cao, W. Q.; Zheng, W. J.; Fan, C. D.; Chen, T. F. Ruthenium complexes containing 2,6-bis(benzimidazolyl)pyridine derivatives induce cancer cell apoptosis by triggering DNA damage-mediated p53 phosphorylation. *Dalton. Trans.* 41:12766-12772; 2012.
- [8] Galanski, M.; Arion, V. B.; Jakupec, M. A.; Keppler, B. K. Recent developments in the field of tumor-inhibiting metal complexes. *Curr. Pharm. Des.* 9:2078-2089; 2003.
- [9] Levina, A.; Mitra, A.; Lay, P. A. Recent developments in ruthenium anticancer drugs. *Metallomics.* 1:458-470; 2009.
- [10] Rademaker-Lakhai, J. M.; Van Den Bongard, D.; Pluim, D.; Beijnen, J. H.; Schellens, J. H. M. A phase I and pharmacological study with imidazolium-trans-DMSO-imidazole tetrachlororuthenate, a novel ruthenium anticancer agent. *Clin. Cancer. Res.* 11:3717-3727; 2004.
- [11] Alessio, E.; Mestroni, G.; Bergamo, A.; Sava, G. Ruthenium antimetastatic agents. *Curr. Top. Med. Chem.* 4:1525-35; 2004.
- [12] Heffeter, P.; Bock, K.; Atil, B.; Hoda, M. A. R.; Korner, W.; Bartel, C.; Jungwirth, U.; Keppler, B. K.; Micksche, M.; Berger, W.; Koellensperger, G.

Intracellular protein binding patterns of the anticancer ruthenium drugs KP1019 and KP1339. *J. Biol. Inorg. Chem.* 15:737-748; 2010.

[13] Groessl, M.; Hartinger, C. G.; Dyson, P. J.; Keppler, B. K. CZE- ICP-MS as a tool for studying the hydrolysis of ruthenium anticancer drug candidates and their reactivity towards the DNA model compound dGMP. *J. Inorg. Biochem.* 102:1060-1065; 2008.

[14] Groessl, M.; Tsybin, Y. O.; Hartinger, C. G.; Keppler, B. K.; Dyson, P. J. Ruthenium versus platinum: Interactions of anticancer metallodrugs with duplex oligonucleotides characterised by electrospray ionisation mass spectrometry. *J. Biol. Inorg. Chem.* 15:677-688; 2010.

[15] Groessl, M.; Zava, O.; Dyson, P. J. Cellular uptake and subcellular distribution of ruthenium-based metallodrugs under clinical investigation versus cisplatin. *Metallomics.* 3:591-599; 2011.

[16] Sava, G.; Alessio, E.; Bergamo, A.; Mestroni, G. Sulfoxide Ruthenium Complex: non toxic tools for the selective treatment of solid tumor metastases. *Metallopharmaceuticals I – Topics in Biological Inorganic Chemistry.* 1:143-169; Elsevier; 1999.

[17] Hartinger, C.G.; Zorbas-Seifried, S.; Jakupec, M.; Kynast, B.; Zorbas, H.; Keppler, B. K. From bench to bedside-preclinical and early clinical development of the anticancer agent indazolium trans-[tetrachlorobis(1H-indazole) ruthenate(III)] (KP1019 or FFC14A). *J. Inorg. Biochem.* 100:891-904; 2006.

[18] Pongratz, M.; Schluga, P.; Jakupec, M. A; Transferrin binding and transferrin-mediated cellular uptake of the ruthenium coordination compound KP1019, studied by means of AAS, ESI-MS and CD spectroscopy. *J. Anal. At. Spectrom.* 19:46-51; 2004.

[19] Millis, K. K.; Weaver, K. H.; Rabenstein, D. L. Oxidation/reduction potential of glutathione. *J. Org. Chem.* 58:4144-4146; 1993.

[20] Jakupec, M. A.; Reisner, E.; Eichinger, A.; Pongratz, M.; Arion, V. B.; Galanski, M.; Hartinger, C. G.; Keppler, B. K. Redox-active antineoplastic ruthenium complexes with indazole: Correlation of in vitro potency and reduction potential. *J. Med. Chem.* 48:2831-2837; 2005.

[21] Reisner, E.; Arion, V. B.; da Silva, M. F. C. G.; Lichteneker, R.; Eichinger, A.; Keppler, B. K.; Kukushkin, V. Y.; Pombeiro, A. J. L. Tuning of redox potentials for the design of ruthenium anticancer drugs - an electrochemical study of [trans-RuCl₄L(DMSO)]⁻ and [trans-RuCl₄L₂]⁻ complexes, where L = imidazole, 1,2,4-triazole, indazole. *Inorg. Chem.* 43:7083-7093; 2004.

[22] Reisner, E.; Arion, V. B.; Eichinger, A.; Kandler, N.; Giester, G.; Pombeiro, A. J. L.; Keppler, B. K. Tuning of redox properties for the design of ruthenium anticancer drugs: Part 2. Syntheses, crystal structures, and electrochemistry of potentially antitumor [Ru^{III}/IrCl₆-n(azole)_n]^z (n = 3, 4, 6) complexes. *Inorg. Chem.* 44:6704-6716; 2005.

[23] Santos, R. L. S. R.; Van Eldik, R.; de Oliveira Silva, D. Kinetic and mechanistic studies on reactions of diruthenium(II,III) with biologically relevant reducing agents. *Dalton Trans.* 42:16796-805; 2013.

- [24] Schluga, P.; Hartinger, C. G.; Egger, A. Reisner, E.; Galanski, M.; Jakupec, M.A.; Keppler, B.K. Redox behavior of tumor-inhibiting ruthenium(III) complexes and effects of physiological reductants on their binding to GMP. *Dalton Trans.* 14:1796-1802; 2006.
- [25] Clarke, M. J.; Bailey, V. M.; Doan, P. E.; Hiller, C. D.; LaChance-Galang, K. J.; Daghlial, H.; Mandal, S.; Bastos, C. M.; Lang, D. ¹H NMR, EPR, UV-vis, and electrochemical studies of imidazole complexes of Ru(III). Crystal Structures of cis-[(Im)₂(NH₃)₄Ru(III)]Br₃ and [(1Melm)₆Ru(II)]Cl₂·2H₂O. *Inorg. Chem.* 35:4896-4903 1996.
- [26] Hartmann, M.; Lipponer, K. G.; Keppler, B. K. Imidazole release from the antitumor-active ruthenium complex imidazolium transtetrachlorobis(imidazole) ruthenate(III) by biologically occurring nucleophiles. *Inorg. Chim. Acta.* 267:137-141; 1998.
- [27] Frasca, D. R.; Clarke, M. J. Alterations in the binding of [Cl(NH₃)₅Ru(III)]²⁺ to DNA by glutathione: Reduction, autoxidation, coordination, and decomposition. *J. Am. Chem. Soc.* 121:8523-32; 1999.
- [28] Warburg O. On the origin of cancer cells. *Science.* 123:309-314; 1956.
- [29] Wallace, D. C. Mitochondria and cancer. *Nat. Rev. Cancer.* 12:685-698; 2012.
- [30] Chan, D. C. Fusion and fission: Interlinked processes critical for mitochondrial health. *Annu. Rev. Genet.* 46:265-287; 2012.
- [31] Kowaltowski, A. J.; Souza-Pinto, N. C.; Castilho, R. F.; Vercesi, A. E. Mitochondria and reactive oxygen species. *Free Rad. Biol. Med.* 47:333-343; 2009.
- [32] Brookes, P. S.; Yoon, Y.; Robotham, J. L.; Anders, M. W.; Sheu, S. S. Calcium, ATP, and ROS: a mitochondrial love-hate triangle. *Am. J. Physiol. Cell. Physiol.* 287:C817-833; 2004.
- [33] Adam-Vizi, V.; Chinopoulos, C. Bioenergetics and the formation of mitochondrial reactive oxygen species. *Trends Pharmacol. Sci.* 27:639-645; 2006.
- [34] Cadenas, E. Mitochondrial free radical production and cell signaling. *Mol. Asp. Med.* 25:17-26; 2004.
- [35] Hermes-Lima, M. Oxygen in biology and biochemistry: Role of free radicals. In: *Functional Metabolism: Regulation and Adaptation*, Wiley-Liss, 319-368; 2004.
- [36] Navarro, A. Mitochondrial enzyme activities as biochemical markers of aging. *Mol. Asp. Med.* 25:37-48; 2004.
- [37] Cardoso, R. C.; Lima, M. V. S.; Chelesk, J.; Peterson, E. J.; Venâncio, T.; Farrell, N. P.; Carlos, R. M. Luminescent ruthenium complexes for theranostic applications. *J. Med. Chem.* 57:4906-4915; 2014.
- [38] Vicentino, C.; Constantin, J.; Bracht, A.; Yamamoto, N. S. Long-chain fatty acid uptake and oxidation in the perfused liver of Walker-256 tumour-bearing rats. *Liver.* 22:342-350; 2002.

- [39] Mizuno, M.; Minato, K.; Ito, H.; Kawade, M.; Terai, H.; Tsuchida, H. Anti-tumor polysaccharide from the mycelium of liquid cultured *Agaricus blazei* mill. *Biochem. Mol. Biol. Int.* 47: 707-714; 1999.
- [40] Pfaffl, M. W. A new mathematical model for relative quantification in real-time RT-PCR. *Nucleic. Acids. Res.* 29:2002-7; 2001
- [41] Chen, Y.; Wang, M.; Rosen, R. T., Ho, C. T. 1.1-Diphenyl-2-picrylhydrazyl radical-scavenging active components from *Polygonum multiflorum thunb.* *J. Agric. Food. Chem.* 47:2226-2228; 1999.
- [42] Jiang, Z. Y.; Woollard, A. C.; Wolff, S. P. Lipid hydroperoxide measurement by oxidation of Fe^{2+} in the presence of xylenol orange. Comparison with the TBA assay and an iodometric method. *Lipids.* 26:853-856; 1991.
- [43] Aebi, H. Catalase in vitro. Orlando: Academic. Press. 121-126; 1984.
- [44] Gao, R.; Yuan, Z.; Zhao, Z.; Gao, X. Mechanism of pyrogallol autoxidation and determination of superoxide dismutase enzyme activity. *Bioelectrochem. Bioenerg.* 45:41-45; 1998.
- [45] Habig, W. H.; Papst, M. J.; Jakoby, W. B. Glutathione S-transferases: the first enzymatic step in mercapturic acid formation. *J. Biol. Chem.* 249:7130-7139; 1974.
- [46] Sedlak, J.; Lindsay, R. H. Estimation of total, protein-bound, and nonprotein sulfhydryl groups in tissue with Ellman's reagent. *Anal. Biochem.* 25:192-205; 1968.
- [47] Bradford, M. A rapid and sensitive method for the quantitation of microgram quantities of protein utilizing the principle of protein dye binding. *Anal. Biochem.* 72: 248-254; 1976.
- [48] Barakat, W.; Elshazly, S. M.; Mahmoud, A. A. *Spirulinaplatis* lacks antitumor effect against solid ehrlich carcinoma in female mice. *Adv. Pharmacol. Sci.* 2015:132873; 2015.
- [49] Gnaiger, E. Bioenergetics at low oxygen: dependence of respiration and phosphorylation on oxygen and adenosine diphosphate. *Respir. Physiol.* 128:277-297; 2001.
- [50] Renner, K.; Amberger, A.; Konwalinka, G.; Kofler, R.; Gnaiger, E. Changes of mitochondrial respiration, mitochondrial content and cell size after induction of apoptosis in leukemia cells. *Biochim. Biophys. Acta.* 1642:115-123; 2003.
- [51] Hutter, E.; Unterluggauer, H.; Garedew, A.; Jansen-Durr, P.; Gnaiger, E. High resolution respirometry – a modern tool in aging research. *Exp. Gerontol.* 41:103-109; 2006.
- [52] Gnaiger, E. Capacity of oxidative phosphorylation in human skeletal muscle: new perspectives of mitochondrial physiology. *Int. J. Biochem. Cell. Biol.* 41:1837-1845; 2009.
- [53] Scandurra, F. M.; Gnaiger, E. Cell respiration under hypoxia: facts and artefacts in mitochondrial oxygen kinetics. *Adv. Exp. Med. Biol.* 662:7-25; 2010.

- [54] Clarke, M. J.; Bitler, S.; Rennert, D.; Buchbinder, M.; Kelman, A.D. Reduction and subsequent binding of ruthenium ions catalyzed by subcellular components. *J. Inorg. Biochem.* 12:79-87; 1980.
- [55] Novohradský, V.; Bergamo, A.; Cocchietto, M.; Zajac, J.; Brabec, V.; Mestroni, G.; Sava, G. Influence of the binding of reduced NAMI-A to human serum albumin on the pharmacokinetics and biological activity. *Dalton Trans.* 44:1905-13; 2015.
- [56] Jiang, M.; Wei, Q.; Wang, J.; Du, Q.; Yu, J.; Zhang, L.; Dong, Z. Regulation of PUMA- α by p53 in cisplatin-induced renal cell apoptosis. *Oncogene.* 25:4056-4066; 2006.
- [57] Dugbartey, G. J.; Peppone, L. J.; de Graaf, I. A. An integrative view of cisplatin-induced renal and cardiac toxicities: Molecular mechanisms, current treatment challenges and potential protective measures. *Toxicology.* 4:58-66; 2016
- [58] Mohanraj, M.; Ayyannan, G.; Raja, G.; Jayabalakrishnan, C. Synthesis, spectral characterization, DNA interaction, radical scavenging and cytotoxicity studies of ruthenium(II) hydrazone complexes. *J. Photochem. Photobiol. B.* 158:164-73; 2016.
- [59] Jeddi, F.; Soozangar, N.; Sadeghi, M. R.; Somi, M. H.; Samadi, N. Contradictory roles of Nrf2/Keap1 signaling pathway in cancer prevention/promotion and chemoresistance. *DNA Repair (Amst).* 54:13-21; 2017.
- [60] Milkovic, L.; Zarkovic, N.; Saso, L. Controversy about pharmacological modulation of Nrf2 for cancer therapy. *Redox Biol.* 12:727-732; 2017.
- [61] Sharma, A. R.; Gangrade, D. M.; Bakshi, S. D.; John, J. S. Ruthenium complexes: potential candidate for anti-tumour activity. *Int. J. Chem. Tech. Res.* 6:828-837; 2014.
- [62] Harris, A. L. Hypoxia? a key regulatory factor in tumour growth. *Nat. Rev. Cancer.* 2:38-47; 2002.
- [63] Ferrara, N.; Gerber, H. P.; LeCouter, J. The biology of VEGF and its receptors. *Nat. Med.* 9:669-76; 2003.
- [64] Chen, L.; Endler, A.; Shibasaki, F. Hypoxia and angiogenesis: regulation of hypoxia-inducible factors via novel binding factors. *Exp. Mol. Med.* 41:849-857; 2009.
- [65] Fischer, B.; Heffeter, P.; Kryeziu, K.; Gille, L.; Meier, S. M.; Berger, W.; Kowol, C. R.; Keppler, B. K. Poly(lactic acid) nanoparticles of the lead anticancer ruthenium compound KP1019 and its surfactant-mediated activation. *Dalton Trans.* 43:1096-104; 2014.
- [66] Bartel, C.; Egger, A. E.; Jakupec, M. A.; Heffeter, P.; Galanski, M.; Berger, W.; Keppler, B. K. Influence of ascorbic acid on the activity of the investigational anticancer drug KP1019. *J. Biol. Inorg. Chem.* 16:1205-15; 2011.
- [67] K V, A.; Madhana, R. M.; Kasala, E. R.; Samudrala, P.K.; Lahkar, M. Morin hydrate mitigates cisplatin-induced renal and hepatic injury by impeding

oxidative/nitrosative stress and inflammation in mice. *J. Biochem. Mol. Toxicol.* 30:571-579; 2016.

[68] Lau, A. H. Apoptosis induced by cisplatin nephrotoxic injury. *Kidney Int.* 56:1295–1298; 1999.

[69] Lieberthal, W.; Triaca, V.; Levine, J. Mechanisms of death induced by cisplatin in proximal tubular epithelial cells: apoptosis vs. necrosis. *Am. J. Physiol. (Renal Physiol).* 39:F700–F708; 1996.

[70] Palipoch, S.; Punsawad, C. Biochemical and histological study of rat liver and kidney injury induced by cisplatin. *J. Toxicol. Pathol.* 26:293-9; 2013.

[71] Danduga, R. C. R.; Kumar, G. S.; Kumar, K. P.; Swamy, B. M. V.; Kishore, K. V. Nephroprotective activity of *Cissampelos pareira* Linn. extract against cisplatin induced nephrotoxic rats. *Am. J. Pharm. Tech. Res.* 5:480-488; 2015.

[72] Mallick, A.; More, P.; Syed, M. M.; Basu, S. Nanoparticle-mediated mitochondrial damage induces apoptosis in cancer. *ACS Appl. Mater. Interfaces.* 1:13218-31; 2016.

[73] Prabhu, V. V.; Kannan, N.; Guruvayoorappan, C. 1,2-Diazole prevents cisplatin-induced nephrotoxicity in experimental rats. *Pharmacol. Rep.* 65:980-90; 2013.

[74] Ognjanović, B. L.; Djordjević, N. Z.; Matić, M. M.; Obradović, J. M.; Mladenović, J. M.; Stajin, A. Š.; Saičić, Z. S. Lipid peroxidative damage on cisplatin exposure and alterations in antioxidant defense system in rat kidneys: a possible protective effect of selenium. *Int. J. Mol. Sci.* 13:1790-803; 2012.

[75] Flocke, L. S.; Trondl, R.; Jakupec, M. A.; Keppler, B. K. Molecular mode of action of NKP-1339 - a clinically investigated ruthenium-based drug - involves ER- and ROS-related effects in colon carcinoma cell lines. *Invest. New Drugs.* 34:261-8; 2016.

[76] Mohanraj, M.; Ayyannan, G.; Raja, G.; Jayabalakrishnan, C. Synthesis, spectral characterization, DNA interaction, radical scavenging and cytotoxicity studies of ruthenium(II) hydrazone complexes. *J. Photochem. Photobiol. B.* 158:164-73; 2016.

[77] Camargo, C. A.; da Silva, M. E.; da Silva, R. A.; Justo, G. Z.; Gomes-Marcondes, M. C.; Aoyama, H. Inhibition of tumor growth by quercetin with increase of survival and prevention of cachexia in Walker-256 tumor-bearing rats. *Biochem. Biophys. Res. Commun.* 25:638-42; 2011.

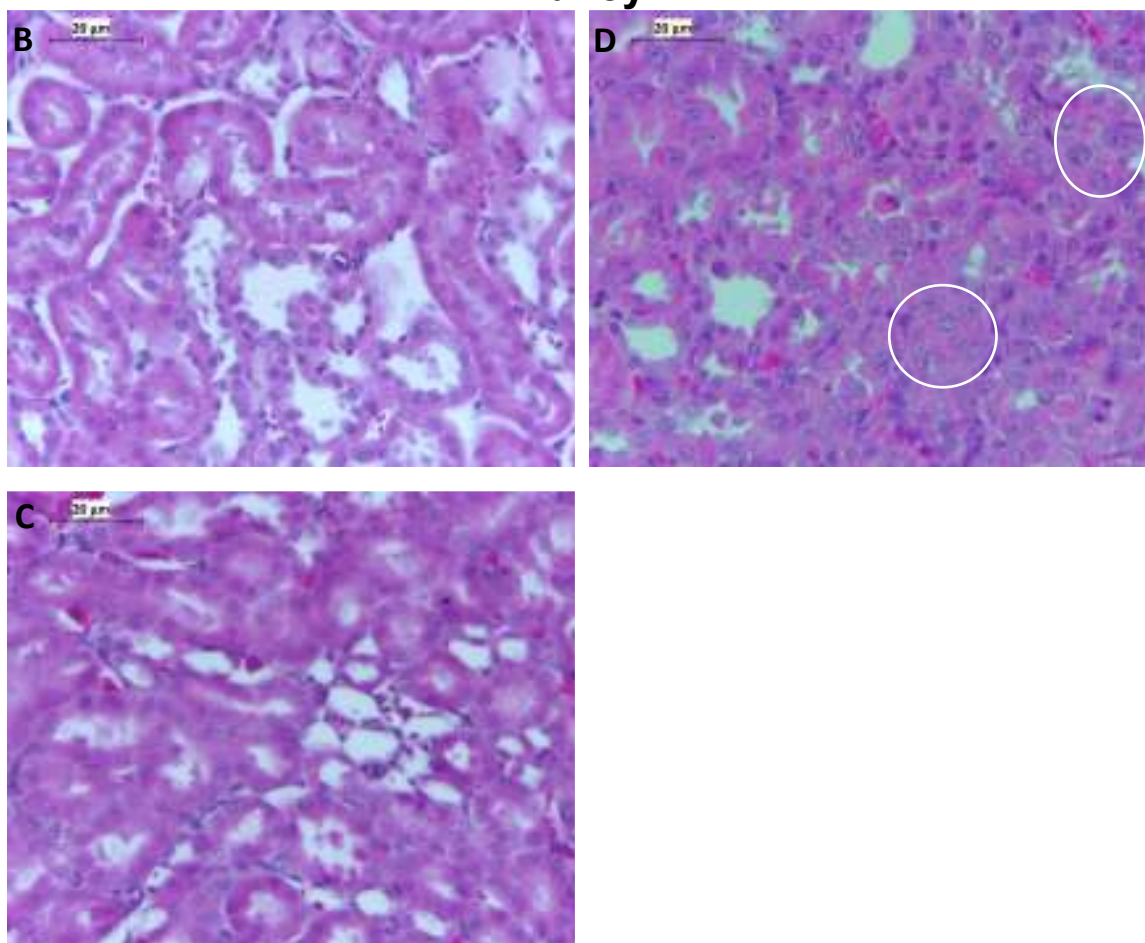
4.10. Supplementary Figure

A

Liver	
Treatment	Hepatocellular tumefaction
Vehicle	-
RuC (10 mg·kg ⁻¹ i.p.)	-
Cisplatin (2 mg·kg ⁻¹ i.p.)	+

Grade: (-) negative, (+) mild.

Kidney



SUPPLEMENTARY FIGURE S1. Histological observations of liver (A) and kidney of healthy rats treated with vehicle (B), 10 mg·kg⁻¹ RuC (C) or 2 mg·kg⁻¹ cisplatin (D) for 13 days. Typical tubular cells are represented in B and C. White circles indicate discrete to moderate tumefaction of the tubular epithelium, stained with hematoxylin and eosin.

5. CONSIDERAÇÕES FINAIS

As células neoplásicas não são responsivas aos controles de crescimento normais e expandem-se além de seus limites anatômicos normais, tendo um potencial de replicação ilimitado (SANTOS *et al.*, 2015). Em vista disso, as células são capazes de se evadir da morte celular programada (apoptose), escapar da resposta imune citotóxica do hospedeiro e fazer metástases. Estes processos tornam a terapia de câncer complicada, pois é preciso bloquear várias funções especializadas das células tumorais para impedir sua proliferação. Grande parte da inovação terapêutica contra o câncer advém de terapias alvo-dirigidas, bloqueando vias bioquímicas ou proteínas mutantes essenciais para a sobrevivência celular (ARAUJO *et al.*, 2017). Neste contexto, o presente trabalho foi realizado com o intuito de investigar os efeitos antineoplásicos de um novo composto, sintetizado a partir do metal rutênio, denominado RuphenImH ou RuC, como uma nova possibilidade terapêutica para tumores sólidos. O conjunto de resultados permite concluir que:

- 1) O composto RuC apresentou efeitos antineoplásicos *in vivo* contra o carcinoma murino Walker-256 e *in vitro* contra as linhagens cancerígenas humanas HepG2 e HeLa;
- 2) Os efeitos antineoplásicos parecem ser dependentes da interferência no metabolismo celular, principalmente reduzindo a respiração celular, estimulando a glicólise e elevando a produção de lactato e piruvato;
- 3) Níveis elevados de lactato celular podem ocasionar redução do pH celular, favorecendo a redução de Ru (III) para Ru (II) no microambiente tumoral, o que pode fomentar ainda mais seus efeitos nas células cancerígenas;
- 4) A transformação de Ru (III) para Ru (II) ocorre por agentes redutores, como o GSH, cujos níveis foram aumentados pelo tratamento com RuC no tecido tumoral, favorecendo a ação do rutênio nas células cancerígenas;
- 5) O GSH é apenas um dos parâmetros relacionados à regulação redox celular afetados pelo tratamento com RuC. No tecido tumoral Walker-

256 houve também aumento da taxa de LPO, o que favorece danos celulares por estresse oxidativo;

- 6) Em contrapartida, o RuC parece ter efeito dual na regulação do estresse oxidativo, pois aumentou o estresse no tecido tumoral favorecendo a morte de células cancerígenas, e reduziu o estresse oxidativo em órgãos saudáveis, como fígado e rins;
- 7) O efeito de proteção do RuC em células saudáveis foi também detectado nos estudos *in vitro*, uma vez que a linhagem de células renais embrionárias (HEK293) mostrou-se pouco sensível ao composto;
- 8) Das linhagens celulares humanas testadas, a HepG2 e a HeLa se mostraram mais sensíveis ao RuC, colocando-o como uma possível droga para o tratamento de tumores sólidos de fígado e cérvix uterina;
- 9) Em comparação com a cisplatina, controle positivo deste estudo, o composto de rutênio mostrou-se mais seletivo para células tumorais, tanto *in vivo* quanto *in vitro*, o que poderia representar menos efeitos adversos em indivíduos eventualmente tratados com o RuC;
- 10) Enquanto a cisplatina induziu morte de células cancerígenas por apoptose, o RuC parece induzir morte por necrose.

Em uma visão mais abrangente, considerando o câncer como um fenômeno multifatorial e multifacetado que supera os níveis biológicos e até pessoais de quem o apresenta, torna-se de altíssima importância em saúde pública estratégias de prevenção, combate e cuidados paliativos (SANTOS *et al.*, 2015). Neste sentido, o presente trabalho contribui com dados pré-clínicos de uma nova possibilidade terapêutica para cânceres, mais especificamente para tumores sólidos, a exemplo do hepatocarcinoma e do tumor cervical. Ressalta-se, no entanto, algumas limitações deste estudo, que não avaliou em profundidade a toxicidade do RuC e utilizou apenas um modelo sólido *in vivo*, não permitindo a extrapolação plena dos resultados para humanos. Mais estudos envolvendo toxicidade, caracterização do mecanismo de morte celular, farmacocinética e farmacodinâmica, são necessárias para estabelecer um perfil de segurança com a utilização do RuC em futuros estudos.

6. REFERÊNCIAS BIBLIOGRÁFICAS

ACCO, A.; BASTOS-PEREIRA, A. L.; DREIFUSS, A. A. Characteristics and Applications of the Walker-256 Rat Tumour. . In: S.G. Pandalai; Daniel Pouliquen. (Org.). *The Rat in Cancer Research: A Crucial Tool for All Aspects of Translational Studies*. 1 Ed. Trivandrum: **Research Signpost/ Transworld Research Network**. 2012.

AGOSTINO, D.; CLIFFTON, E.E. The Growth and Transplantability of the Carcinosarcoma of Walker 256 in the Ascitic Form. **Experientia**, v.24, n.2, p. 166-168, 1968.

AKIMOTO, M., YOSHIKAWA, M., EBARA, M., *et al.*, Relationship between therapeutic efficacy of arterial infusion chemotherapy and expression of P-glycoprotein and p53 protein in advanced hepatocellular carcinoma. **World J Gastroenterol**. v. 14; n.12; p. 868-73. 2006.

ALBUQUERQUE, K. M. *et al.* Cobertura do teste Papanicolaou e fatores associados à não realização: um olhar sobre o Programa de Prevenção do Câncer do Colo do Útero em Pernambuco, Brasil. **Cadernos de saúde pública**, Rio de Janeiro. v. 25, p. 301-309, 2009. Suplemento 2.

ALESSIO, E., MESTRONI, G., BERGAMO, A., SAVA, G. Ruthenium antimetastatic agents. **Curr. Top. Med. Chem.** v. 4; p. 1525–35. 2004.

ALVES, R.C., ALVES, D., GUZ, B. *et al.*, Advanced hepatocellular carcinoma. Review of targeted molecular drugs. **Ann Hepatol**. v. 10; p. 21-7. 2011.

ALVES-DE-SOUZA, C.E.; ALVES DE SOUZA H.M.; STIPP, M.C.; CORSO C R.; GALINDO, C.; CARDOSO, C.R.; DITTRICH, R.L.; CAVALIERI, E.A.S.R.; KLASSEN, G.; CARLOS, R.M.; CADENA, S.M.S.C.; ACCO A. Ruthenium complex exerts antineoplastic effects that are mediated by oxidative stress without inducing toxicity in Walker-256 tumor-bearing rats. **Free Radical Biology & Medicine**. Accepted on June 16, 2017.

AM, I., HUSSEIN, Y., HASANIN, M.T., ELBEHAIRI, S.E. Anti-proliferative Activities of Metallic Nanoparticles in an in Vitro Breast Cancer Model. **Asian Pac J Cancer Prev**. v. 16; n. 14; p. 6039-46. 2015.

ANTELMANN, H.; HELMANN, J. D. Thiol-Based Redox Switches and Gene apoptosis. **Free Radical Biology and Medicine**, v. 48, p. 749-762, 2010.

ARAUJO, R.L.; RIECHELMANN, R.P.; FONG, Y. Patient selection for the surgical treatment of resectable colorectal liver metastases. **J Surg Oncol**. 2017 Feb;115(2):213-220. Review.

ARVELO, F. Establishment and characterization of cell lines from the Walker carcinoma 256 able to grow in suspension culture and deficient in thymidine kinase. **In vitro**, v. 20, n. 7, p.549-565, 1984.

ATTWA, M.H. and EL-ETREBY, S.A. Guide for diagnosis and treatment of hepatocellular carcinoma. **World J Hepatol.** v. 28; n.7; p. 1632-51. 2015

BANERJEE, H.N., HYMAN, G., EVANS, S., *et al.*, Identification of the Transmembrane Glucose Regulated Protein 78 as a Biomarker for the Brain Cancer Glioblastoma Multiforme by Gene Expression and Proteomic Studies. **J Membr Sci Technol.** v. 15; n. 4(1); pii: 1000126. 2014.

BARRY, N.P.E.; SADLER, P.J. Exploration of the medical periodic table: towards new target. **Chem Commun.** 49; 5106. 2013.

Bastos-Pereira AL, Lugarini D, Oliveira-Christoff Ad, Ávila TV, Teixeira S, Pires Ado R, Muscará MN, Cadena SM, Donatti L, Cristina da Silva de Assis H, Acco A Celecoxib prevents tumor growth in an animal model by a COX-2 independent mechanism. **Cancer Chemother Pharmacol.** 65;2:267-76. 2010. doi: 10.1007/s00280-009-1031-8.

BOGLIOLO, L.; BRASILEIRO, F. G. **Bogliolo Patologia.** Rio de Janeiro: Guanabara Koogan, 2011.

BRASIL. Ministério da Saúde. Departamento de DST, Aids e Hepatites Virais. SUS passa a ofertar vacina contra HPV a partir de 10 de março. 2014b. Disponível em: Acesso em: 24 jan. 2014.

BRASIL. Ministério da Saúde. Instituto Nacional do Câncer. Diretrizes brasileiras para o rastreamento do câncer do colo do útero. Rio de Janeiro: Inca, 2011c. p. 106.

BUPATHI M, KASEB, A., MERIC-BERNSTAM, F. *et al.*, Hepatocellular carcinoma: Where there is unmet need. **Mol Oncol.** v. 9; n. 8; p. 1501-9. 2015.

CAMILO, M.R., CARDOSO, C.R., CARLOS, R.M. *et al.*, Photosolvolytic of cis-[Ru(α -diimine) $_2$ (4-aminopyridine) $_2$] $^{2+}$ Complexes: Photophysical, Spectroscopic, and Density Functional Theory Analysis. **Inorg. Chem.** v. 53; p. 3694–3708. 2014.

CARDOSO, C.R., LIMA, M.V.S., CHELESK, J., *et al.*, Luminescent Ruthenium Complexes for Theranostic Applications. **J Med Chem.** v. 57; p. 4906–4915. 2014.

CHABNER, B.A., 2012. PRINCÍPIOS GERAIS DA QUIMIOTERAPIA DO CÂNCER, IN: BRUNTON, L.L., CHABNER, B.A., KNOLLMANN, B.C. (Eds.), **As Bases Farmacológicas da Terapêutica** de Goodman & Gilman, 12 ed ed. AMGH, Porto Alegre, pp. 1667-1674.

CHENG, Y. C. *et al.*, Transarterial chemoembolization for intrahepatic multiple recurrent HCC after liver resection or transplantation. **Ann Transplant.** v. 30; n. 19; p. 309-16. 2014.

CHENG, Y., ZHANG, C., ZHAO, J. Correlation of CpG island methylator phenotype with poor prognosis in hepatocellular carcinoma. **Exp Mol Pathol.** v. 88; n. 1; p. 112-7. 2009.

CIRCU, M. L.; AW, T. Y. Reactive oxygen species, cellular redox systems, and

CLARKE, M.J. Ruthenium metallopharmaceuticals. **Coord. Chem. Rev.** v. 232; p. 69-93. 2002.

CRIPPA, S., BITTONI, A., SEBASTIANI, E., PARTELLI, S., ZANON, S. *et al.*, Is there a role for surgical resection in patients with pancreatic cancer with liver metastases responding to chemotherapy? **Eur J Surg Oncol.** v. 29. pii: S0748-7983(16)30605-9. 2016.

CROCE, C.M.,. Oncogenes and cancer. **The New England journal of medicine** 358, 502-511. 2008.

DE BERARDINIS, R.J., CHENG, T. Q's next: the diverse functions of glutamine in metabolism, cell biology and cancer. **Oncogene.** v. 29; p. 313–324. 2010.

DONATO, M.F., AROSIO, E., MONTI, V., *et al.*, Proliferating cell nuclear antigen assessed by a computer-assisted image analysis system in patients with chronic viral hepatitis and cirrhosis. **Dig Liver Dis.** v. 34; n. 3; p. 197-203. 2002.

DREIFUSS, A.A.; BASTOS-PEREIRA, A.L.; FABOSSI, I.A.; LÍVERO, F.A.; STOLF, A.M.; ALVES-DE-SOUZA, C.E.; GOMES, L.DE.O.; CONSTANTIN, R.P.; FURMAN, A.E.; STRAPASSON, R.L.; TEIXEIRA, S.; ZAMPRONIO, A.R.; MUSCARÁ, M.N.; STEFANELLO, M.E.; ACCO, A. Uncaria tomentosa exerts extensive anti-neoplastic effects against the Walker-256 tumour by modulating oxidative stress and not by alkaloid activity. **PLoS One.** 8;2:e54618. 2013. doi: 10.1371/journal.pone.0054618.

EASL-EORTC. Clinical practice guidelines: management of hepatocellular carcinoma. **J Hepatol.** v. 56; n. 4; p. 908-43. 2012.

EL-SERAG, H. B. Hepatocellular carcinoma. **N Engl J Med.** v. 22; n. 365(12); p. 1118-27. 2011.

EL-SERAG, H.B. and RUDOLPH KL. Hepatocellular carcinoma: epidemiology and molecular carcinogenesis. **Gastroenterology.** v. 132; n. 7; p. 2557-76, Review. 2007.

FARRELL N. Biomedical uses and applications of inorganic chemistry an overview. **Coord Chem Rev.** 232; 1-4. 2002.

FISCHER, B., HEFFETER, P., KRYEZIU, K., GILLE, L., MEIER, S.M., BERGER, W., KOWOL, C.R., KEPPLER, B.K. Poly(lactic acid) nanoparticles of the lead anticancer ruthenium compound KP1019 and its surfactant-mediated activation. **Dalton Trans.** v. 43; p. 1096-104. doi: 10.1039/c3dt52388h. 2014.

FISHER, E. R.; FISHER, B. Electron Microscopic, Histologic, and Histochemical Features of the Walker Carcinoma. **Cancer research**, v.21, p. 527-531, 1961.

FITZMORRIS, P. and SINGAL, A.K., Surveillance and Diagnosis of Hepatocellular Carcinoma. **Gastroenterol Hepatol**. v. 11; n. 1; p. 38-46. 2015.

FRASCA, D. R. and CLARKE, M. J. Alterations in the binding of $[Cl(NH_3)_5Ru(III)]^{2+}$ to DNA by glutathione: Reduction, autoxidation, coordination, and decomposition. **J. Am. Chem. Soc.** v. 121; p. 8523– 32. 1999.

GALLUZZI, L.; VITALE, I.; ABRAMS, J. M.; ALNEMRI, E. S.; BAEHRECKE, E. H.; BLAGOSKLONNY, M. V.; DAWSON, T. M.; DAWSON, V. L.; EL-DEIRY, W. S.; FULDA, S.; GOTTLIEB, E.; GREEN, D. R.; HENGARTNER, M. O.; KEPP, O.; KNIGHT, R. A.; KUMAR, S.; LIPTON, S. A.; LU, X.; MADEO, F.; MALORNI, W.; MEHLEN, P.; NUNEZ, G.; PETER, M. E.; PIACENTINI, M.; RUBINSZTEIN, D. C.; SHI, Y.; SIMON, H. U.; VANDENABEELE, P.; WHITE, E.; YUAN, J.; ZHIVOTOVSKY, B.; MELINO, G.; KROEMER, G. Molecular definitions of cell death subroutines: recommendations of the Nomenclature Committee on Cell Death 2012. **Cell Death and Differentiation**, v. 19, p. 107-120, 2012.

GALUPPO LF, DOS REIS LÍVERO FA, MARTINS GG, CARDOSO CC, BELTRAME OC, KLASSEN LM, CANUTO AV, ECHEVARRIA A, TELLES JE, KLASSEN G, ACCO A. Sydnone 1: A Mesoionic Compound with Antitumoral and Haematological Effects In Vivo. **Basic Clin Pharmacol Toxicol**. 119;1:41-50. . 2016. doi: 10.1111/bcpt.12545. Epub 2016.

GHEZZI, M., BERRETTA, M., BOTTACIN, A., PALEGO, P., SARTINI, B., *et al.*, Impact of Bep or Carboplatin Chemotherapy on Testicular Function and Sperm Nucleus of Subjects with Testicular Germ Cell Tumor. **Front Pharmacol**. v. 13;n. 7; p. 122. 2016.

GLASAUER, A, CHANDEL, N. S. Targeting antioxidants for cancer therapy. **Biochem Pharmacol**. 2014 Nov 1;92(1):90-101. doi: 10.1016/j.bcp.2014.07.017.

GO, R.S.; ADJEL, A.A. Review of the comparative pharmacology and clinical activity of cisplatin and carboplatin. **J Clin Oncol**. v. 17; p. 409-22. 1999.

GUAITANI, A. *et al.* Two lines of Walker carcinoma 256: their peculiarities and different interactions with the host. **Tumori**, v.1, p.1-9, 1983.

GUIMARAES, F. *et al.*, Tumor Growth Characteristics of the Walker 256 AR Tumor, a Regressive Variant of the Rat Walker 256 A tumor. **Brazilian archives of biology and technology**, v.53, n. 5, p. 1101-1108, 2010.

HALLIWELL, B., GUTTERIDGE, J. Free Radicals in Biology and Medicine. New York, USA: **Oxford University Press**. 2007.

HANAHAN, D.; WEINBERG, R. A. Hallmarks of cancer: the next generation. **Cell**, v. 144, n. 5, p. 646-674, 2011.

HARTINGER, C.G., JAKUPEC, M.A., ZORBAS-SEIFRIED, S., GROESSL, M., EGGER, A., BERGER, W., ZORBAS, H., DYSON, P.J., KEPPLER, B.K. KP1019, a new redox-active anticancer agent--preclinical development and results of a clinical phase I study in tumor patients. **Chem Biodivers**. v. 5; n. 10; p. 2140-55. 2008.

HATZARAS, I. *et al.*, Treatment option and surveillance strategie after therapy of hepatocellular carcinoma. **Ann Surg Oncol**, v. 21; n. 3; p. 758-66. 2014.

HEIDI, H.; HARRIS, S. R.; DONALD, M. C.; GOLAN, D. E. Princípios de Farmacologia Antimicrobiana e Antineoplásica. In: Koogan, G. (Ed.). **David E. Golan - Princípios de Farmacologia - A Base Fisiopatológica da Farmacoterapia**, 2009, p.529-537.

HOLM, R.H.; KENNEPOHL, P.; SOLOMON, E.I.; Structural and Functional aspects of metal sites in biology. **Chem Rev**. 96;2239-2314. 1996.

HSIEH, M.C., HUANG, C.H., CHIANG, P.H., CHEN, Y.Y., TANG, Y., SU, Y.L. Tailored Selection of First-Line Cisplatin-Based Chemotherapy in Patients with Metastatic Urothelial Carcinoma of Bladder. **J Cancer**. v. 27; n. 7; p.1347-52. 2016.

INCA. Instituto Nacional de Câncer José Alencar Gomes da Silva. **Estimativa 2014: Incidência de Câncer no Brasil**. Rio de Janeiro, 2016

INDRAN, I. R.; TUFO, G.; PERVAIZ, S.; BRENNER, C. Recent advances in apoptosis, mitochondria and drug resistance in cancer cells. **Biochimica Et Biophysica Acta-Bioenergetics**, v. 1807, p. 735-745, 2011.

JAKUPEC, M. A., REISNER, E., EICHINGER, A., PONGRATZ, M., ARION, V. B., GALANSKI, M., HARTINGER, C. G., KEPPLER, B. K. Redox-active antineoplastic ruthenium complexes with indazole: Correlation of in vitro potency and reduction potential. **J. Med. Chem**. v. 48; p. 2831-2837. 2005.

JOHANSEN, T.; RUSTEN, T. E.; BRECH, A.; BAEHRECKE, E. H.; STENMARK, H. Autophagic degradation of dBruce controls DNA fragmentation in nurse cells during late Drosophila melanogaster oogenesis. **Journal of Cell Biology**, v. 190, p. 523-531, 2010.

JONES, D. P. Redefining oxidative stress. **Antioxidants & Redox Signaling**, v. 8, p.1865-1879, 2006.

KHAN, K.N., YATSUHASHI, H., YAMASAKI, K., *et al.*, Prospective analysis of risk factors for early intrahepatic recurrence of hepatocellular carcinoma following ethanol injection. **J Hepatol**. 32; 2; 269-78. 2000.

KIM, T.K., LEE, E., JANG, H.J. Imaging findings of mimickers of hepatocellular carcinoma. **Clin Mol Hepatol**. v. 21; n. 4; p. 326-43. 2016.

KROEMER, G.; GALLUZZI, L.; BRENNER, C. Mitochondrial membrane Regulation. **Antioxidants & Redox Signaling**. 14; 1049-1063. 2011.

KROEMER, G.; GALLUZZI, L.; VANDENABEELE, P.; ABRAMS, J.; ALNEMRI, E. S.; BAEHRECKE, E. H.; BLAGOSKLONNY, M. V.; EL-DEIRY, W. S.; GOLSTEIN, P.; GREEN, D. R.; HENGARTNER, M.; KNIGHT, R. A.; KUMAR, S.; LIPTON, S. A.; MALORNI, W.; NUNEZ, G.; PETER, M. E.; TSCHOPP, J.; YUAN, J.; PIACENTINI, M.; ZHIVOTOVSKY, B.; MELINO, G. Classification of cell death: recommendations of the Nomenclature Committee on Cell Death 2009. **Cell Death and Differentiation**. 16; 3-11. 2009.

KUMAR, V.; ABBAS, A. K.; FAUSTO, N.; MITCHELL, R. N. **Robbins & Cotran Pathologic Basis of Disease**. Philadelphia: Elsevier Editora Ltda, 2010.

KUO C.W.; TSAI, M. H.; LIN, T. K.; TIAO, M. M.; WANG, P. W.; CHUANG, J. H. CHEN, S. D.; LIOU, C. W. mtDNA as a Mediator for Expression of Hypoxia-Inducible Factor 1 α and H_2O_2 in Hypoxic Neuroblastoma **Cells. Int J Mol Sci**. 7;18, 2017.

LAU, W. K.; CUI, L. Y.; CHAN, S. C., IP, M. S; MAK, J. C. The presence of serotonin in cigarette smoke - a possible mechanistic link to 5-HT-induced airway inflammation. **Free Radic Res**. 50;5:495-502. 2016.

LEE, J. M, Park, J.W, Choi BI. 2014 KLCSSG-NCC Korea Practice Guidelines for the management of hepatocellular carcinoma: HCC diagnostic algorithm. **Dig Dis**. v. 32; n. 6; p. 764-77. 2014.

LEONARDUZZI, G.; SOTTERO, B.; POLI, G. Targeting tissue oxidative damage by means of cell signaling modulators: The antioxidant concept revisited. **Pharmacology & Therapeutics**, v. 128, p. 336-374, 2010.

LLOVET, J.M. and BRUIX, J. Molecular targeted therapies in hepatocellular carcinoma. **Hepatology**. v. 48; n. 4; p. 1312-27. 2008.

LORENZATO, F. R. B. Organização do rastreamento do câncer do colo do útero em países desenvolvidos. In: COELHO, F. (Org.). et al. Câncer do colo do útero. São Paulo: **Tecmedd**, 2008. p. 114-125.

MARTINDALE, J. L; HOLBROOK, N.J. Cellular response to oxidative stress: signaling for suicide and survival. **J Cell Physiol**. 192;1:1-15. Review. 2002.

MARTINS GG, LÍVERO FA, STOLF AM, KOPRUSZINSKI CM, CARDOSO CC, BELTRAME OC, QUEIROZ-TELLES JE, STRAPASSON RL, STEFANELLO MÉ, OUDE-ELFERINK R, ACCO A. Sesquiterpene lactones of *Moquiniastrum polymorphum* subsp. *floccosum* have antineoplastic effects in Walker-256 tumor-bearing rats. **Chem Biol Interact**. 25;228:46-56. 2015. doi: 10.1016/j.cbi.2015.01.01.

MÉNDEZ-SÁNCHEZ, N., RIDRUEJO, E., ALVES DE MATTOS, A. *et al.*, Latin American Association for the Study of the Liver (LAASL) clinical practice guidelines: management of hepatocellular carcinoma. **Ann Hepatol**. 13; Suppl 1; p. S4-40.; Review. 2014.

MILKOVIC, L; ZARKOVIC, N; SASO, L. Controversy about pharmacological modulation of Nrf2 for cancer therapy. **Redox Biol**. 8;12:727-732. 2017.

MONGE, A.; CHORGHAE, M.; ERHARDT, P.W.; GANELIN, C.R.; KOGA, N.; LINDBERG, P.; PERUN, T.J.; TOPLESS, J.G.; TIVEDI, B.K.; WERMUTH, C.G. Medicinal chemistry in the development of coceties. **Eur J Med Chem.** 35; 1121-1125. 2000.

MURATA, S., MINE, T., SUGIHARA, F., *et al.*, Interventional treatment for unresectable hepatocellular carcinoma. **World J Gastroenterol.** 7; 20; 13453-65. 2014.

NARASIMHAN, B., SHARMA, D., KUMAR, P. Biological importance of imidazole nucleus in the new millennium. **Med Chem Res.** 20; 1119-1140. 2011.

NEZIS, I. P.; SHRAVAGE, B. V.; SAGONA, A. P.; LAMARK, T.; BJORKOY, G.; OSBURN, W. O.; KENSLER, T. W. Nrf2 signaling: An adaptive response pathway for protection against environmental toxic insults. **Mutation Research-Reviews in Mutation Research**, v. 659, p. 31-39, 2008.

PLECITÁ-HLAVATÁ, L.; ENGSTOVÁ, H.; ALAN, L. *et al.*, Hypoxic HepG2 cell adaptation decreases ATP synthase dimers and ATP production in inflated cristae by mitofilin down-regulation concomitant to MICOS clustering. **FASEB J.** 30; 5; 1941-57. 2016.

POTTER R. *et al.* Definitive radiotherapy based on HDR brachytherapy with iridium 192 in uterine cervix carcinoma; report on the Vienna University Hospital. 2010.

RADES, D., SEIDL, D., JANSSEN, S., BAJROVIC, A., HAKIM, S.G., WOLLENBERG, B. *et al.*, Chemoradiation of locally advanced squamous cell carcinoma of the head-and-neck (LASCCHN): Is 20mg/m(2) cisplatin on five days every four weeks an alternative to 100mg/m(2) cisplatin every three weeks? **Oral Oncol.** 59; 67-72. 2016.

REISNER, E., ARION, V. B., EICHINGER, A., KANDLER, N., GIESTER, G., POMBEIRO, A. J. L., KEPPLER, B. K. Tuning of redox properties for the design of ruthenium anticancer drugs: Part 2. Syntheses, crystal structures, and electrochemistry of potentially antitumor [RuIII/II]Cl_{6-n}(azole)_n]z (n = 3, 4, 6) complexes. **Inorg. Chem.** 44; 19; 6704-6716. 2005.

REUTER, S.; GUPTA, S. C.; CHATURVEDI, M. M.; AGGARWAL, B. B. Oxidative stress, inflammation, and cancer How are they linked? **Free Radical Biology and Medicine**, 49, 1603-1616, 2010.

RIBEIRO, K. C. B. Epidemiologia do câncer do colo do útero: fatores demográficos e fatores de risco. In: COELHO, F. (Org.) *et al.* Câncer do colo do útero. São Paulo: **Tecmedd**, 2008. 18-23.

RIBEIRO, L. Prevalência e fatores associados a não realização do exame citopatológico do colo do útero na zona norte do município de Juiz de Fora. 2012. 125f. Dissertação (Mestrado em Saúde Coletiva)– Universidade Federal de Juiz de Fora, **Faculdade de Medicina**, Juiz de Fora, 2012.

RIJT, S.H.V.; SADLER, P.J. Current applications and future ptencial for bioinorganic chemistry in the development of anticancer drugs. **Drug Discov Today**. 14; 1089-87. 2009.

SAINI, V; MANRAL, A; ARORA, R; MEENA, P; GUSAIN, S; SALUJA, D; TIWARI, M. Novel synthetic analogs of diallyl disulfide triggers cell cycle arrest and apoptosis via **ROS** generation in MIA PaCa-2 cells. **Pharmacol Rep**. 14;69;4:813-821. 2017.

SANKARANARAYANAN, R. *et al.* O desafio de controlar o câncer do colo do útero no mundo em desenvolvimento. In: COELHO, F. (Org.) *et al.* Câncer do colo do útero. São Paulo: **Tecmedd**, 2008. p. 104-113.

SANTOS, R. L. S. R., VAN ELDIK, R., DE OLIVEIRA SILVA, D. Kinetic and mechanistic studies on reactions of diruthenium(II,III) with biologically relevant reducing agents. **Dalton Trans**. 42; 16796. 2013.

SANTOS, T.G.; LOPES, M.H.; MARTINS, V.R. Targeting prion protein interactions in cancer. **Prion**. 2015;9:165-73. Review.

SAVA, G., GAGLIARDI, R., BERGAMO, A., ALESSIO, E., MESTRONI, G. Treatment of metastases of solid mouse tumours by NAMI-A: comparison with cisplatin, cyclophosphamide and dacarbazine. **Anticancer Res**. 19; 2A; 969-72. 1999.

SCHLUGA, P., HARTINGER, C.G., EGGER, A. *et al.*, Redox behavior of tumor-inhibiting ruthenium(III) complexes and effects of physiological reductants on their binding to GMP. **Dalton Trans**. 14; 1796-1802. 2006.

SCHWEICH.JU; MERKER, H. J. MORPHOLOGY OF VARIOUS TYPES OF CELLDEATH IN PRENATAL TISSUES. **Teratology**, v. 7, p. 253-266, 1973.

SIMPKINS, H. A Morphological and Phenotypic Analysis of Walker 256 Cells. **Cancer research**, 5, 1334-1338, 1991.

STIPP, M. C.; BEZERRA, I. L.; CORSO, C. R.; DOS REIS LIVERO, F. A.; LOMBA, L. A.; CAILLOT, A. R.; ZAMPRONIO, A. R.; QUEIROZ-TELLES, J. E.; KLASSEN, G.; RAMOS, E. A., SASSAKI, G. L.; **ACCO A.** Necroptosis mediates the antineoplastic effects of the soluble fraction of polysaccharide from red wine in Walker-256 tumor-bearing rats. **Carbohydr Polym**. 15;160:123-133. 2017. doi: 10.1016/j.carbpol.2016.12.047.

SUGIYAMA, T., OKAMOTO, A., ENOMOTO, T., HAMANO, T., AOTANI, E., *et al.*, Randomized Phase III Trial of Irinotecan Plus Cisplatin Compared With Paclitaxel Plus Carboplatin As First-Line Chemotherapy for Ovarian Clear Cell Carcinoma: JGOG3017/GCIG Trial. **J Clin Oncol**. v. 11. pii: JCO669010. 2016.

TABRIZIAN, P., JIBARA, G., SHRAGER, B. *et al.*, Recurrence of hepatocellular cancer after resection: patterns, treatments, and prognosis. **Ann Surg**. v. 261; n. 5; p. 947-55. 2014.

VALKO, M., RHODES, C.J., MONCOL, J., IZAKOVIC, M., MAZUR, M. Free radicals, metals and antioxidants in oxidative stress-induced cancer. **Chem Biol Interact.** 160:1-40. 2006.

VANDER HEIDEN, M.G., CANTLEY, L.C., THOMPSON, C.B. Understanding the Warburg Effect: The Metabolic Requirements of Cell Proliferation. **Science.** 324; 1024-33. 2009.

VIDAL M. L. B. et al., Efeitos Adversos tardios subsequentes ao tratamento radioterápico para câncer de colo uterino na bexiga, reto e função sexual. Dissertação (Mestrado em Ciência) – **Instituto Nacional de Câncer**, 2008.

VOUSDEN, K. H. Outcomes of p53 activation - spoilt for choice. **Journal of CellScience**, v. 119, p. 5015-5020, 2006.

WARBURG, O. On the origin of cancer cells. **Science.** v. 123; p. 309–314. 1956.

WARBURG, O. Uber den Stoffwechsel der Carcinomzelle. **Klin Wochenschr Berl.** v. 4; p. 534–536. 1925.

WHO. World Health Organization. Guide to cancer early diagnosis. **Geneva, Switzerland.** 2017. ISBN 978-92-4-151194-0.

WOO CC, Chen WC, Teo XQ, Radda GK, Lee PT. Downregulating serine hydroxymethyltransferase 2 (SHMT2) suppresses tumorigenesis in human hepatocellular carcinoma. **Oncotarget.** v. 6. 2016. doi: 10.18632/oncotarget.10415.

WOO, S.M.; KWON, S.C; KO, S. G., CHO, S. G. Barley grass extract causes apoptosis of cancer cells by increasing intracellular reactive oxygen species production. **Biomed Rep.** 6;6:681-685. 2017.

WRZESINSKI, S.H., TADDEI, T.H., STRAZZABOSCO, M. Systemic therapy in hepatocellular carcinoma. **Clin Liver Dis.** v. 15; n. 2; p. 423-41. 2011.

ZANETTI A,R., VAN DAMME, P., SHOUVAL, D. The global impact of vaccination against hepatitis B: a historical overview. **Vaccine.** v. 18; n. 26; p. 6266-73. 2008.

ZHU, X.; JU, S.; YUAN, F.; CHEN, G.; SHU, Y.; LI, C.; XU, Y.; LUO, J.; XIA, L. microRNA-664 enhances proliferation, migration and invasion of lung cancer cells. **Exp Ther Med.** 13;6:3555-3562. 2017.